CLINICAL AND EXPERIMENTAL STUDY ON THE BIOMECHANICS OF BREASTFEEDING

by

Lin Jiang

APPROVED BY SUPERVISORY COMMITTEE:

Dr. Fatemeh Hassanipour, Chair

Dr. John H.L. Hansen

Dr. Yonas Tadesse

Dr. Giacomo Valerio Iungo

This dissertation is dedicated

to my family and friends,

who have always supported me, encouraged me and directed me to be better;

to my mom and dad,

who have contributed so much to provide me with all the opportunities to pursue this work;

to my husband,

who always stands by me and has faith in me;

to my two kids,

who bring the most happiness and joy to my life.

CLINICAL AND EXPERIMENTAL STUDY ON THE BIOMECHANICS OF BREASTFEEDING

by

LIN JIANG, BS, MS

DISSERTATION

Presented to the Faculty of

The University of Texas at Dallas

in Partial Fulfillment

of the Requirements

for the Degree of

DOCTOR OF PHILOSOPHY IN

MECHANICAL ENGINEERING

THE UNIVERSITY OF TEXAS AT DALLAS

May 2021

ACKNOWLEDGMENTS

First and foremost, I would like to give sincere gratitude to my advisor, Dr. Fatemeh Hassanipour, for her patient guidance and encouragement, not only in academic study but also in all aspects of life. It is her continuous support that helped me transform, from one who does not know much about experimental research in human lactation to one who can handle experiments independently and solves problems with mature plans. Dr. Hassanipour provided the resources, tools, and independence necessary for the successful execution of this research and offered mentorship, guidance, and encouragement to her best extent along the way. I am thankful to have had the opportunity to work in Dr. Hassanipour's research group. All I learned from her makes me grow and become a better person.

I would like to thank all my respectful committee professors, Dr. John Hansen, Dr. Yonas Tadesse, Dr. Giacomo Valerio Iungo, and Dr. Jin Liu. I am grateful for the technical guidance and suggestions I received from Dr. Tadesse, Dr. Hansen, and Dr. Iungo on this research. I am also immensely thankful for the supports and recommendations from Dr. Hansen and Dr. Tadesse as my professional references, who helped me target a dream career in academia.

I would like to thank all members of the Advanced Research in Thermofluid Systems (ARTS) Laboratory, who have worked along with me in these years. Thank you for all your help and support, Xudong An, Sarvenaz Sobhan, Mohammad Aliakbari, Diana Alatalo, Adolfo Lozano III, Jamasp Azarnoosh, Shadi Zaheri, Robin, Navid, Shazi, and Blossom.

On a personal note, I would like to thank my family, friends, and loved ones for their continuous love and support. Most significantly, I would like to thank my parents for providing me the opportunity to receive the best education when I was young and encouraging me wholeheartedly to be brave and explore the world when I grew up. They support and care about me in all aspects of my life. Specifically, I am thankful to my mom for helping me raise my two kids during my 5-1/2 years of PhD study. I am also grateful to my husband, Fenglin Zhou, who has been supportive and understanding throughout this long journey as I pursued my dream of earning a PhD.

Finally, I would like to thank my advisor again, Dr. Fatemeh Hassanipour, for offering me assistantships during my Ph.D. study. The financial support from National Science Foundation (NSF CAREER, Grant #1454334) makes my research project and this dissertation possible.

April 2021

CLINICAL AND EXPERIMENTAL STUDY ON THE

BIOMECHANICS OF BREASTFEEDING

Lin Jiang, PhD
The University of Texas at Dallas, 2021

Supervising Professor: Dr. Fatemeh Hassanipour, Chair

Breastfeeding benefits mothers and infants in both physical and mental health. An infant develops complex oral dynamics on the breast to extract milk. The present study aims to understand the breastfeeding mechanism through *in vivo* clinical analysis and *in vitro* experimental work, which can answer several bio-mechanical questions that arise from the infant's oral interaction on the breast during breastfeeding.

In the clinical study, the positive (compression) and negative (vacuum) pressure values were obtained simultaneously on multiple lactating mother-infant dyads. Parallel to the pressure data measurements, ultrasound images were captured and processed to reveal the nipple deformations and the displacements of infants' tongues and jaw movements during breastfeeding. The results showed an oscillatory positive pressure profile on the breast under both maxilla and mandible, which differed from clinical observations that only the mandible of an infant moves during breastfeeding. The nipple deformations varied between mothers and indicated a large volume change in the anatomy.

In the experimental work, a new and unique bio-inspired breastfeeding simulator (BIBS) was constructed to mimic infant oral behavior and milk extraction, with the intent to study the breastfeeding mechanism *in vitro*. The simulator replicated the intra-oral vacuum pressure,

compression pressures from the infant's jaw, tongue and upper palate, and nipple deformation on the breast areola area. All mechanisms were successfully coordinated to mimic the infant's feeding mechanism during breastfeeding. Results were matched with the *in vivo* clinical pressure data and nipple deformation in ultrasound images. Integrated with graphical user interface and feedback controllers, the BIBS adjusted automatically based on vacuum magnitude and frequency and served as a physiologically accurate test-bed for studying the biomechanics of breastfeeding.

Finally, the flow dynamics in the bifurcated milk ducts of a lactating breast model during breastfeeding simulation using BIBS was analyzed with a particle image velocimetry (PIV) system. A clear human milk-mimicking fluid (HMMF) achieved with composition of 15.69% NaI, 30.27% glycerin, 54.02% water and 0.02% xanthan gum by weight percentage provided a non-Newtonian density, viscosity, and refractive index matched fluid for use in PIV experiments. The oscillatory flow under vacuum pressure provided a higher maximum velocity magnitude at the outlet compare to when an infant applies both vacuum and oral compression pressures, however mean velocity was higher when compression was combined with vacuum. Additionally, the average milk flow rate of vacuum-only operation was less than that of vacuum plus oral compression, thus further explaining the effectiveness of applying compressive suckling dynamics on the breast in human lactation.

TABLE OF CONTENTS

LIST OF FIGURES

LIST OF TABLES

LIST OF ABBREVIATIONS AND ACRONYMS

D	Diameter
DW	Distilled Water
GA	Genetic Algorithm
Gly	Glycerin
GUI	Graphical User Interface
HMMF	Human Milk Mimicking Fluid
HP	Hard Palate
ID	Inner Diameter
J	Hard-soft Junction
L1-L7	Lower Jaw Sensel 1 - 7
M	Milk Flow
max	maximum
MAXE	Maximum absolute error
min	minium
N	Nipple
NaI	Sodium Iodide
NH	Nipple Height
NL	Nipple length
PC	Personal Computer
PID	Proportional-integral-derivative
PIV	Particle Image Velocimetry
RMSE	Root mean square error
RI	Refractive of Index
SD	Standard Deviation
SP	Soft Palate
T	Tongue
U1-U7	Upper Palate Sensel 1 - 7
U	Uncertainty
XG	Xanthan Gum

CHAPTER 1

INTRODUCTION

1.1 Motivation

Breastfeeding is strongly recommended for infants as breast milk contains necessary nutrition and boosts immune defenses. However, many mothers introduce supplementary food or stop nursing in the first month postpartum due to breastfeeding difficulties (Schwartz et al., 2002; Scott et al., 2006). Early termination is largely associated with neurological and physical health issues for both mother and child (Odom et al., 2013). Infant sucking and latching difficulties are commonly cited as reasons for ceasing breastfeeding during the initiation of lactation (Li et al., 2008), yet there is little knowledge regarding sucking dynamics, specifically tongue movement, during this period. Studying the biomechanics of breastfeeding and understanding the infant's oral interaction with the mother's breast can assist in solving breastfeeding difficulties.

Some of the well-studied clinical assessment of breastfeeding has explored the mechanism of milk production (Newton and Newton, 1950), the rhythmic vacuum pressure for milk extraction (Woolridge, 1986), as well as the relationship between the tongue position and the milk ejection (Geddes et al., 2012). While intra-oral pressure can yield adequate volumes of milk for infant consumption, more recent work has demonstrated that mouthing dynamics is also as effective as the vacuum at milk removal (Alekseev and Ilyin, 2016; Alatalo and Hassanipour, 2020). Furthermore, a study regarding the effect of breast milk ejection on infant oral motor skills is needed in defining the correct technique for suckling to be used in the clinical assessment and physical therapy for breastfeeding.

Beyond clinical studies, some recent works have attempted to examine the mechanics of lactation using computation software (Quezada and Vafai, 2014; Mortazavi et al., 2015; Elad et al., 2014). These simulations of milk flow within the breast consider applied vacuum pressure values from clinical experiments but largely ignore the compression from the infant's oral movement. Meanwhile, the assumption that the human breast is a homogeneous, incompressible material is commonly made. To the best of the author's knowledge, there is no attempt in considering the effect of oral interaction to the breast during breastfeeding. The compressive forces exerted by the infant on the nipple require further study both *in vivo* and *in vitro* for better simulation model construction.

The purpose of this work is to develop an easy-to-control, fully-coordinated experimental apparatus to mimic various forces that an infant would apply on the mother's breast, and use the apparatus to study the bio-mimicking human milk transportation in breastfeeding procedure in vitro. With this aim, my dissertation will focus on:

1. processing clinical data on oral pressure and ultrasound images to understand the physiology of the human lactation and infant's oral suckling skills,
2. developing an autonomous Bio-inspired Breastfeeding Simulator (BIBS) to mimic infant's oral interaction with breast during breastfeeding,
3. integrating BIBS with graphical user interface (GUI) and feedback controllers to allow a visualize and robustness simulation on breastfeeding process with user-defined oral suckling profile,
4. formulating human milk mimicking fluid (HMMF) for refractive index matching (ROI) in flow experiments,
5. conducting *in vitro* flow experiments to measure the bio-fluid in the flexible milk ducts with a lactating human breast phantom using particle imaging velocimetry (PIV) system.

1.2 The Physiology of Human Lactation

Human lactation is the process by which milk is synthesized and secreted from the mammary glands of the postpartum female breast in response to an infant sucking at the nipple.

The process describes the secretion of milk from the mammary glands and the period that a mother lactates to feed her young. In humans, the process of feeding milk is called breastfeeding or nursing.

1.2.1 Lactating Human Breast

Studies involving the use of ultrasound to locate and measure milk-yielding ducts noted that ducts are easily compressed and diameter varied with milk ejection and volume under infant's oral movement during breastfeeding (Hassiotou and Geddes, 2013; Geddes, 2007a,b; Ramsay et al., 2005). The mechanical resistance in the bifurcated milk ducts and hundreds of lobes along with the manipulation of the nipple to release milk are important mechanism factors that affect milk flow speed. However, the complex anatomy of the breast as well as the physical dysfunctions of infants cause feeding on the breast difficult and sometimes make breastfeeding impossible (Odom et al., 2013; Stuebe et al., 2014). Breast engorgement, breast abscess, ductal blockage provide inadequate milk production and poor milk supply. Also, the blocked milk ducts cause more resistance in milk transportation in the lactating breast and contribute to infants' inability to sustain sucking. Hence, understanding the physiology of breastfeeding and the milk transport in the breast ductal system from anatomy is very important.

Various imaging modalities have been used to study the anatomy of the breast. A lactating human breast contains nipple, areola, milk ducts, lobes and lobules, adipose tissue, lymph nodes, and skin and muscles (Jütte et al., 2014). The nipple is located at the tip of each breast and at the center of the areola, which is a dark, circular area of skin that surrounds the nipple. The nipple of the breast provides the exit for breast milk and has multiple openings for the milk to come through. Lobules are connected to the ducts, which transport the milk to the nipple, and are compressed by the infant's oral cavity to draw the milk out of the ducts through the nipple. The breast contains an average of 15 to 20 lobes that generates breast

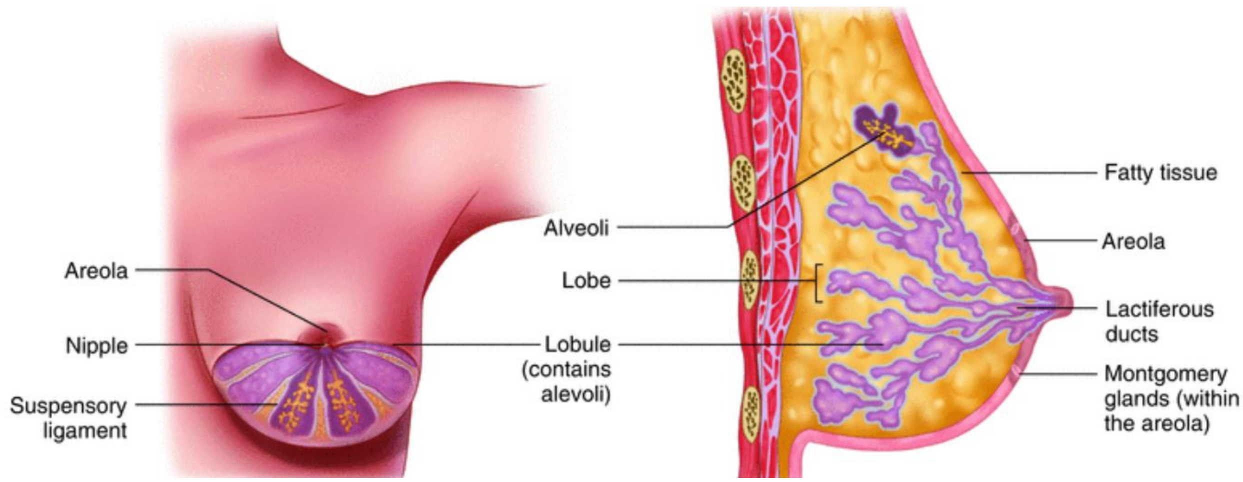

Figure 1.1: The internal and external anatomy of a lactating human breast, image adapted from (Dahl, 2015)

milk. Each lobe consists of lobules, the glands responsible for producing milk in lactating women. Tiny and bifurcated tubes that carry the milk from the lobes and lobules (where the milk is produced) to the nipple are called milk ducts. The reported number of lactiferous ducts varies among studies, often due to differences in methodologies, with values ranging from 4 to 30 ductal openings with most studies reporting 5-9 milk-yielding ducts (Love and Barsky, 2004a; Ramsay et al., 2005; Geddes, 2007b; Hassiotou and Geddes, 2013; Koyama et al., 2013). Duct diameter within the nipple exist varies from 0.1 mm (Taneri et al., 2006) to 4.4 mm (Ramsay et al., 2005).

Among all the studies on the anatomy of the human breast, few have focused on the effect of lactating breast ducts deformation to milk production. *In vivo* mammography of the lactating breast is difficult because of the expansion in radiodensity due to the increase in glandular tissue and the secretion of human milk (Moore, 2010). Limitations in imaging techniques also inhibit the visualization of milk-flow *in vivo* beyond second and third bifurcations because of the diameter of milk ducts (Mortazavi et al., 2015). Due to the limitation in image mapping *in vivo* and the complexity of the unique ductal system in a lactating human breast, challenges exist in studying the bio-transport processes in the human lactating breast. Modeling and fabricating the soft human lactating breast phantom with the appropriate tissue-mimicking, bifurcated, and micro size milk ducts based on the anatomy structure of a lactating human breast is of great importance to study breastfeeding process during *in vitro* breast milk flow experiments.

1.2.2 Infant's Suckling Mechanism

Every component or structure in the anatomy of an infant's oral cavity as shown in Figure 1.2 has its function in mouthing dynamics and cooperatively controls the milk flow rate in the mouth during breastfeeding. The anatomy of a neonate allows it: (1) to breathe even with a teat filling his mouth and his nose pressed up against the breast; and (2) to swallow milk without the worry of having the liquid spill into the trachea. The palate is a soft object and is deformable in the early stage of oral cavity development. It alternated depending on what is placed in the mouth (artificial nipple, pacifiers, and feeding tubes). Wilson-Clay and Hoover (Wilson-Clay and Hoover, 2008) measured the oral geometries of 98 breastfeeding infants ranging in age from 35 weeks of gestation to 3 months. The hard palate is 19-32mm in length and approximately 20-25mm in width. Pressure from these items can easily mold the shape of the palate. The human nipple in the infant's mouth contributes to a rounded U-shaped palate configuration. The tongue assists in sealing the mouth anteriorly and posteriorly to hold intra-oral vacuum pressure during breastfeeding. Tongue and jaw move together to enable suckling during breastfeeding. The tongue needs to extend past the gums, lateralize, and lift from the back of the mouth. The average width of the tongue from 85 infants is 25mm and the average length is 40mm (Siebert, 1985). The configuration of the tongue also changes to provide compression to the nipple to extract milk. As the tongue lifts, the jaw raises as well to compress the nipple-areola complex. The jaw (mandible) raises to help generate positive pressure during swallowing, and the drops during suction (vacuum pressure) seal the oral cavity.

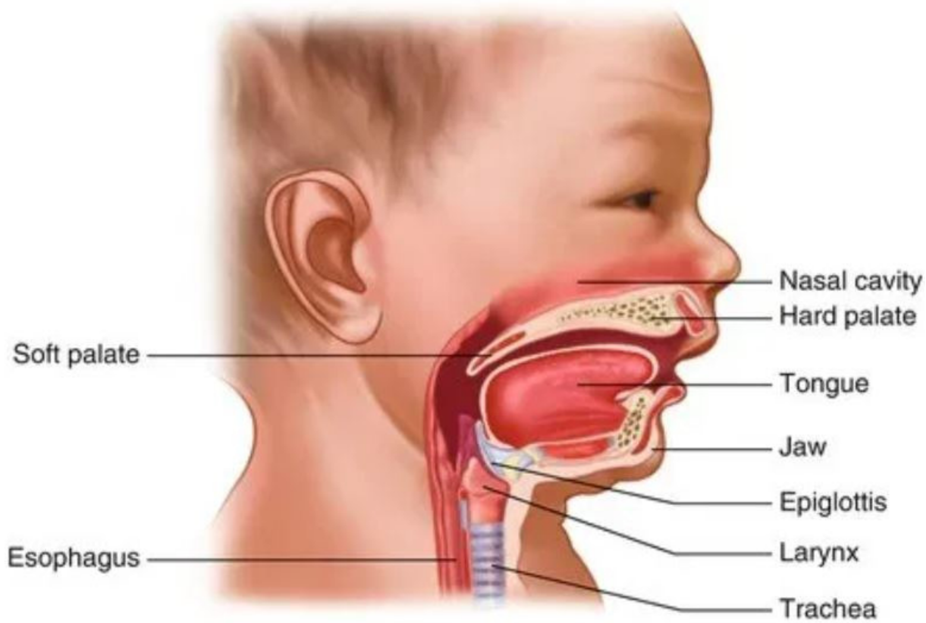

Figure 1.2: This anatomy of infant oral cavity, image adapted from (Dahl, 2015)

Researchers demonstrated the oral geometry and its movement in breastfeeding based on cineradiography studies in the 1950s and confirmed by ultrasound in the 1980's (Weber et al., 1986). The mouth or the oral cavity mainly consists of the lips, upper gum (maxilla), lower jaw (mandible), cheeks, tongue, hard and soft palate, hard-soft palate junction (J), and gum ridges (as described in Figure 1.3a). The lips help locate the nipple and bring it into the mouth and lock the position of the nipple-areola complex within the mouth. An infant's maxilla or upper palate is used to compress the nipple and assist the posterior seal. The soft palate is located behind the upper hard palate. Hard and soft palates are connected by smooth hard-soft palate junction.

The infant uses his anatomic structures, physiological activities, reflexive behaviors, and nutritional needs to initialize and control milk supply during breastfeeding. Infants first latch onto the breast and drag the nipple into its mouth. Then, the infant moves his tongue up and down, compressing the nipple-areola complex and extracts the milk into its mouth. A peristaltic motion from the infant's tongue helps to draw milk from the ducts and guide the milk to the throat during each cycle. Figure 1.3b shows a schematic configuration of this procedure with four stages: 1) maxilla and mandible clamp the nipple-areola complex, 2) tongue extends out and pulls the nipple into the oral cavity, 3) tongue pushes the nipple to the hard palate, and 4) upper palate and lower jaw compress the nipple to squeeze out the milk.

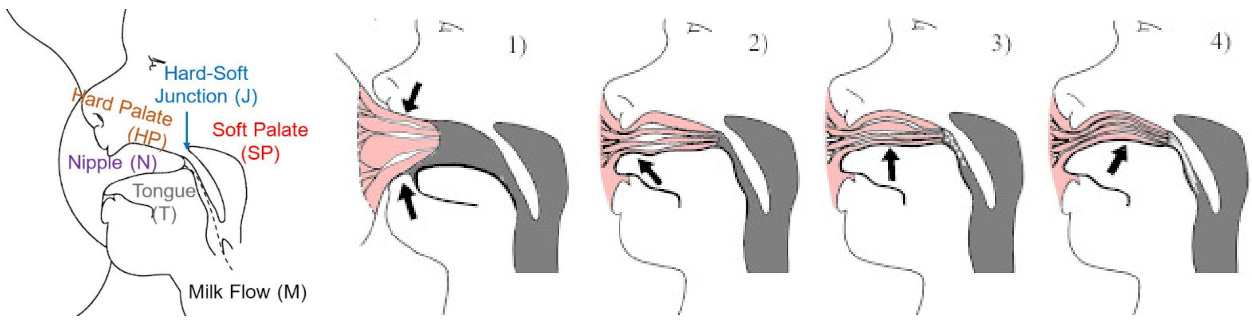

(a) (b)

Figure 1.3: (a) schematic mid-sagittal plane of the infant's oral cavity, (b) schematic configurations of breastfeeding procedure in one cycle.

Infants' suckling during breastfeeding has been observed to have a coordination between facial and tongue muscles, palate compression, and intra-oral vacuum pressure. Suckling, swallowing, and breathing (FEŞTILĂ et al., 2014) all occur in a synchronized interaction in the infant's oral cavity. The observation of oral pressure to the breast and nipple displacement in infant oral cavity during breastfeeding is important for attachment to the breast, proper positioning of the nipple, and for milk removal (McClellan et al., 2008; Geddes et al., 2012; Weber et al., 1986; Alekseev et al., 1998). Rhythmic pressure change from the infant's oral cavity during breastfeeding has also been shown to be vital for milk removal (McClellan et al., 2008; Ilyin et al., 2019). However, neurological and physical disabilities can cause developmental issues in the muscles and bone structure inside the infant's oral cavity, and as a consequence, make latching difficult. For example, infants with neurological diseases, such as Down syndrome, may have weakened tongue muscles which can lead to abnormal control of the oropharyngeal structures, contributing to an uncoordinated and/or insufficient suck, as well as difficulty swallowing (Stuebe et al., 2014). In infants born with a cleft lip and/or a cleft palate, the oral cavity cannot be adequately separated from the nasal cavity during feeding, making it difficult to create the suction needed to breastfeed successfully (Vazirinejad et al., 2009). If the infant has a tongue-tie, he cannot maintain the tongue over the lower gum during sucking. The chewing process is then triggered. This action will cause inefficient milk transfer, low milk supply, and nipple trauma. Among these studies, diagnose and classify the abnormality of breastfeeding mechanics among mothers and infants is based on clinical investigation. Understanding an infant's oral interactions with the lactating human breast is essential in evaluating the nursing efficiency as well as recognizing how the physiological deviations affect the breastfeeding process. Research on understanding the biomechanics of breastfeeding ranges from the mathematical and computational simulations to *in vivo* clinical studies with different imaging techniques and *in vitro* experimental studies with various assessment systems.

1.3 Review on Mathematical and Computational Methods

Several mathematical modeling methods (Zoppou et al., 1997; Quezada and Vafai, 2014) and computational simulations (Mortazavi et al., 2015; Elad et al., 2014; Azarnoosh and Hassanipour, 2020) have investigated the biomechanics of breastfeeding by considering both complex geometry of the ductal structure and the oral cavity movement.

(Zoppou et al., 1997) developed a mathematical model of breastfeeding was developed based on quasi-linear poroelastic theory to compare milk extraction between infant breastfeeding and the use of a breast pump. They showed the critical role of tongue movement, leading to a high volume of expressed milk. (Quezada and Vafai, 2014) modeled the mammary glands and studied the transport mechanism of three types of toxins from blood to breast milk. (Mortazavi et al., 2015) Mortazavi et. al. used mathematical modeling to study milk flow transport in the breast ductal system. They reported that for the minimum flow resistance, there is an optimal range of branch generations leading to the easiest milk flow. (Elad et al., 2014) Elad et. al. simulated the mechanics of breastfeeding considering a symmetric two-generation ductal model with periodic pressure cyclings. Their observation from ultrasound images and simulation emphasized the importance of vacuum pressure in milk expression during breastfeeding. (Mortazavi et al., 2017) In another study by the same authors, a numerical simulation of lactation within a six-generation ductal system was performed with the assumption of the ductal system as a rigid body. They showed that the maximum intra-oral vacuum pressure was not relevant to the highest milk expression from the nipple. (Azarnoosh and Hassanipour, 2020) developed a 3-D computational breast-/mouth model for the FSI (fluid-structure interactive) simulations. This work provided a more realistic and detailed analysis of the biomechanics of breastfeeding including the change of oral pressures, tongue and nipple deformation, as well as the fluid dynamic in the milk ducts.

These simulations of milk flow within the breast considered applied vacuum pressure values from clinical experiments and ignored compressive pressure values (Elad et al., 2014; Mortazavi et al., 2015, 2017). One recently modeled the complex biophysical simulation of breastfeeding with intra-oral vacuum applied and stated that milk extraction from the breast mostly resulted from cycling subatmospheric pressures (Elad et al., 2014), which does not match with what clinical studies have concluded. The latest CFD study from the author's research group (Azarnoosh and Hassanipour, 2020) modeled the infant's oral cavity using the finite element method and applied both compressive pressure and vacuum pressure on the breast to investigate the flow dynamics in the milk ducts with fidelity boundary conditions of infant suckling. Vacuum pressure and tongue movement were found closely related to nipple stress. The biomechanics of milk extraction from the breast by infants continues to elude full understanding. The effect of compressive forces exerted by the infant on the nipple requires further study.

1.4 Review on Clinical Imaging Techniques

The compressive forces on the nipple-breast areola area depend on the infant's latch-on position, vacuum strength, tongue movement, and swallowing coordination. The oral movements of an infant during active suckling in breastfeeding are visualized using various imaging techniques, including 2D ultrasound (Smith et al., 1985, 1988; Geddes et al., 2008a), video-fluoroscopy (Goldfield et al., 2010), direct filming (Eishima, 1991; Niikawa et al., 2012), and 3D ultrasound (Burton et al., 2013).

(Smith et al., 1988) measured the human nipple and tongue deformation during breastfeeding in vivo for the first time. They found that nipple compression may draw milk into the ducts but that the actual stimulus for release is a vacuum phenomenon caused by the rapid enlargement of the oral cavity. (Geddes et al., 2008a) used ultrasound images to study the relationship between the tongue movement, negative vacuum pressure by the infant's mouth, and milk ejection from the breast. They observed that milk expression increases as the intra-oral vacuum pressure increases with the simultaneous downward movement of the tongue. But no rolling peristaltic motion of the tongue was noted. (Goldfield et al., 2010) utilized video-fluoroscopy to measure tongue movements during bottle-feeding in preterm infants reported that suckling is characterized by an anterior-posterior lingual wave that may serve the function of moving liquid to the back of the mouth. (Eishima, 1991) analyzed the suckling behavior of 287 health infants using a milk bottle integrated with a miniature video camera. This study reveals that the suckling behavior contains both peristaltic tongue movement and oral pressures, with peristalsis predominating when milk flow was slow but diminishing with faster flow. They also found that tongue movement is synchronized with jaw movement and sucking pressure automatically adjust to minimize the energy required. Niikawa et al., studied the force of the infant's tongue during active suction using an artificial nipple with a built-in measurement unit and direct filming of infant mouth (Niikawa et al., 2012). The force from the root of the tongue is about two times the force from the tip of the tongue. Research of (Burton et al., 2013) evaluate an infant's tongue movement using 3D ultrasound for the first time. They also revealed a peristaltic infant tongue movement in the majority of infants.

Besides tongue movement and its effect on breast deformation, the coordination of sucking, swallowing and breathing, are studied with various imaging techniques, including clinical observation (Waller, 1936; Woolridge et al., 1980), cineradiography (Weber et al., 1986), in vivo ultrasound with oral vacuum measurement (Geddes et al., 2012; McClellan et al., 2008; Nowak et al., 1994), and video recording using electric breast pumps (Kent et al., 2006).

(Woolridge et al., 1980) studied the effect of two nipple shields (Mexican Hat and Thin Latex) on suckling pattern and milk intake under clinical observations. The suckling pattern was analyzed based on direct filming of the infant's mouth, and milk intake was measured using an electronic weight scale. (Weber et al., 1986) observed healthy neonate's suckling, swallowing, and breathing coordination ultrasonographically during breast- and bottle-feeding. Sucks were found to either occur on their own or in combination with swallow, whereas swallows were found not to occur on their own. (Geddes et al., 2012) used sub-mental 2D ultrasound scans of the infant oral cavity performed simultaneously with the measurement of intra-oral vacuums. (McClellan et al., 2008) found that when intra-oral vacuums and oral cavity dimension change were measured in submental mid-sagittal ultrasound images, infants of mothers with persistent nipple pain experienced stronger peak vacuum (minimum pressure) to the breast and transferred less milk during one monitored feed, despite professional lactation counseling. (Nowak et al., 1994) used real-time ultrasonography to visualize the deformation of an artificial nipple in vivo during infant sucking. They proposed that the ultrasound imaging technique could be used to define which nipple would best be used for an infant with feeding difficulty. (Kent et al., 2006) addressed the importance of vacuum using an electric breast pump. This work demonstrated that maximum milk yield was produced by the use of the mother's maximum comfortable vacuum.

1.5 Review on Experimental Assessment Systems

Some previous experimental studies on the physiology of breastfeeding have measured the intra-oral vacuum pressure and its effect on milk removal (Sandholm, 1968; Weber et al., 1986; Geddes et al., 2008a, 2012). (Sandholm, 1968) compared the amount of milk and the vacuum pressures between multiparae and primiparae mothers and found that multiparae had a higher milk ejection response during suckling and the higher intramammary pressure. (Geddes et al., 2008a) demonstrated that the infant's intra-oral vacuum pressure showed a sinusoidal dynamic and ranges from -10 to -25kpa over the entire feeding period. Flow meters and weight measurement scales are also widely used in the assessment systems to evaluate the effect of infant suckling on milk ejection (Woolridge et al., 1982; Dewey et al., 1984; Kent et al., 1999; Cobo, 1993). (Woolridge et al., 1982) measured instantaneous milk flow with a flow meter in the nipple shield. They found that suck volume was relatively constant but that suckling bursts and pauses varied among infants. This change in suckling pattern resulted in a decrease of average suck volume for a feed (usually about 15 minutes) from 0.14 ml/suck to 0.01 ml/suck. They further referenced that changes in the suckling rate relate to decreased milk availability, infant satiation, or the breast reacting to infant cues depending on whether suck volume decreases. (Dewey et al., 1984) looked at how a decline in milk volume affected composition when breastfeeding after 6 months of age. Milk volume decreased from exclusive breastfeeding at >500 ml/day over 6 feeds to partial weaning at $300 - 500$ ml/day over 4 feeds to weaning at < 300 ml/day over 3 feeds. Significant composition changes were noted during weaning (< 300 ml/day) when compared to exclusive or partial weaning. (Kent et al., 1999) examined breast volume from before conception through weaning. An increase of breast tissue volume (not including milk) from preconception was not related to 24-hr milk production. When breast tissue volume decreased after 6 months, 24-hr milk production remained the same, possibly due to increased efficiency of breast tissue, redistribution of fat stores, or loss of mammary cells. When breast volume returned to pre-conception size at 15 months, significant milk production continued. Infants rarely emptied breasts, so storage capacity responds to the degree of emptying, not infant intake. (Cobo, 1993) compared spontaneous milk ejection with milk ejection in response to infant suckling. Infant suckling produced uncoordinated spurts of contraction waves in mammary ductal pressure for as long as suckling persisted. Spontaneous milk ejection either occurred in a single contraction wave or multiple contraction waves in decreasing amplitudes. Overall findings were that oxytocin release increases progressively during the first 2 months of lactation and spontaneous ejection occurs more frequently when the breast is full and ready for another breastfeeding session (relates to control system of lactation).

While feeding at the breast, infants control the milk expression by adjusting both intra-oral vacuum and oral compression pressure on the nipple-areola complex (Goldfield et al., 2006; Woolridge, 1986). An oscillatory movement from the upper palate (maxilla) and tongue and jaw assembly (mandible) is observed through previous clinical studies (Geddes et al., 2012; Alatalo and Hassanipour, 2020), and usually defined by nipple deformation in the oral cavity with *in vivo* ultrasound images. Weber et al. (Weber et al., 1986) noted the importance of taking into account both oral compression and vacuum pressure. The positive oral pressure, or normal force, exerted by the infant's mouth on the breast has received limited attention in recent decades. Pioneering experiments compared milk ejection rates in breastfeeding mothers using a breast pump that applied only vacuum and a designed pump with both a vacuum and compression (Alekseev et al., 2000). When the compression component was active (pressure amplitude controlled by mother), milk flow began before the first milk reflex was active, and peaks in milk excretion occurred sooner and more frequently. Further experiments noted that when ductal pressure was not at its peak, suction and compression combined resulted in faster milk release from the breast whereas when ductal pressure was at its peak then suction alone removed milk faster (Alekseev and Ilyin, 2016). Out of all the studies mentioned, only one study measured the peak compression value tolerated by mothers, which was 35-40 kPa (Alekseev et al., 2000).

Existing milk pumps (Ramsay et al., 2005; Goldfield et al., 2006) usually focus on extracting the milk with vacuum pressure only. These devices have limitations in mimicking a natural suckling behavior because they neglect the positive compression and tongue movement which has been stated to be important in the breastfeeding process (Alatalo et al., 2020). A review in 1988 (Woolridge and Baum, 1988) summaries that the factors that influence milk flow at a feed are not only from both the mother and her infant but also the specific interaction between them. Hence, it indicates the need for a detailed study of how sucking patterns and reflex milk ejection interact in determining milk transfer and how they change with alternations in the oral dynamics of feeding and with infant appetite.

A series of studies on oral stimulation or oral massage in developing infant suckling skills have used different assessment tools or protocols. (Field et al., 1986) first developed an infant massage therapy (iMT) based on a tactile/kinesthetic protocol specifically for preterm infants. (Fucile et al., 2002) presented a clinical practice of non-nutritive oral massage therapy (NNOMT) for preterm infants. They found that early oral stimulation accelerates the transition of preterm infants to full oral feeding mechanism. (Lau et al., 2012) compared and combined two clinical massage therapy methods for developing preterm infant's oral feeding skills. (Sandholm, 1968) investigated changes in intramammary pressure (about 2 cm into the duct) in response to oxytocin doses administered i.v. or intranasally in comparison to suckling. (Perrella et al., 2020) evaluated a commonly used clinical assessment tool, Preterm Breastfeeding Assessment Tool (PBAT), to determine if it accurately estimates milk transfer during breastfeeding. Using PBAT, clinicians assess infant attachment to the breast and suckling/swallowing. Using test weighing, vacuum tubes, and ultrasound, they found that the PBAT is not a reliable tool for clinical use.

Most of the preliminary experimental work has been focused on exploring the intra-oral vacuum dynamics applied on the breasts by infants during breastfeeding. Although some clinical and experimental studies developed certain devices to stimulate an infant's oral mouthing activities, the effect of positive compression pressure (compression by jaw, tongue, and hard palate) on nipple stress and milk flow dynamics in duct structures are still unknown. Further understanding of the infant's oral dynamics including both vacuum and positive compression allows the researchers and clinicians to evaluate the nursing efficiency and to recognize how the physiological deviations affect breastfeeding effectively.

1.6 Dissertation Outline

During breastfeeding, suckling, swallowing, and breathing are coordinated by the central nervous system in a way that allows the infant to feed continuously without breathing interruptions. These activities of the infant's oral movement that is interfered with human lactating breast represent the most complex neuromuscular function in the human body. Recent clinical research on recording the intra-oral vacuum pressure and the ultrasound image simultaneously provide an insight into understanding the relationship between the vacuum changes and tongue motion (Geddes et al., 2012). However, to the best of the authors' knowledge, there is no attempt in evaluating the effect of both vacuum pressure and compressive forces exerted by the infant on the nipple-areola complex with experimental demonstrations of the physic of breastfeeding.

- **Chapter 2** processes the *in vivo* clinical data from 8 mother-infant dyads to provide a comprehensive knowledge of the physiology of infant suckling during breastfeeding. Although previous studies have successfully measured the oral vacuum pressure and captured the tongue movement using imaging techniques, the positive pressure or compression pressure that an infant would apply on the mother's nipple-areola area is still unknown. Results from the clinical data and ultrasound images show that compression pressure is found to be as strong as the intra-oral vacuum pressure. Positive compression also results in deforming the nipple and extract milk from the breast during natural suckling.

- **Chapter 3** develops a bio-inspired breastfeeding simulator (BIBS) to mimic an oral suckling pattern on the breast for the first time. The experimental protocol can be used as a potential screening tool for developmental disabilities such as the infant's oral abnormalities by varying the operations in the apparatus. In the clinical experiments, we capture the oral peripheral pressure and intra-oral pressure, collect the milk consumption over the entire feeding period for 15 participants. Based on the clinical data and observations, the pressure values, number of sucks, and nipple deformation are all considered as initial input in the apparatus. Automotive actuators and soft robotic motors are designed and developed in the apparatus for studying the breast-infant interaction mechanism during breastfeeding. All components in the apparatus can be modified and customized based on pressure pattern and oral geometry, which assist in evaluating the milk consumption responses of breastfeeding activities from mothers and infants.

- **Chapter 4** integrates the BIBS setup with a graphical user interface (GUI) and multiple feedback controllers. The GUI allows for user-defined inputs to the BIBS, and the proportional–integral–derivative (PID) feedback control provides fast-tracking, robustness, and reliable signal outputs for vacuum pressure, tongue movement, and compressive pressures.

- **Chapter 5** formulates the human milk mimicking fluid (HMMF) with glycerin (Gly), xanthan gum (XG), and sodium iodide (NaI) to mimic the density, kinematic viscosity of the human milk, as well as the refractive index matching in the spherical breast phantom.

- **Chapter 6** studies the flow dynamics in the milk ducts with a particle image velocimetry (PIV) system. The study of the fluid-structure interaction in human lactation has benefits in areas ranging from effective drug delivery to health condition diagnosis. Using the bio-mimicry experimental protocol on BIBS setup and fluorescent particles in HMMF, the flow speed and the flow pattern in the bifurcated milk ducts can be quantitatively measured by the PIV system. The size of the milk ducts is designed based on the specific geometry and the generation of branching for individual applications. Three generations of the milk ducts in the breast phantom allow for the flow analysis of milk in deeper bifurcated generations under a user-defined infant's oral movement.

- **Appendix** provides the LabVIEW configurations in BIBS, MATLAB code for clinical data and image processing, MATLAB simulation on system identification and PID control parameter design, Processing 3 IDE for GUI design and development.

CHAPTER 2

CLINICAL STUDY ON INFANT APPLIED PRESSURES ON BREAST[1]

2.1 Introduction

Understanding the biomechanics of breastfeeding requires capturing both positive and negative pressures exerted by infants on the breast. This clinical experimental work utilizes thin, flexible pressure sensors to capture the positive oral pressures of fifteen mother-infant dyads during breastfeeding while simultaneously measuring vacuum pressures and imaging of the infants' oral cavity movement via ultrasound. Eight sets of data from the participant dyads are complete for analysis.

Methods for de-noise biological signals and evaluating ultrasound images are discussed. Nipple width and length changes are measured to analyze nipple deformation in an infant's mouth during breastfeeding. The results reveal that pressures from the infant's upper palate (maxilla) and lower jaw (mandible) are evenly distributed in an oscillatory pattern corresponding to the vacuum pressure patterns. Variations in nipple dimensions are considerably smaller than variations in either pressure but the ultrasound shows positive pressure dominates structural changes during breastfeeding. Clinical implications for infant-led milk expression and data processing are discussed.

---

[1] © 2018 Reprinted, with permission, from Lin Jiang, Diana L. Alatalo, Donna T. Geddes, and Fatemeh Hassanipour. "A Clinical Experiment on Infant Applied Pressures During Breastfeeding." In American Society of Mechanical Engineers (ASME) International Mechanical Engineering Congress and Exposition, vol. 52026, pp. 41-50.

2.2 Clinical Experimental Study

2.2.1 Data Acquisition

This study was approved by the Internal Review Board at The University of Texas at Dallas (IRB 16-41) and the Human Research Ethics Committee of The University of Western Australia.

Fifteen mother-infant dyads were initially recruited through either the Australian Breastfeeding Association or community health centers in Western Australia. Positive oral pressure and negative vacuum data were successfully obtained from eight dyads, with one dyad providing two sets of data on separate days. The ages of infants ranged from 6 days to 21 months. All infants were successfully breastfed with the use of a nipple shield.

2.2.2 Ultrasound Image Processing and Nipple Deformation

The ultrasound images and vacuum pressure were obtained by an endocavity convex transducer (Acuson, XP10, Siemens, Mountain View, California, USA) placed under infant chin and a silicon vacuum tube (650×4mm) connected to a disposable pressure transducer (Cobe Laboratories, Frenchs Forest, NSW2086, Australia) as outlined by Geddes et al. (Geddes et al., 2008a), except the supply line for the pressure transducer was filled with water instead of mother's expressed breast milk and placed alongside the nipple on top of the nipple shield, when in use. Raw data of Infant 6's intra-oral pressure is given in Figure 2.1 and shows a periodic pattern during the entire nursing period. The ultrasound imaging is used to determine periods of nutritive and non-nutritive suckling, as well as to visualize the changes in the nipple dimensions from infant pressures. Figure 2.2a shows a single image with the oral structure marked in the image from ultrasound videos of Infant #6 during his clinical experiment.

All ultrasound movie analyses were performed using MATLAB for observing the nipple dimension changes inside infants' mouths during breastfeeding. The original ultrasound

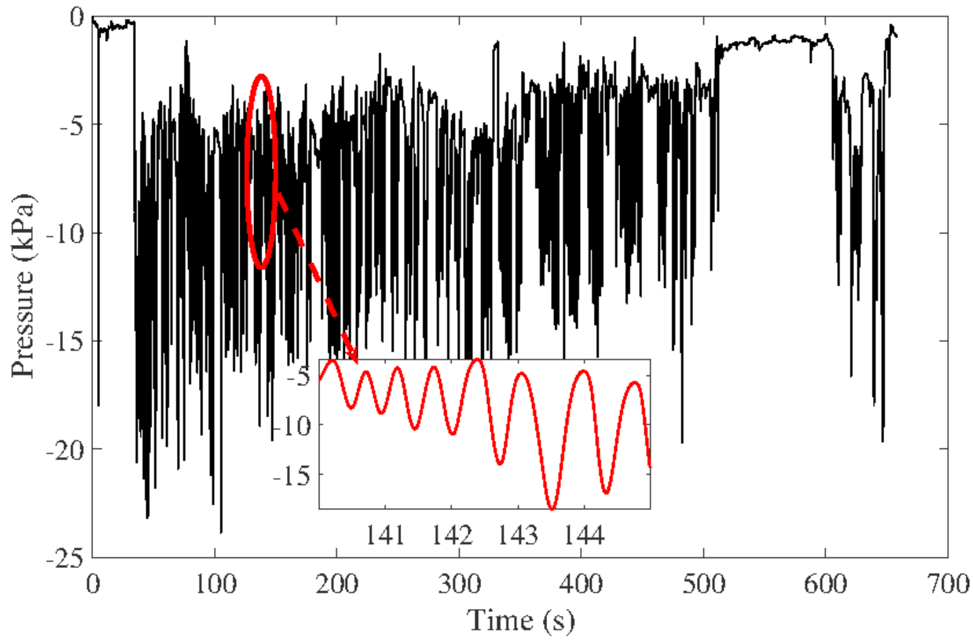

Figure 2.1: Raw intra-oral pressure data for Infant #6

images extracted from the ultrasound video clips (Figure 2.2b) show a large space of speckle-noise that may contain information unnecessary information for evaluation. Although the ultrasound imaging equipment already has a filter embedded in the recording system, the biomedical images during breastfeeding clinical experiments contain tremendous uncertainties and variables. Taking that into account, a local statistic filter called Wiener filter (Wiener et al., 1949) is applied on the original images to deduct the signal-to-noise ratio. However, after smoothing the images, the contrast of the images is decreasing due to the signal elimination by the Wiener filter. To solve this, imaging sharpening is applied on the filtered image to better display the outlines in Ultrasound images.

Calibration is made with a self-decided baseline in images. A manual designation of the approximate edge on each frame was used to outline the boundaries for the nipple, the infant's hard palate, and tongue, pictured in Figure 2.2a. A self-programmed measurement system was achieved in MATLAB to get average dimensions to change the nipple width and length with the tongue moving up and tongue moving down. Figure 2.3c shows a schematic

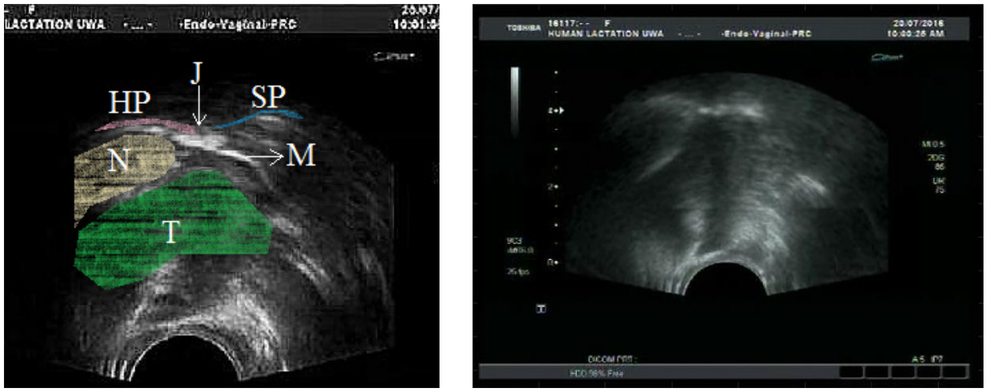

(a) (b)

Figure 2.2: (a) Ultrasound imaging of Infant #6's oral cavity during breastfeeding visualizes the structure of hard palate (HP), soft palate (SP), hard-soft juction part (J), nipple (N), and tongue (T); (b) Original ultrasound image from Infant# 6

description of nipple dimension change measurement. Nipple Height at its maximum value (NH_{max}) and Nipple Length at its minimum value (NH_{min}) are chosen in ultrasound imaging as a start point when the tongue is at the lowest position during one effective nursing cycle. The amount of deformation is recorded when nipple length reaches its maximum length and nipple height is at its minimum height observed in ultrasound images. Average nipple dimension changes plus standard deviations are derived from multiple NS suckling cycles for statistic evaluation purposes.

2.2.3 Pressure Measurements and Data Analysis

Two flexible resistance pressure sensor strips 9801 and 9830 with the I-Scan System (Tekscan Inc. Boston, MA, USA) are attached to the breast with tape[2] and covered with a breast shield to minimize moisture exposure to the strips and prevent the strips from entering the mouth of the infant (see Figure 2.4). Each sensor has been cut and edges smoothed to prevent the sensor edge from cutting into the mother's skin. For infants who are regularly breastfed

[2]The tape is placed away from the areola.

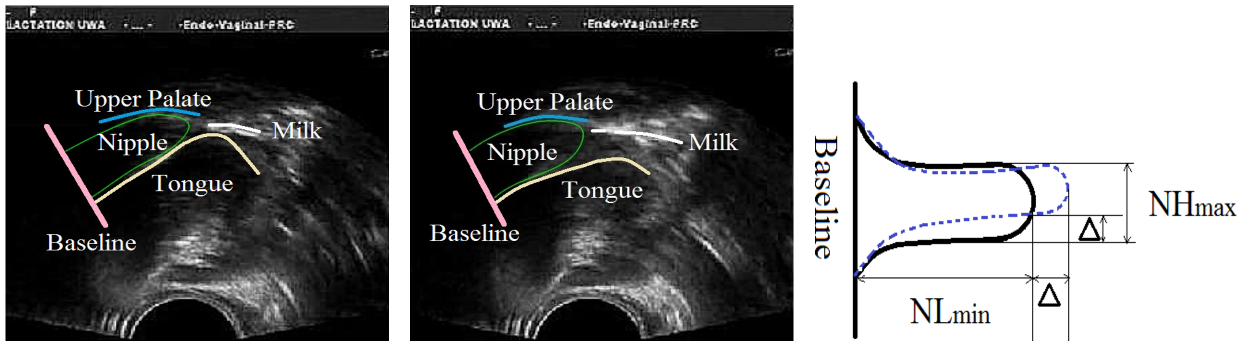

(a) (b) (c)

Figure 2.3: (a) Ultrasound image for Infant #6 during sucking with tongue moving up, (b) with tongue moving down, and (c) Schematic description of nipple dimension measurement in ultrasound imaging

without a nipple shield, the tip of the shield is cut off to allow the nipple to move normally within the oral cavity. Since the width of the strips is too wide to comfortably fit around the nipple under a shield, the strips are placed along the top and bottom of the areola as close to the base of the nipple as possible. Initial experiments attempted different layouts (see Figure 2.4) using Sensor 9830 to approximate pressure ranges. The T-type and V-type sensor layouts were not considered as the sensor strips distracted the infant's attention and interfered greatly with infants' oral mechanics. Additionally, the data from these initial layouts with those dyads are incomplete and not included in these findings. On the final layout, the strips are oriented to approximate the location of the upper and lower gums and lips of the infant while suckling as seen in Figure 2.5b. The position of sensors during experiments can be seen in Figure 2.4c, where U1-U7 represents the displacements of the sensor cells that were under the maxilla of infants while L1-L7 represents the sensors cells placed under the infant's mandible. Since the amount of areola that each infant takes into the mouth differs, the exact location of sensels varies as seen in Figure 2.5a.

The maximum pressures are 69 kPa and 34 kPa for Sensors 9830 and 9801, respectively. Sensors with lower pressure ranges are more sensitive and will be more inclined to produce readings induced by the curvature of the sensor (Tekscan^{TM}, 2017). Once the final layout

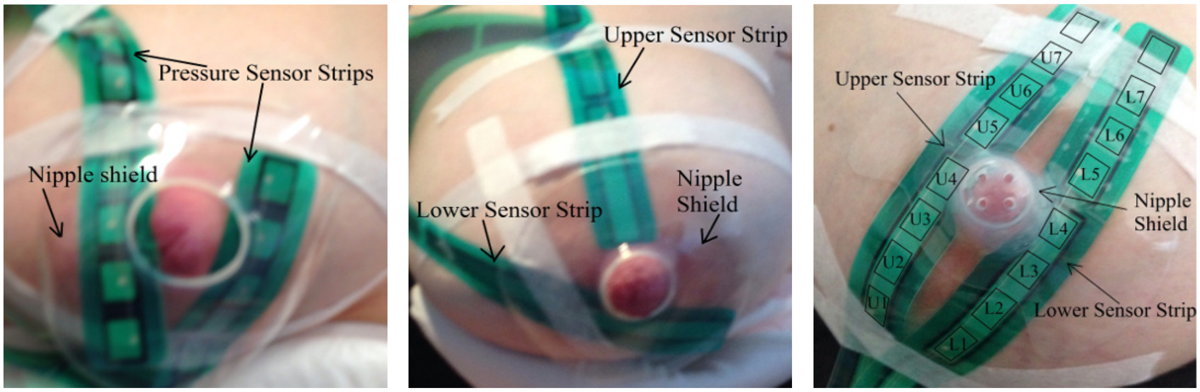

(a) (b) (c)

Figure 2.4: Multiple layouts for peripheral pressure sensor strips on mothers: (a) T-type placement with nipple shield tip cut off, (b) V-type placement with nipple shield tip cut off, (c) Parallel placement with entire nipple shield.

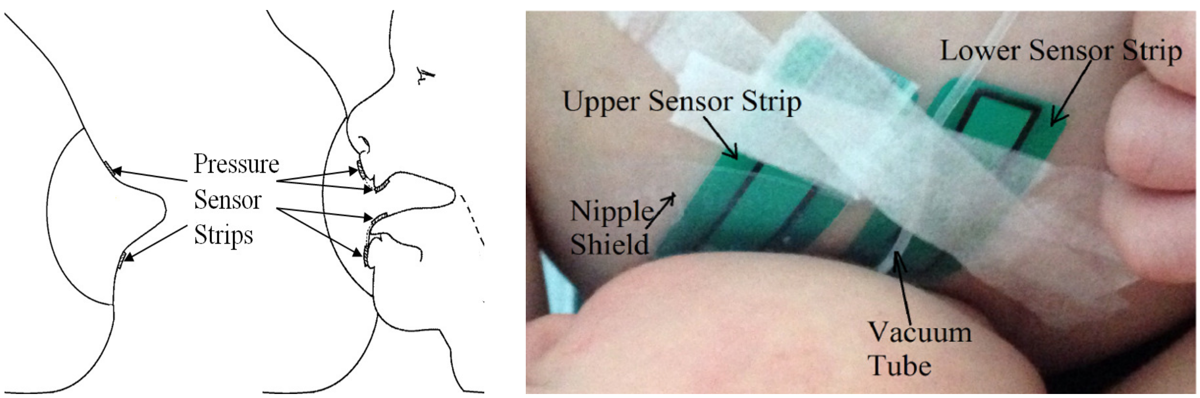

(a) (b)

Figure 2.5: a) Pressure sensor strips position during experimentation, and b) Tekscan sensor strip clinical experiment setup for Infant #6

of sensor strips is determined, Sensor 9801 with lower sensitivity captures data for the first round of experiments, then validated with the higher sensitivity set, Sensor 9830. As the curvature of the surface increases, the level of accuracy changes. The sensors are zeroed and calibrated according to manufacturer guidelines using the I-Scan built-in multi-point calibration algorithm. Examination of individual sensel cells reveals that one sensel displays a constant value, likely caused by wrinkling, crimping, or folding of the individual sensel that results in the high-pressure reading (Tekscan^{TM}, 2017). Before data processing, those sensel values are removed to keep the pattern of the original data. Figure 2.6 elaborates the raw data from each sensel cell of Sensor 9830 used by Infant #6 in this clinical experiment. Data from each sensel varies significantly with their positions. Sensels placed right under the infants' mouth have more contact space with the infant's maxilla and mandible. However, not all sensels are placed exactly under the infant's mouth during the whole nursing period due to the pressure strip curvature and infant's feeding position change. To demonstrate the average pressure applied on mum's breast, average raw values of all sensels are calculated to analyze the total pressure applied on the breast by the infant's oral cavity with different sensor strips.

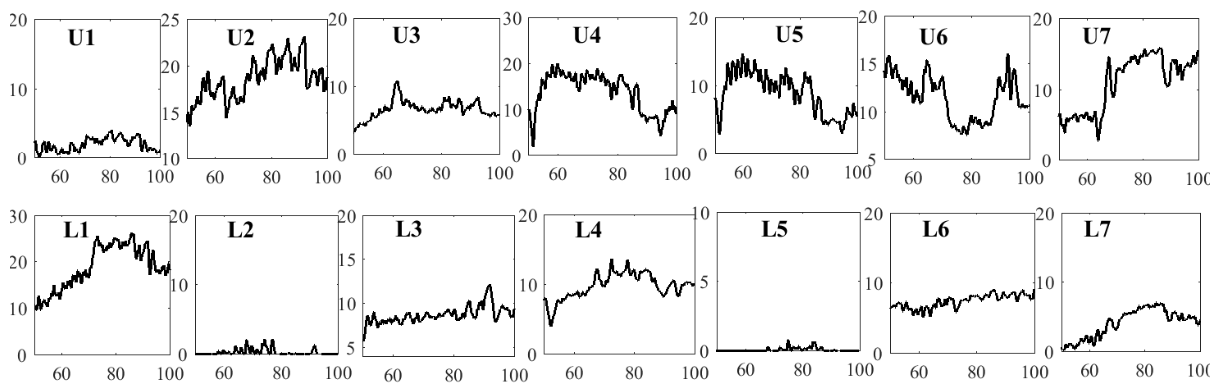

Figure 2.6: Raw peripheral oral pressure data of Infant #6 from Sensor 9830

Two different sensor systems are used to measure both the intra-oral vacuum and the peripheral oral pressures, thus time-line matching for relating both sets of pressure data with infant's suckling during breastfeeding is essential in the data analysis part. Each sensor module includes a sensor responsive to time recording, as well as data storing for information. Using the ultrasound to visualize milk ejection, the dynamic pattern of infants' peripheral oral pressures are correlated to the intra-oral vacuum pressures for six infants to eliminate the experimental time gaps. Files of raw sensor readings are downloaded from software specific for each measuring system and imported into MATLAB with user-defined programs. Raw sensor data shows an arbitrary range of white noise and some unpredictable outlines that needed to be eliminated before any analysis. A post-processing filter-based polynomial de-noising algorithm known as BUTTERWORTH with a MATLAB command BUTTER (MATLAB, 2010) are applied for the overlapped experimental and the noise signals.

2.3 Results

In ultrasound movies, cycling motion of infant's anterior tongue and palate was visualized. From Figures 2.3a and 2.3b, the nipple was observably elongated and compressed when infants moved their tongue up versus when they moved their tongue down. Average dimension changes (Δ) in elongation of Nipple Height (NH) and Nipple Length (NL) for all NS cycles with observable tongue up and tongue down are measured and presented in Table 2.1 for all mother and infant dyads. The elongation of nipple length ranges from 2.51 mm to 3.66 mm, and the compression of the nipple in the height ranges from 1.26 mm to 1.91 mm. Nipple dimension change in length is approximately twice of height change.

During clinical experiments with mother and infant dyads, we observe multiple resting times of infants during nursing. Pressure values are relatively smoothier and lower during resting times than suckling time. With the evidence of multiple resting times from infants during breastfeeding, time frame matching of different recording systems from multiple sensor modules is resolved. Optimal results of pressure data can be obtained based on this time-matching method. Ignoring time periods when the infants are not actively suckling, the average pressure values from both maxilla sensor strip and mandible sensor strip plus standard deviation are calculated for all infants and are reported in Table 2.1.

All infants exhibited an oscillatory pattern for positive oral pressures for both maxilla and mandible. The oscillatory pattern of pressure under the maxilla has not been previously

Table 2.1: Clinical experiment data on nipple measurement and pressure changes from the Infant's oral cavity of participant dyads

Dyad No.	Infant age	NH (mm) Δ±SD	NL (mm) Δ±SD	Vacuum(kPa) Max±SD	Maxilla(kPa) Mean±SD	Mandible(kPa) Mean±SD
#1	4.5 month	1.45±0.53	2.11±0.47	-11.53±0.85	2.14±2.06	1.27±1.62
#2	10 weeks	1.91±0.53	2.71±0.69	-14.43±0.35	0.18±0.09	1.86±3.35
#3	4.5 month	1.55±0.32	2.51±0.62	-7.14±0.13	2.70±4.18	0.36±0.26
#4	6 days	1.64±0.50	3.03±0.98	-13.79±1.99	1.01±0.60	0.84±0.28
#5	21 month	Ultrasound Not Captured			0.37±0.33	1.57±2.16
#6	4 weeks	1.80±0.37	3.22±0.28	-10.04±0.34	7.92±1.81	5.01±2.54
#7a	10 weeks	1.47±0.35	3.06±0.27	-20.32±1.78	0.96±0.31	1.03±0.24
#7b	11 weeks	1.26±0.19	3.66±0.49	-19.56±1.33	2.37±0.27	1.24±0.92
#8	3.5 weeks	1.32±0.73	2.83±0.37	-11.09±0.57	1.40±0.82	1.54±0.95

reported and would not be obvious to external observers since the maxilla does not appear to move after forming a teat. Rather movement of the mandible is generally evaluated for correct suckling patterns. While the mean pressure values were below 3 kPa for all infants except Infant #3, the maximum pressure values showed greater variations. The mean positive pressure for all infants combined was 2.78±2.62 kPa for maxilla and 1.67±1.68 kPa for the mandible. Peak pressure values averaged 7.88±6.59 kPa and 5.30±3.63 kPa for maxilla and mandible, respectively. The higher mean applied pressure exerted by Infant #3 likely was from sensor placement. As seen in Figure 2.4c, the sensor strips were placed close to the base of the nipple ($\leq 5\ mm$) but with enough distance to prevent the edges from rubbing against the nipple base and causing damage to the skin. The actual placement of the sensor during suckling varied since the amount of areola drawn into the infant's mouth differed for each dyad. As a result, some sensels may have captured lip or chin pressure values instead of gum pressures. Variations in denoised pressure values on individual sensels on sensor strips under the maxilla and mandible for Infant #3 are shown in Figure 2.7. However, since a large portion of the areola must be drawn into the oral cavity for the nipple

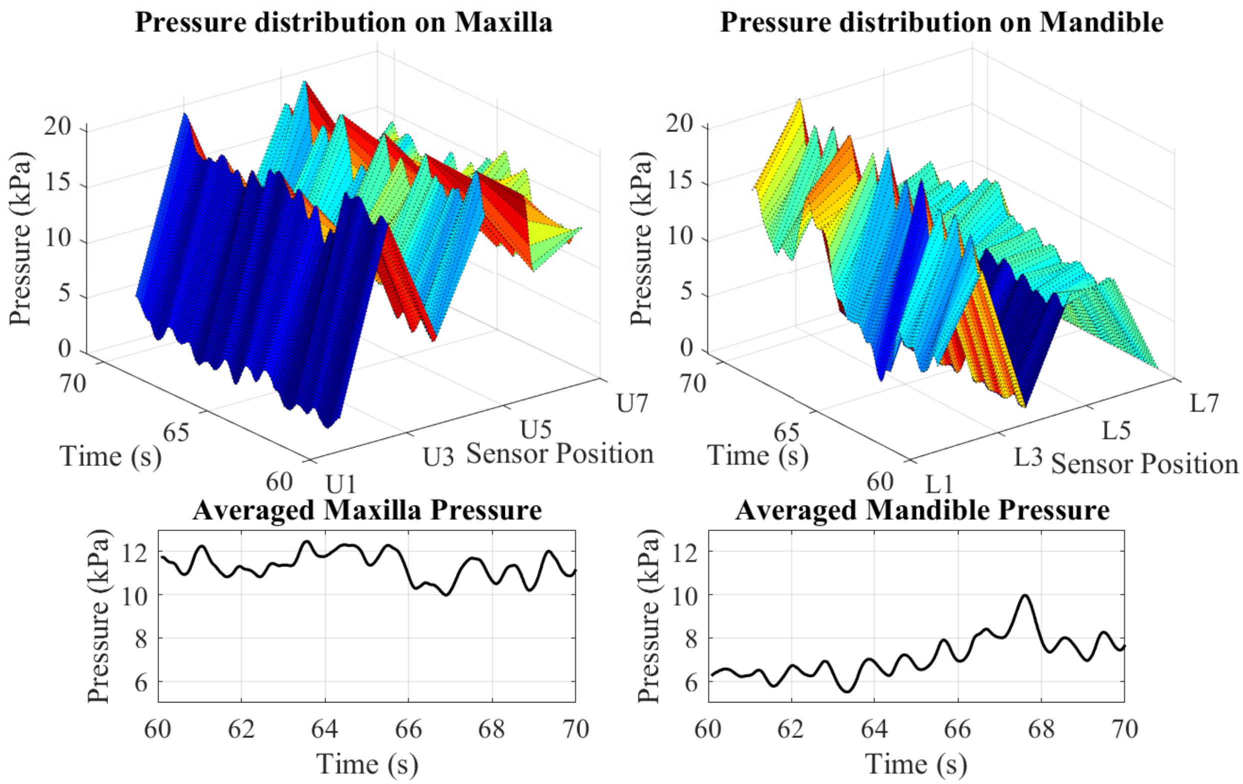

Figure 2.7: Denoised pressure distribution along the sensor position (upper) and average for maxilla pressure and mandible pressure of Infant #3 (lower) with milk transfer.

to reach the hard-soft palate junction, it is more likely that the pressure values are from the maxilla or mandible.

The denoised peripheral oral pressure sensor data for Infant 6 gives smooth sinusoidal signals, as well as, keeps the original peaks of the waves as shown in Figure 2.8. The peripheral oral pressure demonstrates a rhythmic, oscillatory pattern with pressure changes for both the maxilla and mandible. A closer look at 10 seconds of nutritive suckling for Infant 6 (seen in Figure 2.8) provides new insights into breastfeeding biomechanics with implications for clinical application. During this period, the total pressure of 11.23 kPa is applied on the breast from the maxilla and 5.65 kPa is from the mandible motion of the infant during breastfeeding. The deviation in maxilla movement is 1.81 kPa compared to the deviation in mandible movement at 2.94 kPa which indicates the maxilla moves steadier than the mandible during these 10 seconds of nutritive suckling. The pattern of maxilla and mandible pressures match the vacuum peaks during these suck cycles. When the vacuum experiences a local minimum (around -20 kPa) the maxilla and mandible pressures reach a local minimum value. This phenomenon matches observations in the ultrasound images where the infant's mandible drops to create a vacuum. Thus positive pressure on all sides of the areola is used by infants to control milk extraction and this bilateral pressure application should be observed by clinicians during normal breastfeeding.

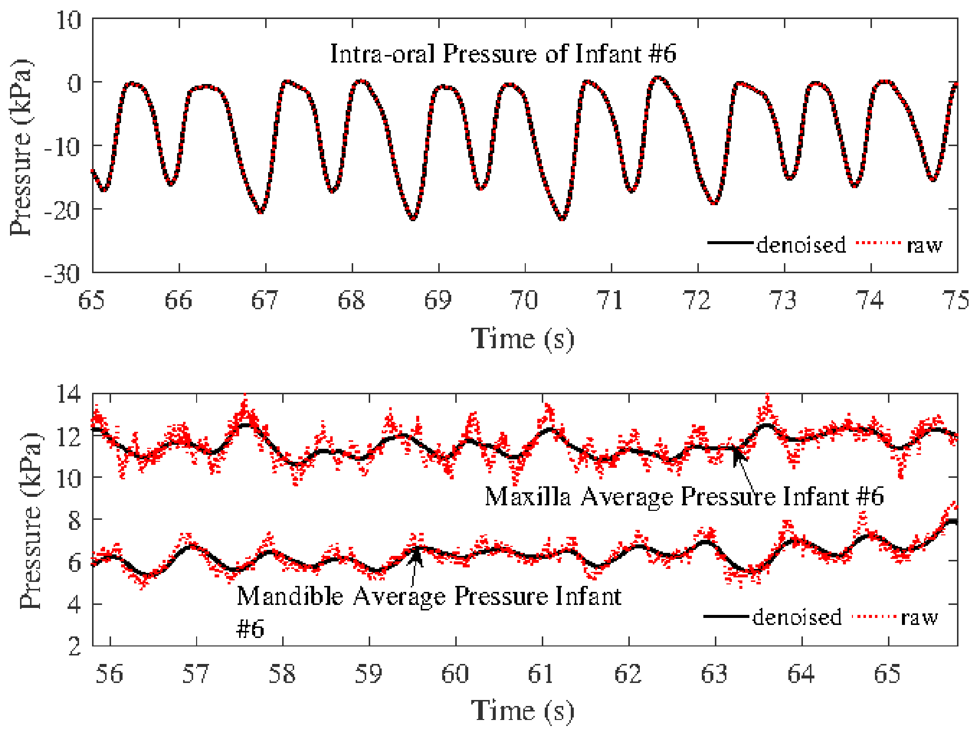

Figure 2.8: Intra-oral pressure and peripheral oral pressure during 10 seconds nutritive breastfeeding of Infant#6

2.4 Discussion

The use of positive and negative pressures in combination are known to positively affect milk flow (Morton et al., 2009; Alekseev et al., 1998), yet the amount of pressure exerted on the nipple-areola complex by the infant is missing from all previous studies. By utilizing two separate measuring systems, this clinical experimental work successfully captures intra-oral vacuum pressure simultaneously with positive peripheral oral pressure applied on the breast by an infant's maxilla and mandible while breastfeeding. By using the well established relationship between oral movements and vacuum pressure, time matching between the two systems is possible. The resulting data provide new insight into the peripheral oral pressure exerted by infants during breastfeeding. The raw data demonstrates an oscillatory pattern with pressure changes for both maxilla and mandible. The distribution of pressure from the maxilla on the breast at times exceeds that of pressure from the mandible. So while the mandible is the only moving joint during suckling (Woolridge, 1986), the pressure distribution on the breast is distributed around the areola. The second order butterworth filter sufficiently removed unwanted noise originating from the measuring system leaving a smooth sinusoidal pattern that matches the sinusoidal vacuum pressure pattern.

Image contrast is essential for distinguishing between anatomical markers in the infant's oral cavity. The use of a Wiener filter smooths the spaces in ultrasound imaging adaptively while the image sharpening enhances the contrast and thus allows for differentiating between nipple, palates, and tongue. From these images, the dominant pressure that results in nipple deformation is identified as compression since images show that when the infant is creating the vacuum, its oral cavity opens and the nipple expands in height and shortens in length. No correlation between variations in nipple dimensions and variations in either pressure is found. Periods of nutritive suckling are identified by milk sprays in the infant's mouth.

Peripheral oral pressure and intra-oral pressure vary considerably among mother-infant dyads. The oscillatory motion of the maxilla with pressure values that can exceed mandible pressures indicates a more active role in milk extraction beyond anchoring of mouth to the breast. Among all the mother and infant dyads, Infant 7 applies the strongest vacuum load on the breast and his mother verbally complained of nipple pain. During Infant 7's first session he initially nursed with a sensor strip and exerted peripheral pressures of 1.0

kPa for both maxilla and mandible with a strong vacuum pressure of 8.5 kPa. Infant 7's second session began with him nursing without the sensor strip. His vacuum pressure was slightly stronger without the sensor strip, 11.5 kPa versus 10.2 kPa, than with the sensor strip. The oral peripheral pressure is stronger than during the first session at 2.4 kPa for maxilla and 1.2 kPa for the mandible. A closer look at Infant 7's mandible pressure over time shows a step up that is not attributed to any sensel saturation. Comparison of peripheral pressures and vacuum pressure during that step up reveals that Infant 7 created a vacuum that he did not lose for over 2 minutes. It has been documented that infants adjust the frequency of their suckling based on milk flow (Woolridge, 1986), so likely infants adjust their applied peripheral pressures as well. This theory is supported by the periodic spikes in the pressure readings (see Figure 2.8). These spikes may originate from the re-positioning of infants (either by mother or infant). However, these spikes may also be from a deliberate action of the infant to control milk extraction. In all the studies that investigated the use of positive and negative pressures for milk extraction, the focus of the studies was on mother-controlled milk extraction using hand or pump expression. Breastfeeding is an infant-led process where the infant controls milk extraction. Thus infants apply pressures to control expression in response to appetite and suck-swallow-breathe requirements. So while a mother-led control system will maximize expression by utilizing pressure values at the maximum of their tolerances, an infant-led control system may operate at lower pressure values with increases as needed to meet the infant's needs. These fundamental differences in control systems are important considerations for clinical investigations in milk extraction.

2.5 Conclusion

Infant-led breastfeeding utilizes both positive compression and negative vacuum pressure to extract milk from the breast. Previous studies on infant feeding biomechanics lacked positive pressure values as applied by infants. This study investigated the two major pressures exerted by infants during breastfeeding and examined the effect of these pressures on the nipple during suckling using a novel method to measure *in vivo* oral pressure forces. Multiple challenges in studies such as this one exist for engineers and clinicians. Using clinical observations, time matching between two separate systems allowed for new insights into the biomechanics of breastfeeding. Data processing, filtering, and image sharpening provided a realistic picture of infant-led milk extraction. Tekscan^{TM} pressure mapping sensors captured the peripheral oral pressure applied to the areola by infants with their maxilla and mandible while intra-oral vacuum pressure and ultrasound video clips were captured and recorded simultaneously. The nipple during continuous suckling deforms primarily by positive pressure applied by the infants to the circumference of the nipple. The maxilla and mandible peripheral pressures varied in an oscillatory pattern that corresponded to the oscillatory pattern of the intra-oral vacuum pressure. Infant's applied pressure on mother's breast was distributed around the areola and varied for both maxilla and mandible. This clinical experiment provides a powerful and practical tool for clinicians and researchers to monitor multiple assessments in biomechanical processes, including sensor system timeframe matching, imaging modality choosing and processing, and data de-noising. These preliminary findings provide insight into the amount of positive pressure the areola experiences during breastfeeding. Differences between mother-led control of milk expression and infant-led control are highlighted and show that infants do not always apply maximum pressures while breastfeeding. Additional work is underway to capture the pressure exerted on the nipple by the tongue.

Certain aspects and limitations of the study methods should be noted as these factors may influence the ability to compare results with future works. The age range of infants was broad so the maturity of latch on and suckling may evolve with age. The crinkling sound of the Tekscan strips that were not in use and the number of study personnel in the room distracted some older infants and led to them turning their heads frequently to find the source of noise and conversations. Although pressure measurements were eliminated during periods when suckling was not occurring, infants can often maintain suckling while turning their heads if the range is not great enough to cause loss of vacuum. Lastly, the use of a nipple shield adds another layer of material between the infant's mouth and breast tissue. Although this layer is thin, medical-grade silicone could have a damping effect (Carl Ward and Timothy Perry, 1981) on the infant applied force.

CHAPTER 3

BIO-INSPIRED BREASTFEEDING SIMULATOR (BIBS): A TOOL FOR STUDYING THE INFANT FEEDING MECHANISM[1]

3.1 Introduction

In this chapter, we introduce a bio-inspired breastfeeding simulator (BIBS), an experimental apparatus that mimics the oral suckling behavior of infants and breast milk extraction from the nipple during natural lactation. Unlike previous assessment tools for analyzing the oral suckling pattern which have used rigid sensing device (Niikawa et al., 2012) or applied vacuum-only stimuli (Barlow, 2009), this work develops an autonomous apparatus that includes all oral movements, such as suction, compression and swallowing from an infant's suckling, and analyzes the effect of oral behaviors on the lactating breast. The fully-developed breastfeeding simulator provides a powerful tool for understanding the biomechanics of breastfeeding and a foundation for future breastfeeding device development.

BIBS is configured with an individually controllable structure of oral dynamics and programmable software and has the ability to operate the system with a wide-ranging vacuum frequency, as well as evaluating and predicting the breastfeeding process objectively. The construction of the apparatus follows a clinical study by the authors to collect measurements of natural intra-oral vacuum pressure, the movements of the infant's jaw, tongue, and upper palate, as well as nipple deformation and compression on the breast areola. A flexible, transparent, and tissue-like breast phantom with a bifurcated milk duct structure is designed and developed to work as the lactating human breast model. Bifurcated ducts are connected with a four-outlet manifold under a reservoir filled with human milk-mimicking liquid. This work improves the flexibility and elasticity of the breast phantom with a combination of two materials: one for breast skin and the other for glandular tissue. To the best of the authors' knowledge, this is the first known attempt to model a lactating human breast with three bifurcated ductal structures and the optical clearness for flow visualization. A vacuum pump compiled with a sinusoidal vacuum profile of the infant is developed to create the infant's suction during breastfeeding. Two linear actuators mimic the infant's maxilla (upper palate) and mandible (lower jaw) movements. A motor-driven gear rotates to duplicate the infant's peristaltic tongue motion. The tongue gear is made of a four-tooth gear-shaped silicone model to represent the infant's tongue. Two materials with different stiffness are used to differentiate the flexibility of the tongue tip and the tongue root. The reservoir filled with human milk-mimicking liquid is connected to the ductal structure inlets with an array of manifolds to simulate the milk flow through the ducts. Piezoelectric sensors and a CCD (charge-coupled device) camera are used to record and measure *in vitro* dynamics of the apparatus. All movements such as suckling, swallowing, and squeezing are coordinated by an open-loop control system that allows for modifying infants' oral patterns. Finally, oral pressure and nipple deformation captured by BIBS are validated with those from *in vivo* clinical experiments.

3.1.1 Experimental Setup, Methodology, Materials, Design & Construction

A clinical experiment was conducted to capture the movement of the infant oral cavity and track the nipple deformation via ultrasound imaging (Alatalo et al., 2020) as mentioned earlier in Chapter 2. Rhythmic patterns were found with an average suckling frequency of approximately 1-2 cycles/s from 6 infants. The applied pressure on the breast had an average vacuum range from -12 to 0 kPa, and an average positive pressure between 2-8 kPa, respectively. As discussed in Chapter 2, vacuum pressure and compression pressure both contribute to the milk extraction out of the ducts in the nipple. In this study, a bio-inspired breastfeeding simulator (BIBS) that can mimic an infant's coordinated control of oral vacuum and oral compression is developed, which can serve as a practical tool to understand the biomechanics of breastfeeding *in vitro*.

To imitate the infant's oral behavior involving coordinated vacuum and compression pressure on the breast, different types of simulators were designed and applied in this apparatus. All components are inspired by the clinical observation of natural breastfeeding. The schematic configuration of the BIBS apparatus is shown in Figure 3.1. The apparatus consists of the following:

- A transparent and flexible breast phantom with bifurcated ductal structure
- A vacuum pump assembly that generates rhythmic intra-oral pressure
- Two linear actuators representing the infant's upper palate and lower jaw motion
- A flexible silicone gear-shaped motor mimicking the tongue motion
- A reservoir filled with milk-mimicking liquid that represents the breast milk and assists the flow visualization in the apparatus
- A set of pressure sensors for measuring the vacuum and compression force
- A CCD camera for capturing the breast-infant interaction
- Drivers and control systems for commanding the inputs and recording the outputs components.

Transparent Tissue Mimicking Breast Phantom

An optically clear, flexible, and soft breast phantom has been designed to mimic a human breast in the setup as shown in Figure 3.2a. The breast phantom contains breast skin, transparent filling gel, and the ductal structure.

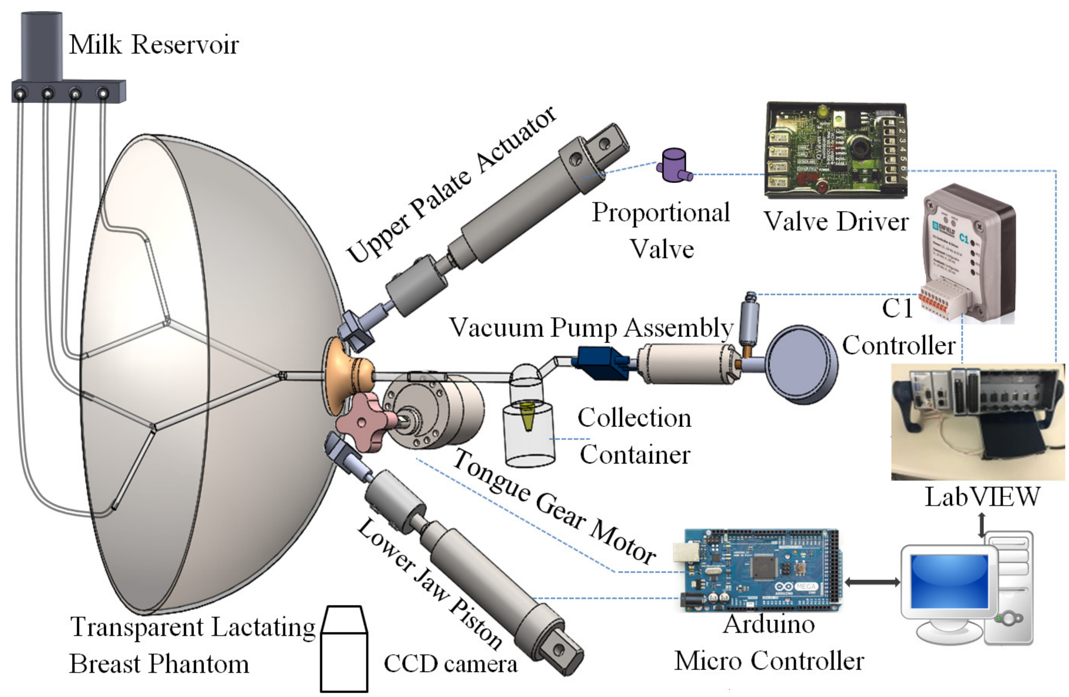

Figure 3.1: A 3D design sketch of the Bio-inspired Breastfeeding Simulator (BIBS).

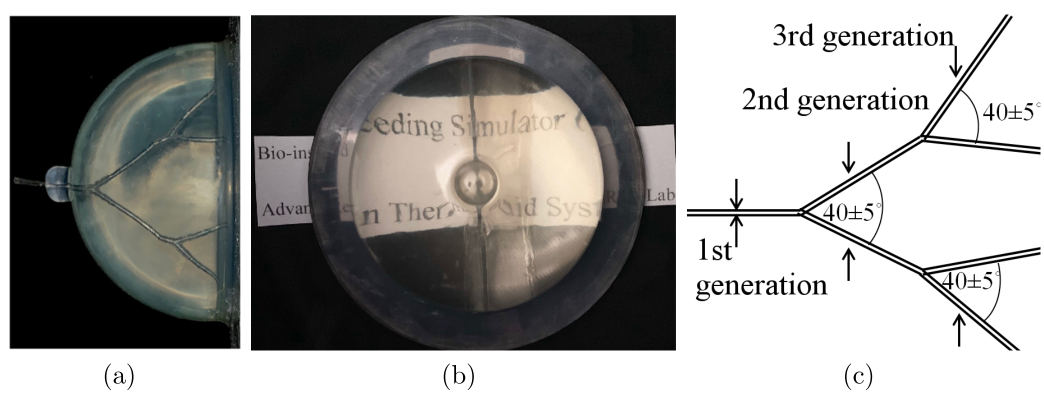

Figure 3.2: A lactating breast phantom (a), which is transparent for visualization (b), with three generation symmetric ductal structure (c).

The dimensions of nipple, areola and breast were measured from the clinical study with methods reported in (Alatalo et al., 2020). Average dimension from clinical work has been utilized for the breast phantom geometry and shown in Table 3.1.

The thin and flexible breast shell is built with Polydimethylsiloxane (PDMS) (Sylgard 184, Dow Corning, Midland, MI, USA), which has been well accepted as an optimal repre-

Table 3.1: *In vivo* versus *in vitro* dimensions of a lactating human breast.

Contents	*In vivo* (Alatalo et al., 2020) (mm)	*In vitro* (mm)
Nipple width	14.44-15.09	15
Nipple length	10.70-13.79	12
Areola width	3.02-6.75	5.0
Breast width	116.70-166.05	120
Breast height	48.12-71.34	60
Breast skin thickness	1.44-2.05 (Berggren et al., 2018)	2.0

sentative for human skin and vascular mimicking (McNamara et al., 2009), to imitate the breast skin with a non-uniform thickness. The fabrication process of the skin consists of three major steps: 1) designing the 3D model in SolidWorks, 2) creating the master mold, and 3) casting the mold with a solution of room temperature vulcanized PDMS. The skin (shell) of the breast phantom model has a 2mm thickness based on the reported numbers from clinical studies (Berggren et al., 2018). The thickness of the nipple part is chosen at 1.5mm to maximize the softness and flexibility. A transparent water-based gel (Zerdine gel, CIRS, Norfolk, VA, USA), which is widely used as the closest mimic of glandular tissue in breast phantom for Young's moduli at 20-40 kPa (Cannon et al., 2011), is filled into the space between breast shell and the supporting base plate to mimic the softness of a human breast. The optical clearness of the breast and ducts (as shown in Figure 3.2b) allows us to visualize milk flow in bifurcated ducts during experiments.

Table 3.2: Duct dimensions in the optical clear lactating breast

Generation	Length (mm)	ID $\pm$ SD (mm)	Thickness $\pm$ SD (mm)
First	35.75	2.00 ± 0.12	0.50 ± 0.15
Second	30.15	1.60 ± 0.08	0.30 ± 0.10
Third	25.04	1.20 ± 0.10	0.20 ± 0.08

To simplify the geometry of milk ducts for the physical setup, symmetric bifurcation with three generations of branching (as shown in Figure 3.2c) is used. The length and diameter of the bifurcated ducts are based on the model reported in (Mortazavi et al., 2015). The detailed dimension of the ductal system and their accuracy are shown in Table 3.2. The angle between the smaller ducts is approximately $40° \pm 5°$ degrees. Flexible silicone tubing (MasterFlex, Cole-Parmer, USA) with 1.2mm, 1.6mm, and 2 mm inner diameter (ID) are used to mimic the ductal structure in a lactating breast.

Vacuum Pump Assembly

The assembly includes a pneumatic proportional valve for creating vacuum pressure, a LabVIEW signal generator, and a tube that connects the vacuum pump to the nipple-areola surface. The vacuum generator, as shown in Figure 3.3, contains a proportional valve (ES-V15, Enfield Technologies, USA) with a built-in valve driver, a controller, an air tank (AVT 12-1, Clippard, USA), a manual switch, a vacuum pump, a pressure gauge and a pressure transducer (PX209, Omega, USA). The inlet of the proportional valve was connected to the external air supply. One of the outlets of the proportional valve was connected to a vacuum pump (Model No.#6909, with 3 cu^3/min capacity, FJC, Mooresville, NC, USA) controlled by a voltage command from the proportional valve until obtaining the required vacuum pressure. The air tank was attached to the other end of the proportional valve to add capacitance to the system for stability. A pressure gauge was added to monitor the pressure change inside the air tank. The pressure transducer detected the vacuum pressure inside the tank and converts the value to a voltage signal feedback to the programmable controller (C1, Enfield Technologies, USA).

The vacuum pressure profile was based on the clinical data collection (Alatalo et al., 2020) of Infant #3, which contained arbitrary pressure frequency and strength during breastfeeding. Figure 3.4 demonstrates the circuit diagram for creating arbitrary periodic vacuum signals using the proportional valve, LabVIEW setup, vacuum pump transducer, and controller. Sinusoidal waves, frequency, and vacuum strength varied during the entire breastfeeding session as shown in Figure 3.5a. The vacuum pressure profile was preloaded in a high

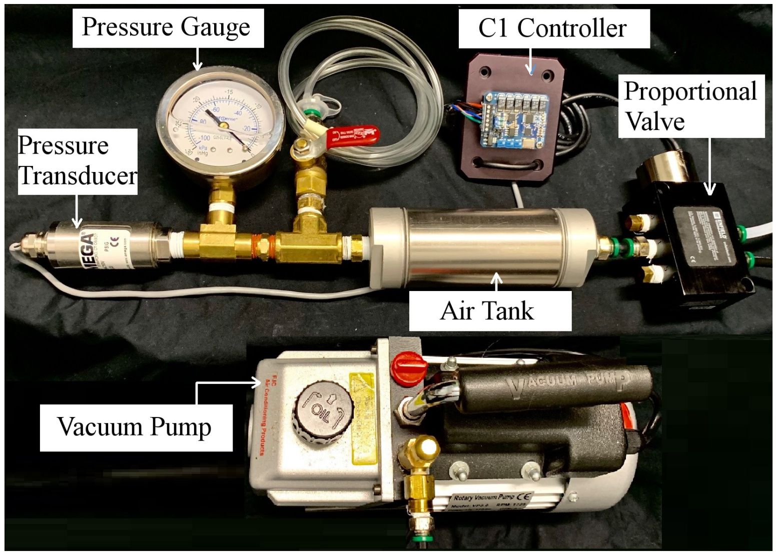

Figure 3.3: The assembly for creating sinusoidal vacuum pressure.

logical programmable LabVIEW Real-Time hardware (National Instrument (NI) Compact RIO 9074) for data generation. PID (proportional-–integral-–derivative) control algorithm was embedded in LabVIEW to control the signal stability. Generated command voltage was the input signal to the proportional valve to control the vacuum pump. Detailed LabVIEW algorithm and implemented diagram is presented in Appendix Part I. Real-time sensor feedback from the transducer and the LabVIEW command signal profile were compared and shown in Figure 3.5b. Signal uncertainty was within ±1%.

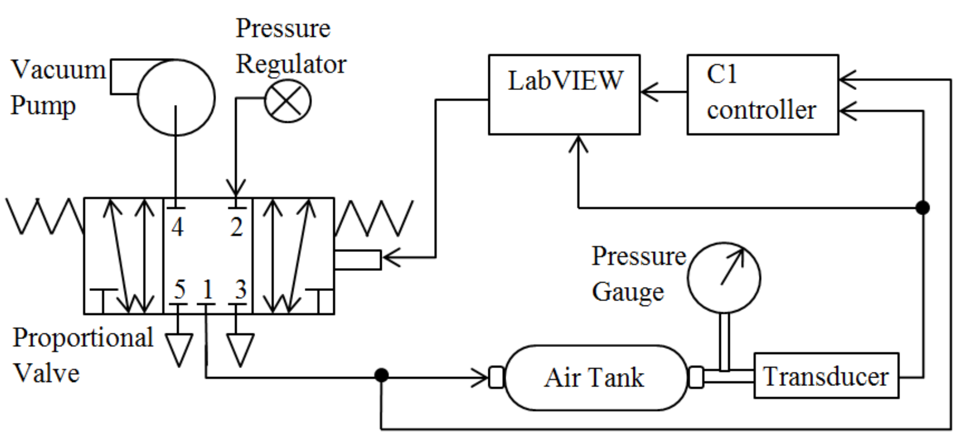

Figure 3.4: Pneumatic circuit diagram for the vacuum generator.

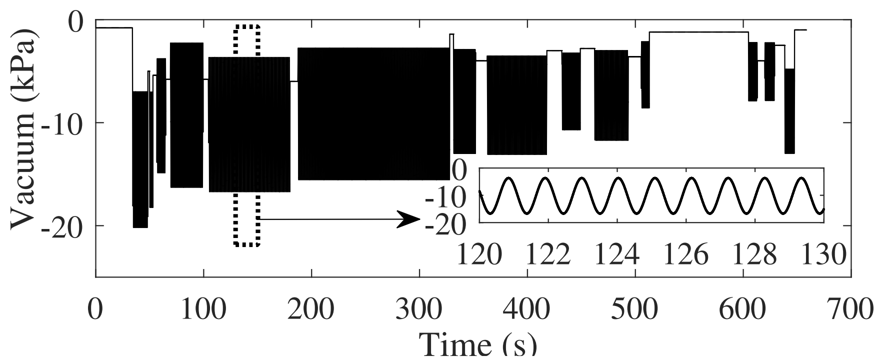

(a)

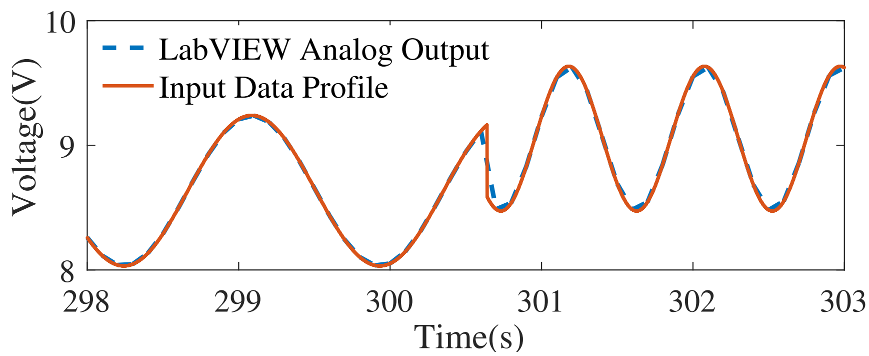

(b)

Figure 3.5: (a) Profile of an infant's natural vacuum pressure during breastfeeding and (b) LabVIEW data output performance.

Upper Palate and Lower Jaw Actuator

The clinical observation shows that the infant's upper palate applies constant pressure on the nipple-areola area and holds the nipple in position for initial oral latching (Alatalo et al., 2020), whereas the lower jaw of the infant generates a periodic wave-shaped force on the areola to compress the nipple and the tissues around it. To mimic this mechanism, the upper palate and lower jaw assemblies contain the 3D prototypes and two sets of linear actuators.

The palate and jaw prototypes are designed and developed based on the measurements from a set of CT scanned images. A sample image is shown in Figure 3.6 from the infants' oral cavities provided by the Dallas Children Health, Plastic & Craniofacial Surgery Department from The University of Texas Southwestern Medical Center. The saddle-shaped upper palate and D-shaped lower jaw are 3D printed mimicking the infant's oral skeleton as shown in Figure 3.6.

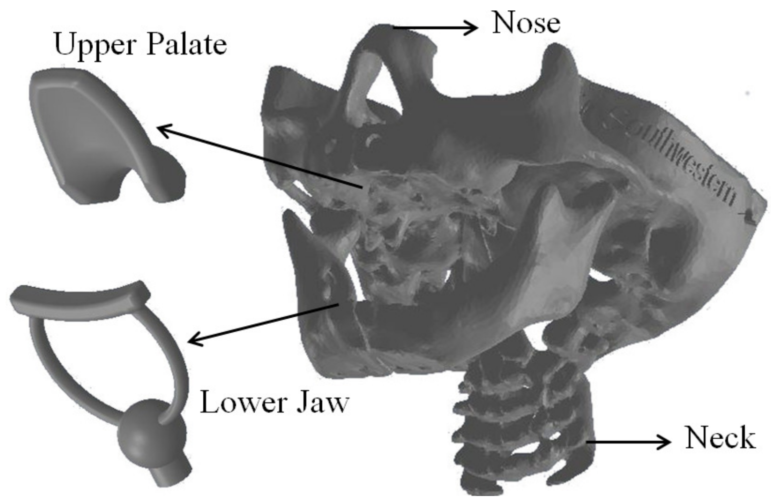

Figure 3.6: The infant's oral cavity CT scan and the corresponding designed prototypes of upper palate (maxilla) and lower jaw (mandible).

The upper palate assembly is controlled by a pneumatic actuator (USN-08-1/2-N, Clippard, Cincinnati, OH, USA) coupled with the 3D printed upper palate model as shown in Figure 3.7. The actuator is connected to a proportional valve (iQ Valve 930212, iQ Valves, Melbourne, FL, USA) and a valve driver (iQ Valves 5-250). The linear correlation between the input pressure and palate position allows the control of the actuator at a commanded position and thus holds the nipple in the right position. The pressure in the pneumatic actuator is controlled by the valve driver triggered with the voltage signal from an analog output module (NI 9264, National Instruments, Austin, TX, USA) with LabVIEW Real-Time signal generator.

The lower jaw assembly includes a 12 V DC linear actuator with a constant travel speed of 50mm/s (GLA750, Gimson Robotics, UK) coupled with the jaw prototype as shown in Figure 3.8b. The controllable linear actuator creates the periodic motion of the infant's jaw. The input profile for jaw movement is designed as a non-uniform saw-toothed piston moving

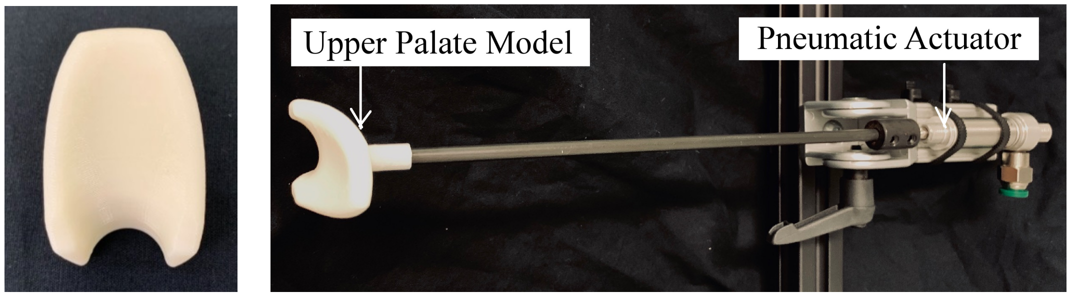

(a) (b)

Figure 3.7: (a) The 3D printed upper palate model, and (b) The upper palate assembly with pneumatic actuator.

distance in the apparatus (as seen in Figure 3.9) and imported into the Arduino Microcontroller (Mega 2580, Arduino). The skin-mimicking material (Eco-Flex 30) is wrapped around the jaw model to imitate the lip on the infant's jaw.

Tongue Gear Motor Assembly

In order to mimic the infant's peristaltic tongue movement, a tongue gear motor assembly was designed and constructed as shown in Figure 3.10. The assembly includes a rotating flexible silicone gear and a DC motor (GB37Y3530-12V-251R, DFRobot, Shanghai, China) with the encoder for speed control as shown in Figure 3.10a. The silicon gear contains four teeth that allow continuous direct contact on the breast while rotating. Each tooth has an ellipse-shaped involute profile to represent the infant's tongue based on the average geometry reported in (Siebert, 1985). The length of the tongue is 36mm and the width of the tongue is 24mm. A previous study (Niikawa et al., 2012) showed that the force from the root of the tongue was approximately two times the force from the tip of the tongue. In order to achieve this mechanism, a stiffer tongue root and a softer tongue tip are designed. QM 240T (Quantum Silicone, Richmond, VA) which is relatively stiffer with a Durometer at 20A is used to shape the root of tongue gear with a thickness of 6mm. Eco-flex 30 (Smooth-on Inc., PA, USA) with a Durometer of 00-30 is utilized to shape the 6mm thick softer part

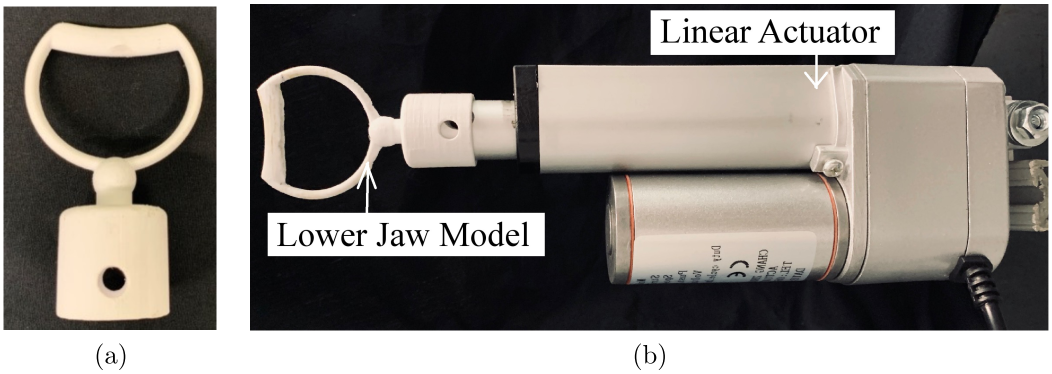

Figure 3.8: (a) The 3D printed jaw model, and (b) The lower jaw assembly with linear actuator.

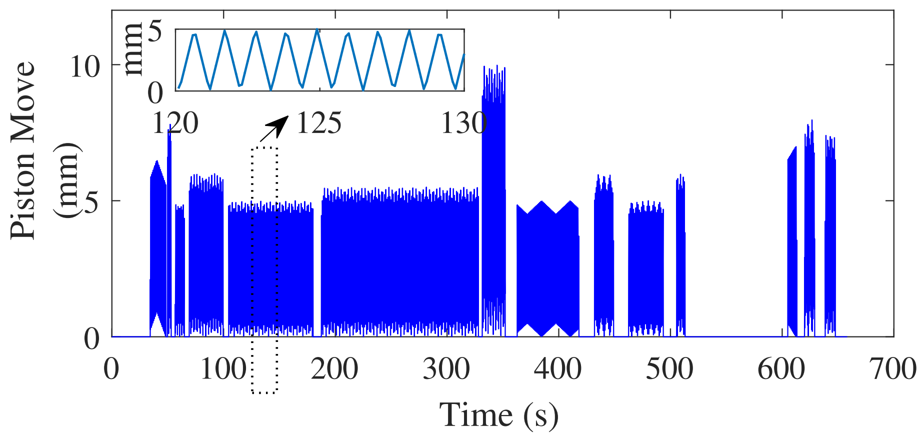

Figure 3.9: The input profile for lower jaw movement.

of the tongue root. The non-uniform rotational speed of the silicone tongue gear results in a peristaltic-like tongue movement during breastfeeding. This soft tissue-mimicking gear model (flexibility shown in Figure 3.10b) is connected to a long shaft toward the end of the rotating motor.

The rotation speed (rpm) is controlled by the DC motor, which has been connected to an Arduino Micro Controller updated with a predefined rotational speed profile (see Figure 3.11) based on the infant's suckling frequency. While rotating, the gear imitates the infant's tongue movement by applying a non-uniform periodic positive pressure on the nipple of the breast.

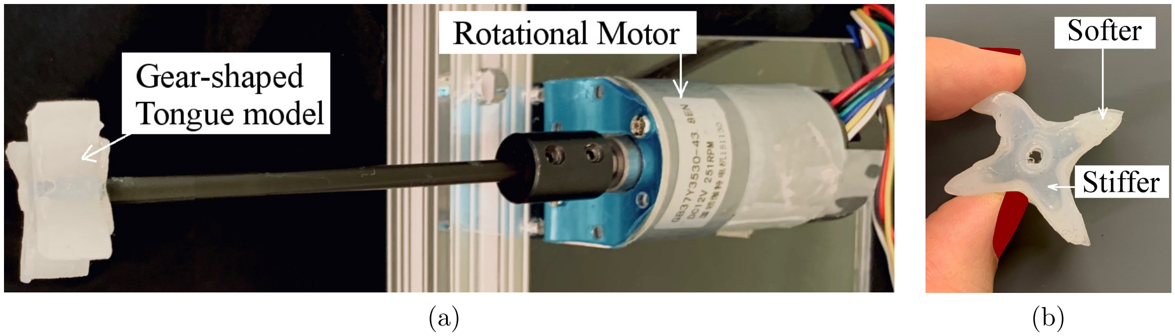

Figure 3.10: (a) Tongue-gear assembly, (b) The flexible gear-shape tongue structure.

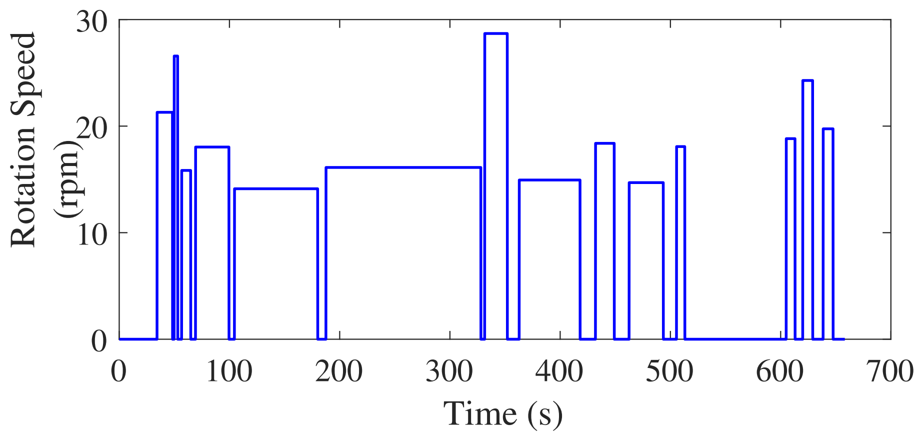

Figure 3.11: Input profile for the rotational gear.

Milk Reservoir

A milk reservoir has been designed to mimic breast milk production during the breastfeeding simulation (as seen in Figure 3.12). The reservoir assembly includes a milk bottle filled with milk-mimicking liquid, a set of manifolds, a shut-off valve and tubes connected to the ductal system in the breast phantom. The milk bottle with milk-mimicking liquid is held by a bottle holder.

The transparent milk-mimicking liquid is prepared with a mixture of 50.21% distilled water, 39.14% glycerol and 10.65% NaI in the lab based on the density and viscosity described in (Alatalo and Hassanipour, 2016). The liquid from the milk bottle flows into the four-outlet metal manifold for diffusion. A shut-off valve connects the tube from the milk bottle to the

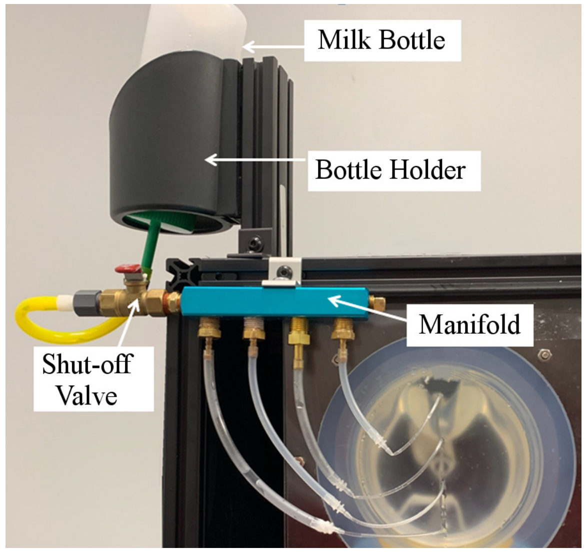

Figure 3.12: Breast milk reservoir setup

manifold and allows manipulation of the milk flow before and after experiments. The four tubes that come out of the manifold are connected to the inlets of the ductal structure in the breast model. The milk-mimicking liquid flows into the ductal structure in the breast phantom when the experiment starts and the shut-off valve opens at the same time. The transparency of the milk-mimicking liquid enables the flow visualization through the duct using the CCD camera.

3.1.2 Complete Design, Control System and Measurement Strategy:

The complete experimental setup for the bio-inspired breastfeeding simulator (BIBS) with the control system is presented in Figure 3.13a. The flexible and transparent breast phantom with bifurcated ducts represents the lactating human breast in the setup. The vacuum pump assembly generates sinusoidal intra-oral pressure with a LabVIEW control and measurement system. The infant's oral cavity is represented by the silicone soft tongue gear model and 3-D printed palate and jaw. Controllable linear actuators work as the palate and jaw of the infant and apply maxilla and mandible pressure on the breast phantom as shown in Figure 3.13b. The rotational tongue-gear motor mimics the infant's peristaltic-like tongue

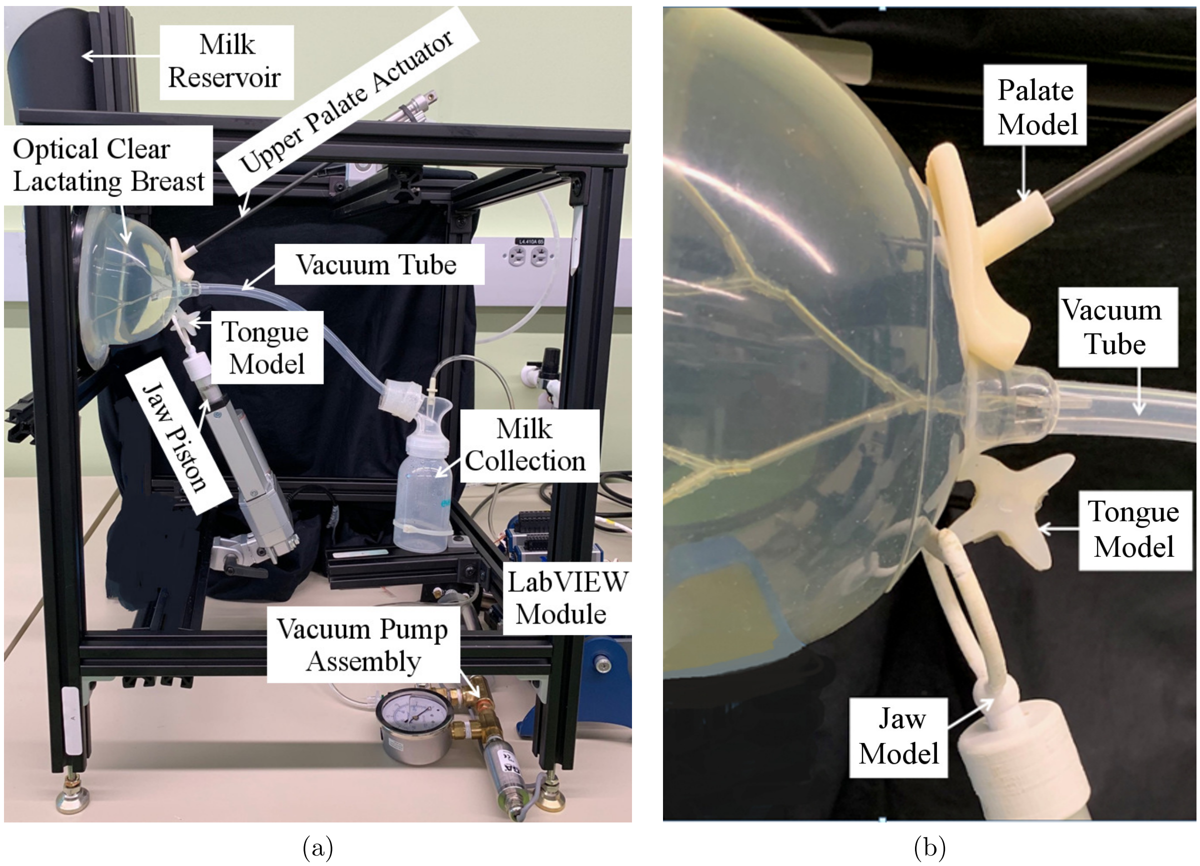

Figure 3.13: (a) The complete Bio-inspired Breastfeeding Simulator (BIBS) setup, and (b) The close look of the oral cavity models on the transparent lactating breast phantom.

movement. This apparatus provides a nonlinear and complete imitation of natural suckling during breastfeeding experiments. A set of piezoelectric sensors over the areola measures the compression of the gear-shaped tongue, mandible, and maxilla while a high-resolution CCD camera captures the movement of the breast and oral cavity and deformation of the nipple and areola. The sensors are not shown in Figure 3.13 for clarity, please see Figure 3.15 for the sensor locations.

A simple open-loop MIMO (Multiple-Input Multiple-Output) control strategy (see Figure 3.14) is designed to manipulate all the actuators, motors, and pumps with one central control system. Feedback from pressure sensors is added for vacuum pressure and jaw piston motion. The sensors are controlled by the LabVIEW program. Input profiles for the jaw piston movement and the frequency for tongue gear rotation are all designed based on clinical observations (Alatalo et al., 2020). A measurement system is designed for capturing the pressure outputs and nipple deformation from the apparatus.

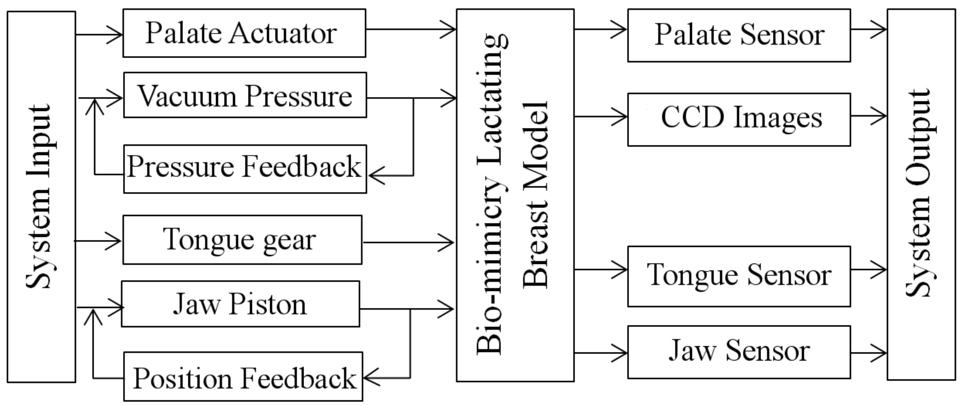

Figure 3.14: Breastfeeding simulator open-loop MIMO control architecture.

Pressure measurements

Two piezoelectric strip sensors (FSR^{TM} 408, Interlink Electronics, Los Angles, USA) as shown in Figure 3.15, measure the pressure from the maxilla (upper jaw) and mandible (lower jaw) plates on the nipple-areola area. The sensors are flexible with a thickness of 0.3mm and have a sensing range of 1-1000N. A pinpoint tip sensor (FSR^{TM} 400) is placed underneath the bottom of the nipple to capture the tongue-nipple contact pressure. The diameter of the tip sensor is 0.16" with a thickness of 0.2mm and has a sensing range of 0.1-100N. The analog readings from pressure sensors are recorded by user-defined software in an Arduino UNO module.

Static and dynamic characteristics of these force sensors were evaluated before the experiments (Dabling et al., 2012). For sensor static characterization, increasing and decreasing random loads were applied to the force sensors from 0 to 50 kPa. Scattered data of static characterizations for both types of sensors were presented in Figure 3.16a and Figure 3.16b. Both types of force sensors showed strong linearity. For dynamic characterization, 25 and

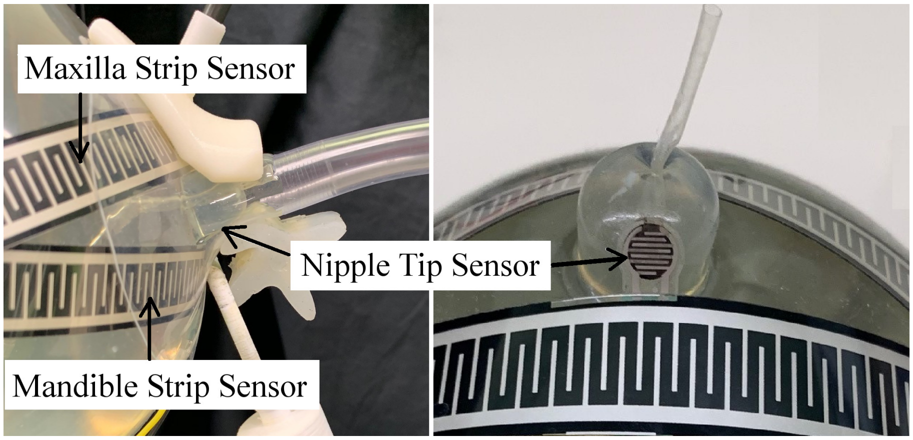

Figure 3.15: Side view (left) and top view (right) of the pressure sensors on the lactation breast phantom.

50 kPa pressure was separately applied on both strip and tip sensors and was manually removed to test the sensor sensitivity. The response time was recorded when the pressure was instantly removed. Figure 3.16c and Figure 3.16d show that the time required for the output to drop from 90% to 10% ranges from 0.03-0.07 seconds, which is less than the profile updating rate at 0.1 seconds during experiments. These sensors proved to have a sufficient dynamic characteristic for the measurement response purpose.

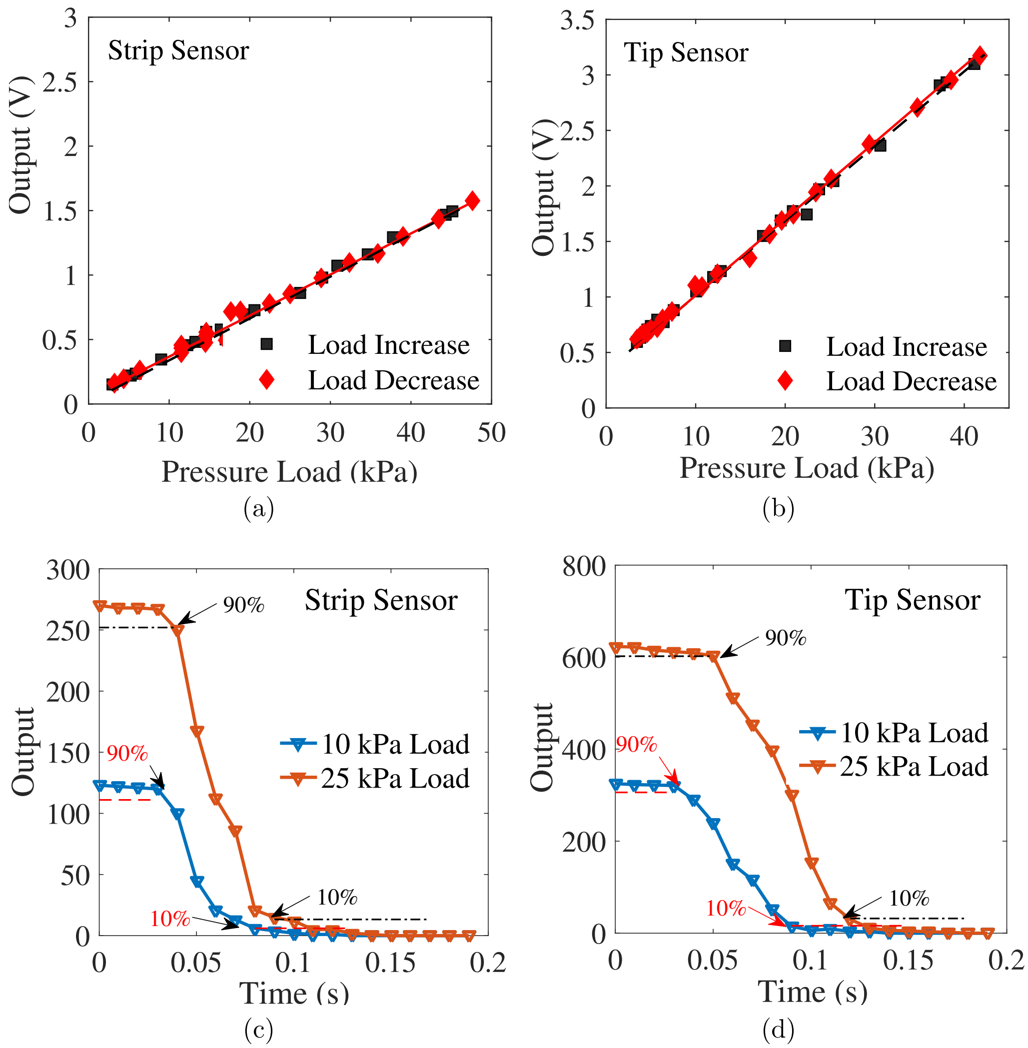

Figure 3.16: Static characteristic by increasing pressure load and decreasing pressure load on the (a) strip and (b) tip sensor, and dynamic characteristic by applying pulse pressure and test the response delay on the (c) strip and (d) tip sensor.

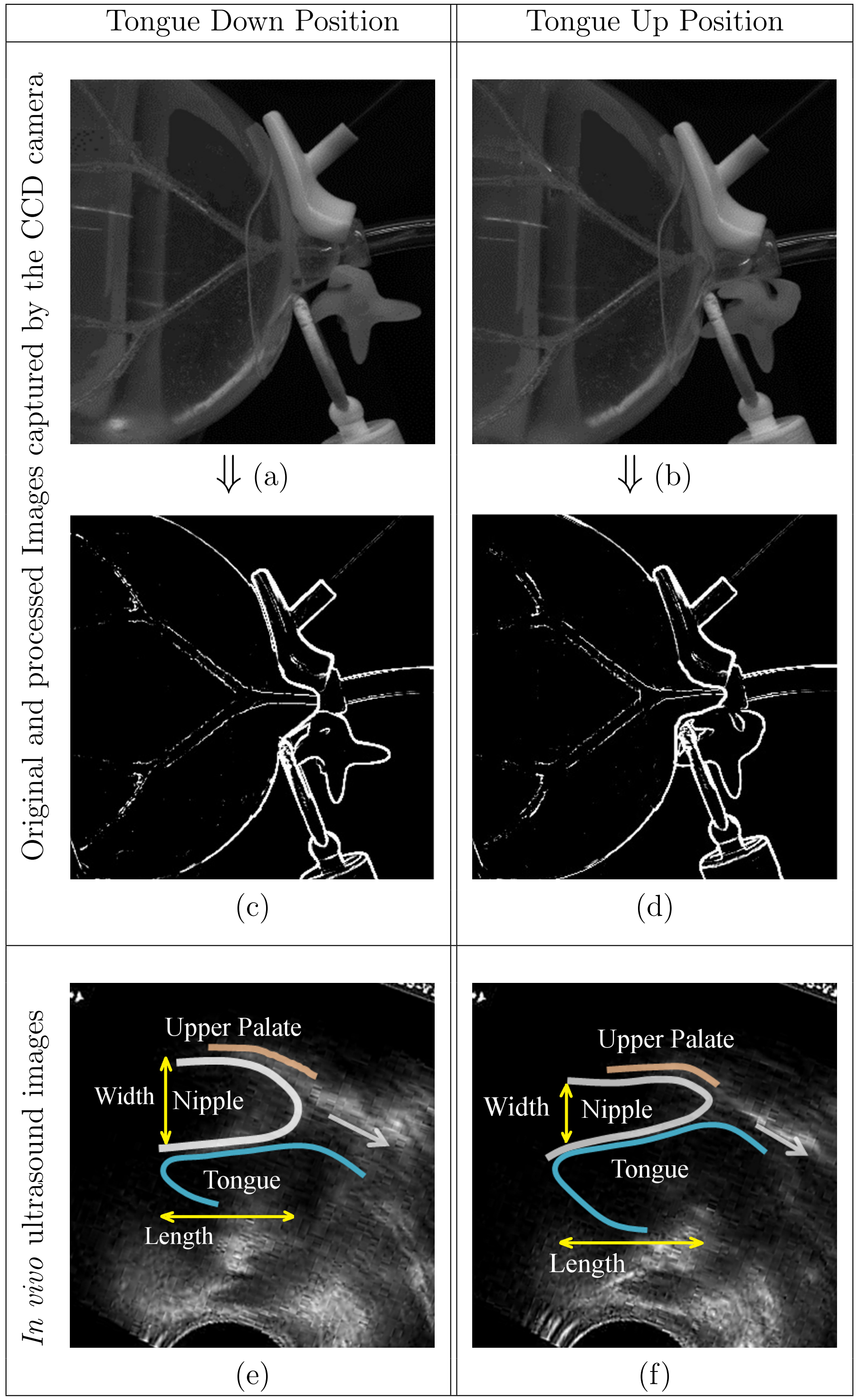

Figure 3.17: Nipple-mouth interaction during one suck cycle (tongue up and down position); (a) and (b) are CCD captured images, (c) and (d) are processed images with detected boundaries, (e) and (f) are *in vivo* ultrasound images.

Nipple Deformation Measurement

A real-time high-speed CCD camera (UNIQ USS-680CL, EPIX, Buffalo Grove, IL, USA) captures images of oral and nipple movements during the experiment with 110 frames per second. The full-frame resolution of the camera is 659×494 pixels. A BUTTERWORTH low-pass filter (Butterworth, 1930) is applied to smooth the images. Nipple deformation measurements from processed images aid in understanding the biomechanics of breast-infant interaction and observation of applied forces that affect milk removal. A programmable measurement system is developed using MATLAB to get dimensions of the nipple width and length with the tongue moving up and tongue moving down. The Canny edge detection method (Canny, 1987) is applied on each image frame to outline the nipple, upper palate, and tongue. Manual edge designation is also drafted on each frame to validate the detected boundaries. Captured and processed images are shown in Figures 4.5. Significant nipple width deformation happens on the areola area when the jaw piston and tongue move up and down on the breast phantom. Figures 4.5 compares experimental images for tongue-up and tongue-down positions with those from ultrasound images.

3.2 Results and Validation

3.2.1 Infant Applied Pressure

A set of experiments are conducted to test the stability and robustness of the apparatus. Results from the experiment for fifteen runs are presented in Figure 3.18 with a shade of error range. The results include the intra-oral vacuum pressure, upper palate pressure, lower jaw pressure, nipple-tongue contact pressure, nipple width, and nipple length variation. The input profile has the total suck cycles of 495 ± 16 during 658.2 s total feeding time, and the average total output suck cycle from LabVIEW feedback in the BIBS is 489 ± 21. Suckling frequency is between 1-2 cycles/s over the feeding time.

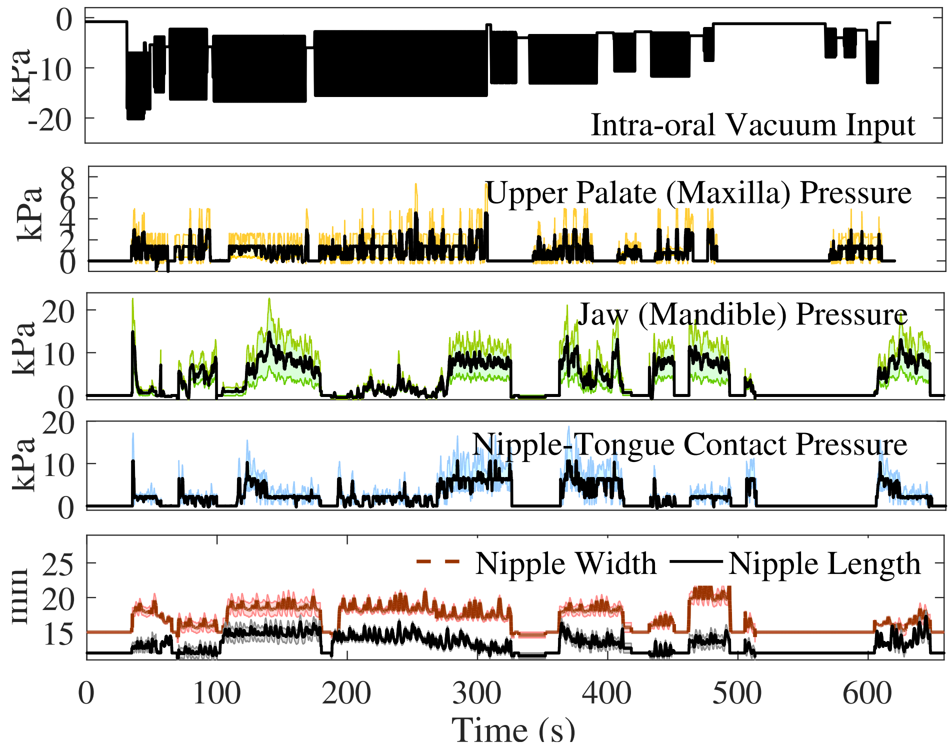

Figure 3.18: Output profile of the infant oral pressures includes: intra-oral vacuum pressure, positive pressures (maxilla, mandible and nipple-tongue contact pressure) and nipple length and height change.

Average data for the multiple runs of the apparatus is presented in Table 3.4 and compared with the clinical results. The *in vivo* (Alatalo et al., 2020) average oral pressure applied on the breast by the infants is around -10.04 kPa for intra-oral vacuum and 12.93 kPa for peripheral oral pressure. The BIBS setup provides an average of -9.98 kPa for vacuum pressure and 13.70 kPa for oral compression pressure.

Average variations and uncertainties from experiments are shown in Table 3.4. The Average upper palate pressure is the lowest in peripheral pressures, whereas lower jaw pressure is the highest. The average pressure change from numerous experiments is 1.76 ± 1.69 kPa for palate pressure, 7.29 ± 3.36 kPa for jaw pressure, and 4.65 ± 2.39 kPa for the nipple-tongue contact pressure. Uncertainties for all pressure results are less than 10%, which indicates real-time stability and robustness of the BIBS to imitate breastfeeding patterns.

Table 3.3: Averaged output results from both *in vivo* and *in vitro* (with BIBS) experiment

Measurements ($\Delta\pm$SD)	*In vivo*	*In vitro*
Total Sucks	495 ± 16	489 ± 21
Intra-oral Vacuum	-10.04 ± 0.34 kPa	-9.98 ± 0.25 kPa
Peripheral Oral Pressure	12.93 ± 4.35 kPa	13.70 ± 5.44 kPa
Nipple Width Change	2.51 ± 0.20 mm	2.48 ± 0.57 mm
Nipple Length change	3.22 ± 0.28 mm	3.08 ± 0.93 mm

Table 3.4: Average variations and uncertainties from experiments

Results Evaluation	Intra-oral Vacuum (kPa)	Peripheral Oral Pressure (kPa)			Nipple Width (mm)	Nipple Length (mm)
		Upper Palate	Lower jaw	Nipple-Tongue Contact		
Average	-9.98	1.76	7.29	4.65	16.78	13.84
Variation	6.35	1.69	3.36	2.39	2.48	3.08
Uncertainty	0.99%	8.72%	9.53%	6.46%	1.23%	1.54%

Ten-second sample pressure results from the BIBS are presented in Figure 3.19. Upper palate pressure, jaw pressure, and the nipple-tongue contact pressure are measured spontaneously *in vitro* for the first time. The results show that pressure values are in good agreement with clinical values over time. As observed from the outlined experimental results in Figure 3.19, mouthing frequency is in good agreement with the intra-oral vacuum frequency. When the vacuum experiences a local minimum (around -15 kPa), the maxilla, mandible, and nipple pressure decrease, whereas when the vacuum is at a local maximum (close to atmosphere pressure), the maxilla, mandible, and nipple pressure increase. All pressures match the clinical study by the author (Alatalo et al., 2020).

3.2.2 Nipple Deformation

The average nipple width and length variations from captured and processed CCD images are 2.48 ± 0.57mm and 3.08 ± 0.93mm, respectively. In the authors' clinical study (Alatalo

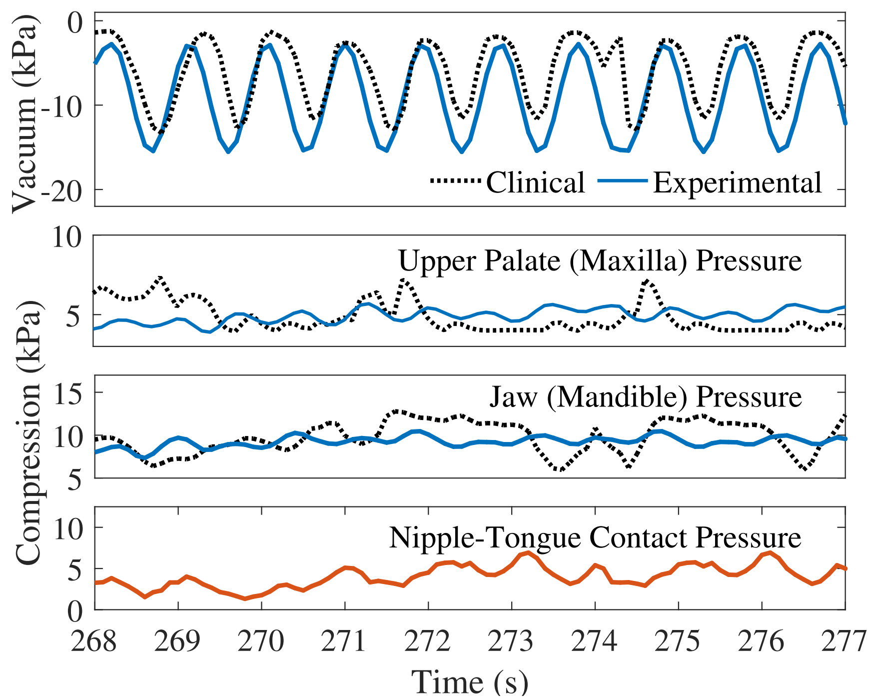

Figure 3.19: Comparisons between clinical results and *in vitro* experimental results in ten seconds show that experimental oral pressure matches the clinical infant oral pressure in BIBS apparatus.

et al., 2020), the average change that was measured in ultrasound images in nipple width and length for Infants was 2.51 ± 0.20 mm and 3.22 ± 0.28 mm, respectively, over the entire feeding period. Nipple deformations from *in vitro* experiments are found to be comparable with those from *in vivo* clinical results.

Figure 3.18 shows the dynamic pattern for nipple deformation in the entire feeding period. The variations in nipple deformation are observed not sensitive to the intra-oral vacuum pressure but actively respond to the compression pressure from maxilla, mandible, and tongue movement. The change in nipple width is mostly controlled by the jaw piston, and the nipple length deformation is affected by the tongue-gear motion and vacuum pressures. In this paper, the compression from palate and jaw piston caused $31 \pm 14\%$ in nipple width change and $25.6 \pm 7.8\%$ in nipple length change. The observation from the milk flow shows that besides the vacuum pressure, the compression contributes to the milk transfer from the nipple. The small differences between the clinical and experimental nipple deformation are due to the mechanical property discrepancy between human tissue and silicone model, which are still under investigation and need further study for both *in vivo* and *in vitro* experiments.

3.3 Discussion

In this study, a bio-inspired breastfeeding simulator (BIBS) was designed and constructed based on clinical observations. The apparatus includes easy-to-control actuators and motors for imitating an infant's rhythmic oral movement during breastfeeding to reveal the biomechanics of breastfeeding. The setup mimics natural breastfeeding by utilizing a transparent and flexible breast model, a tongue-shaped gear, hard palate, and jaw prototypes and actuators to create both positive oral compression and negative oral vacuum pressure for extracting milk from the breast.

Inspired by an infant's oral motor skills during breastfeeding, this novel apparatus is the first known attempt to successfully mimic both the compression and vacuum pressures exerted by an infant, on a transparent and flexible breast model. The setup is equipped with flexible thin-film sensors to evaluate the oral behavior of an actual infant. Using these sensors, the BIBS apparatus captures the pressure values at the upper palate, lower jaw and tongue, and nipple contact area and reports a complete set of pressure results for the first time. A CCD camera captures the interaction of breast and nipple during the action and records the breast and oral cavity movement and deformation.

Pressure profiles from the clinical investigation are imported as inputs and are cross-validated with the results from the BIBS apparatus. Wavelike pressure profile for all models in the BIBS setup successfully mimics the infant suckling patterns in natural breastfeeding. The results also show that the upper palate pressure is lower than the lower jaw pressure but similar to the pressure from the nipple-tongue contact area. Lower jaw pressure is the main force causing the nipple width change, whereas the tongue and vacuum pressures contribute to the nipple length change. Jaw movement produces the strongest peripheral pressure on the breast. These results are in good agreement with the previous clinical studies (Alatalo and Hassanipour, 2016).

We briefly note several challenges in the process of designing and building this apparatus. Some issues were related to inevitable limitations of available materials and mechanical design. For example, the mechanical properties of PDMS and the human breast skin are not identical, therefore the nipple elongation in BIBS cannot fully match the stretch-ability of human breast tissue. This may be addressed by the advent of new materials in the future. Future work may also increase the number of bifurcations of the breast ducts, and possibly the number of lobes. While careful construction of the apparatus has considerably reduced the effect of vibrations and noise on the measurements, this effect has not been completely eliminated.

Despite challenges, this study has achieved its goal to mimic natural breastfeeding suckling behavior *in vitro* with remarkable fidelity. Compared with the previous breastfeeding assessment tools (Wang et al., 2014; Ilyin et al., 2019), the BIBS apparatus provides several advantages and benefits, including an optically clear breast phantom with improved flexibility and softness in the breast and milk ducts. The apparatus can run simulations under various suckling patterns to find optimal milk consumption, considering the fact that each mother and infant dyad is different. BIBS can be used as a potential screening tool for developmental disabilities such as infants' oral abnormalities and mothers' physical lactation problems. BIBS can also be applied towards an educational purpose for understanding the mechanism of breastfeeding. Following the same approach as in the current work, the model can be extended to a better breast pump design by introducing oral compression pressure.

While the model parameters are identified for a specific infant, the model structure is directly applicable to simulate any boundary conditions, especially infants with abnormal oral movement or mothers with breast dysfunctions, to predict the oral behavior and quantify milk production. BIBS can adapt to any shape of the breast, upper palate, lower jaw, and tongue model, which makes it useful for studying infants with physical oral abnormalities when *in vivo* experiment is not practicable. Understanding oral behavior with *in vitro* experiments can also provide objective suggestions for future breast pump design and breastfeeding methods.

3.4 Conclusion

A bio-inspired breastfeeding simulator (BIBS) was designed and developed to mimic the infants, complex natural suckling pattern, including both the intra-oral vacuum and the peripheral oral pressures. The complete design included a transparent lactating breast phantom, a vacuum pump, two actuators represent the infant's oral maxilla and mandible, a rotating tongue-gear motor, a milk reservoir, and a set of measurement systems. Vacuum pressure and compression inputs were inspired by the infant's oral movement mechanism from the clinical study by the authors. The intra-oral vacuum pressure and the peripheral oral pressure values from BIBS were found to be comparable to *in vivo* clinical data. Results indicated that the BIBS setup performance is in good agreement with the infant's oral motion and realized the effect of infant applied forces on the breast with the real-time oral pressures and nipple deformation measurement. BIBS provides a non-invasive and practical assessment tool to imitate and monitor an infant's oral behavior during breastfeeding *in vitro*.

CHAPTER 4

BIBS INTEGRATED WITH GRAPHICAL USER INTERFACE (GUI) AND FEEDBACK CONTROLLERS

The content of this chapter was adapted from a manuscript to be submitted at the time of writing by the author: Lin Jiang, Navid Sadeghi Varnousfaderani, Yonas Tadesse, Fatemeh Hassanipour, "A Bench-top Infant Oral Suckling Simulator for Studying Breastfeeding Mechanics", IEEE Robotic and Automation Letters.

4.1 Introduction

Infant sucking difficulties and oral physical dysfunctions are common reasons for ceasing breastfeeding (Li et al., 2008). The biomechanics of infant oral cavity and breast interaction during breastfeeding have attracted the attention of researchers recently ((Alatalo et al., 2020)). Such knowledge is of importance to the lactation solutions for mothers and infants with breastfeeding difficulties. Studying the biomechanics of infant suckling during breastfeeding helps in getting insights into feasible physical treatments for mothers and infants clinically and practically.

Infant oral suckling is an instinctive action that takes place about 1-2 times per second during natural breastfeeding (Alatalo et al., 2020). A complete infant oral suckling dynamic includes rhythmic vacuum extraction, periodic oral compression on the nipple-aerola complex and frequency coordinated breathe and swallowing (Woolridge, 1986). Complex infant suckling patterns have been studied with various techniques, including clinical observation of oral movement with bottle feeding (Taki et al., 2010; Waller, 1936; Taffoni et al., 2016), in vivo ultrasound mapping of oral cavity during breastfeeding (Geddes et al., 2012; McClellan et al., 2008), and suckling assessment tools using electric breast pumps (Kent et al., 2006; Ilyin et al., 2019).

(Taki et al., 2010) investigated the suckling variables for breast-feeding and bottle-feeding infants of 1, 3, and 6 months using tube pressure transducers and weight scales. They found milk intake increases with the number and frequency of the sucks. (Taffoni et al., 2016) developed a bottle-feed based module with integrated sensors to monitor neonatal breathing patterns during nutritive suckling. (Geddes et al., 2012) used sub-mental 2D ultrasound scans of the infant oral cavity performed simultaneously with measurement of intra-oral vacuums. Their work indicates a peristaltic like tongue movement in ultrasound images, which contributes to milk removal during breastfeeding. (Kent et al., 2006) addressed the importance of vacuum on milk ejection using an electric breast pump. This work demonstrated that maximum milk flow was produced at the maximum vacuum pressure setting of the pump. Among these studies, in vivo measurements were either invasive, restrictive or low quality in resolution and precision. Also, in vitro studies have used open-loop control in design or considers vacuum pressure only (e.g. breast pumps), which potentially excludes the contribution of oral cavity movement.

Motivated by reducing human testing and the need of comparative and quantitative analysis of breastfeeding biomechanics, we have developed a bio-inspired breastfeeding simulator (BIBS) (Jiang and Hassanipour, 2020a) based on a recent clinical study of infant oral motor dynamics (Alatalo et al., 2020). BIBS imitates infant's oral interaction with the breast during active feeding and serves as an in vitro assessment system for evaluating infant's suckling pattern mechanism. In the existing BIBS setup. actuators and vacuum pressure follow a single pre-defined input profile and are controlled with a open-loop strategy. In this work, we constructed the BIBS with addition of feedback control for pressure tracking and a graphical user interface (GUI) for real-time data and image capturing. Specifically, PID (proportional-–integral-–derivative) controlled vacuum generator produces user-defined frequency and strength of vacuum pressure. A PID controlled soft robotic tongue mimics the peristaltic motion of the infant tongue and nipple. Additionally, the BIBS is designed with a solid infant head and jaw model to demonstrate the humanoid behavior of the simulator. The infant's head skeleton and jaw model are modified based on a previously designed infant humanoid robot (Tadesse et al., 2011). The redesigned infant head and jaw models are 3D printed with ABS (Acrylonitrile butadiene styrene) materials. The mechanism of oral cavity opening and closing (mouthing) is controlled by two synchronized servo motors. Measurement system integrated in the updated BIBS includes piezoelectric sensors on the breast nipple and areola for peripheral oral pressure, vacuum transducer for intra-oral vacuum, and the digital flow meter for outlet flow rate. As an external validation, a PIV (particle image velocimetry) measurement system is utilized to visualize and quantify the outlet flow rate from the breast phantom. The BIBS integrated with feedback controllers and GUI interface is also designed to be used as a portable and user-friendly bench-top testing apparatus.

The main contribution of this work is applying feedback controllers for the precise pressure and tongue motion control, as well as adding GUI software interface to customize oral pattern modulation in a physiologically realistic breastfeeding simulator for studying the breastfeeding mechanism quantitatively. The insights gained from the results of this physical simulator can lead to more effective clinical treatment routines for breastfeeding difficulties such as development of medical devices to assist infant feeding.

The schematic configuration of the bench-top apparatus is shown in **Figure ??**. To serve as an open-source, bench-top setup, the infant suckling simulator is designed to be mechanically simple and modular for easy construction, customization, and maintenance. The apparatus consists of the following:

1. A transparent and flexible breast phantom with bifurcated ductal structure, adapted from previously developed BIBS setup (Jiang and Hassanipour, 2020a).

2. An infant head model including a position adjustable upper face, motor-controlled lower jaw and soft tongue actuator as shown in **Figure 4.1**.

3. An Arduino-controlled battery-driven vacuum breast pump that generates rhythmic intra-oral pressure defined by user through GUI (graphical user interface), connected with a digital flow meter for measuring the vacuum frequency.

4. A measuring system with force sensors, digital flow meter and arduino-compatible camera for real-time pressure, flow rate, and image data capturing.

5. A reservoir filled with human milk-mimicking liquid (HMML) outlined in (Jiang et al., 2020) that allows the quantitative flow analysis with PIV experiments, as well as a milk bottle to collect the HMML from the breast.

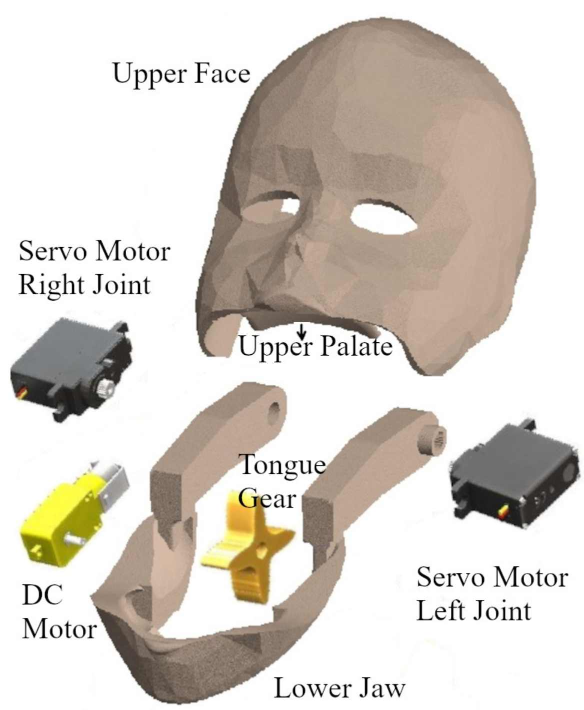

Figure 4.1: Exploded view of the infant head model.

4.1.1 Infant Suckling Simulator Mechanical Design

To serve as an open-source, bench-top setup, the infant suckling simulator is designed to be mechanically simple and modular for easy construction, customization, and maintenance.

The schematic configuration of the bench-top apparatus is shown in Figure 4.2a. A snapshot the assembly is shown in Figure 4.2b. The apparatus consists of the following:

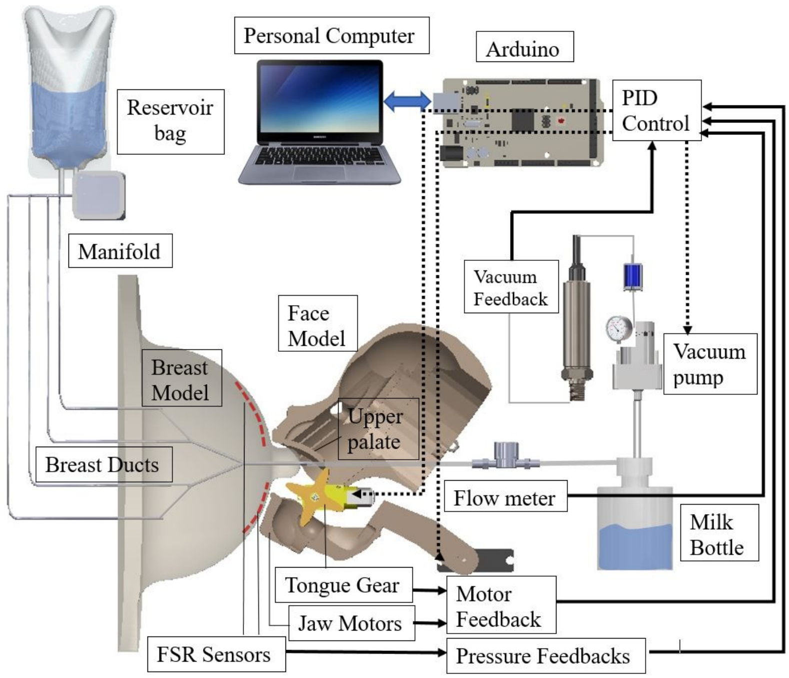

(a)

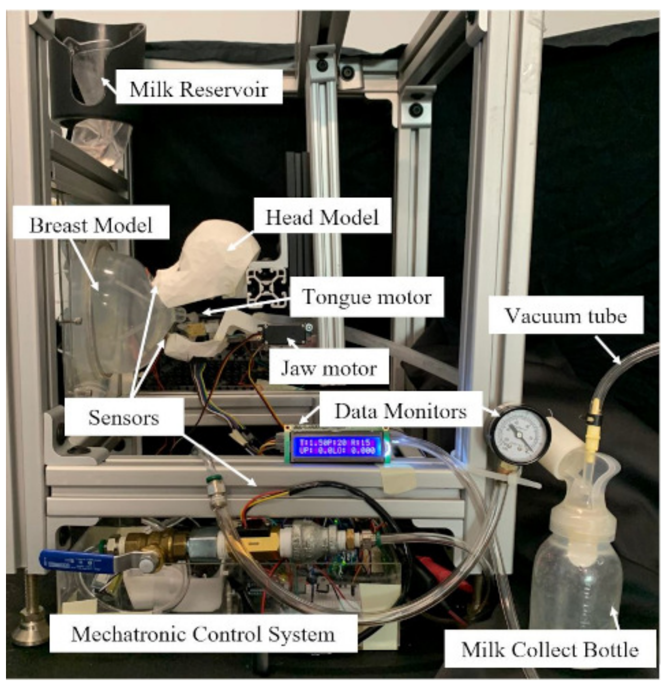

(b)

Figure 4.2: A snapshot and the schematic configuration of the BIB setup and the close-loop control diagram

1. A infant head model consists of position adjustable upper face, motor-controlled lower jaw and soft tongue actuator.

2. A transparent and flexible breast phantom with bifurcated ductal structure, adapted from BIBS setup (Jiang and Hassanipour, 2020a).

3. An Arduino-controlled battery-driven vacuum breast pump that generates rhythmic intra-oral pressure defined by the user through GUI (graphical user interface), connected with a digital flow meter to measure the vacuum frequency.

4. A measuring system with piezoelectric force sensors, digital flow meter, and Arduino-compatible camera for real-time pressure and flow rate data capturing, as well as image capture.

5. A milk bottle to collect HMML from the breast.

6. A reservoir filled with human milk-mimicking liquid (HMML) outlined in (Jiang et al., 2020) that allows the quantitative flow analysis with PIV experiments.

Detailed designs originate in this study are illustrated as below.

4.1.2 Robotic Head and Tongue Models

Solid Head Model: The solid head model consists of a face model with upper hard oral palate representing infant's face and a jaw model designed with motor mounts for servo motor actuation. The infant face and jaw model is modified from humanoid head model presented in (Tadesse et al., 2011). The oral upper palate embedded in the upper face solid design is based on the measurements from a set of CT (computerized tomography) scanned images provided by the Dallas Children Health, Plastic & Craniofacial Surgery Department at The University of Texas Southwestern Medical Center. The upper face and lower jaw are fabricated by 3D printing using ABS (acrylonitrile butadiene styrene) plus plastic on

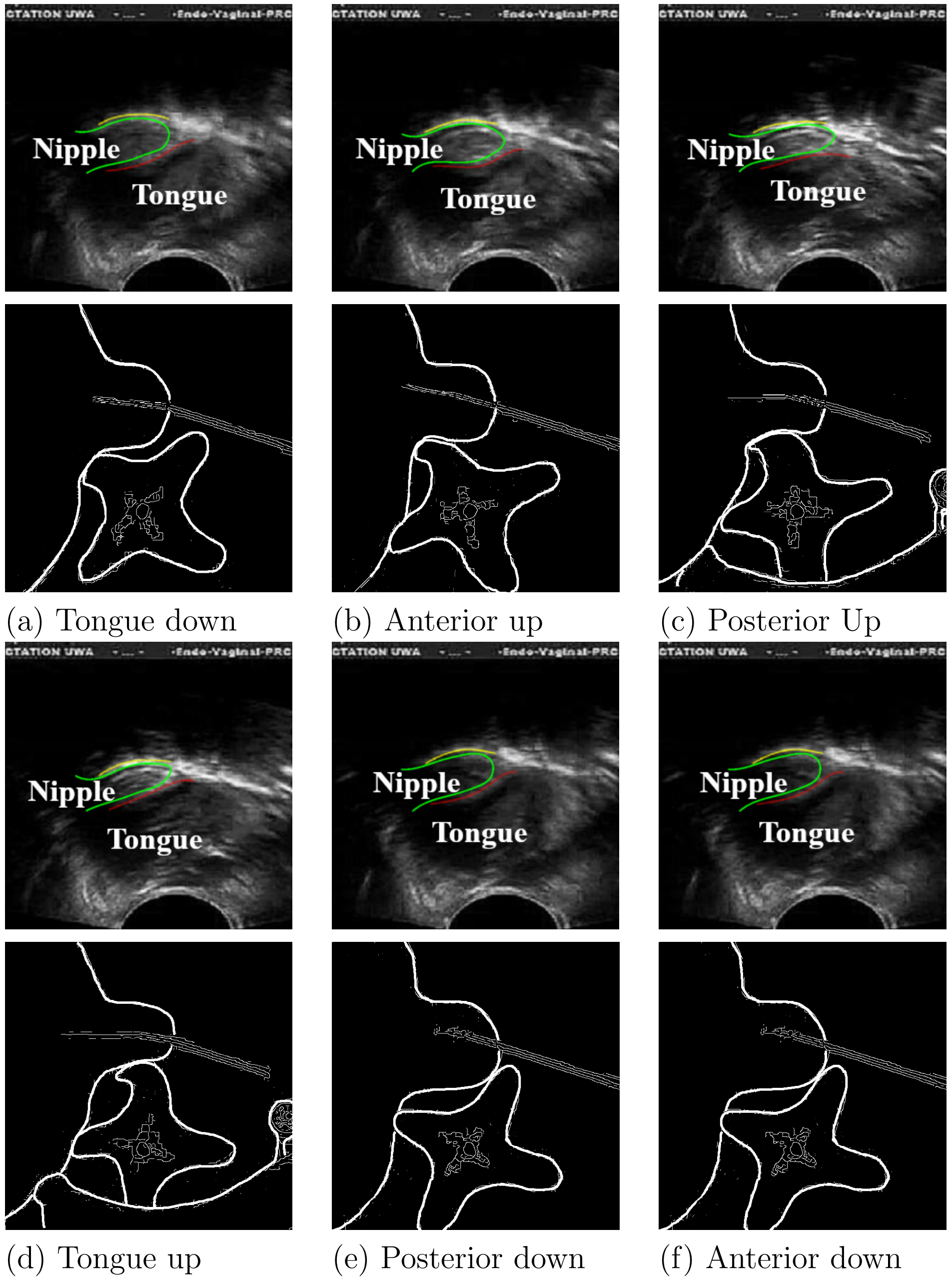

(a) Tongue down (b) Anterior up (c) Posterior Up

(d) Tongue up (e) Posterior down (f) Anterior down

Figure 4.3: Ultrasound and edge detected image sequence of tongue motion in the apparatus.

Fortus 250MC (Stratasys Ltd., Edina, MN, USA). The upper face and lower jaw model are separately mounted on T-slotted frames that allow for the vertical and horizontal positioning of the components. Two small servos motor (HS 81, Hitec) mounted on the frames actuate the jaw in one DOF (degree of freedom) of rotating angle that enables up and down jaw movements toward the breast.

Soft Robotic Tongue Model: The soft robotic tongue model includes a multi-shoreness platinum cured silicone synthetic tongue adapted from BIBS setup (Jiang and Hassanipour, 2020a) and a micro DC motor (DFR429, DFRobot) with an encoder that provides rotation speed feedback. The tongue dimensions are based on the infant tongue size studied by (Siebert, 1985).

Ultrasound videos of clinical studies have shown that the tongue surface has a peristaltic-like movement during breastfeeding (Geddes et al., 2008b). **Figure 4.3 (top row)** present six typical moment of the tongue peristaltic-like motion in each cycle using ultrasound images. The tongue movement during infant breastfeeding suckling mechanism follows: a) infant's maxilla and mandible hold the nipple-areola in the infant's mouth, and oral vacuum generates while tongue is at the lowest position, b) tongue extends out and the anterior of the tongue moves up to pull the nipple into the oral cavity, c) tongue posterior pushes the nipple to the hard palate, and d) tongue reaches at the top and compress the nipple to squeeze out the milk, e) tongue posterior moves down and vacuum start, f) tongue anterior moves down and vacuum peaks.

While rotating, the soft tongue model deforms and compresses the nipple following the six typical moment of realistic tongue motion during suckling. After one gear slides over, the next tongue gear flips up to repeat the peristaltic movement and continues to deform the nipple. **Figure 4.3 (bottom row)** provides post-processed images of the tongue movement captured by the embedded camera in the simulator. The tongue gear tip first attaches to the breast, then slide along with the soft breast phantom to the tip of the nipple. The momentum generated by the stiffer inner part of the tongue gear enable the gear teeth to flip over and leave the space for the next gear teeth. The designed soft robotic tongue mimics the infant's tongue movements during breastfeeding, and provide a more realistic breast-nipple deformation under tongue muscle for in vitro studies.

4.1.3 Mechatronic System Design

The mechatronic system enables the feedback control for three types of motors: DC motor for tongue rotation, RC servo motors for jaw motion, and pump motor for vacuum control. The system can be battery powered or powered by USB port connected to a personal computer (PC). Arduino Mega 2650 serves as the main on-board processor and controller. It handles motor control and low-level data processing. Arduino Uno is responsible for image capture and storing using embedded camera (ArduCAM OV2640 2MP Plus). All communications with PC are enabled with serial ports.

A closed-loop feedback control loop running on a micro-controller provides real-time and robust control on the coordination of the soft robotic tongue rotation, jaw actuation, and vacuum cycles. The control system is designed with two levels. The first level of control is executed on an integrated development environment (Arduino Mega) to acquire real-time data from the sensors, identify the system transfer function with sensor data, simulate the system model in MATLAB using SIMULINK, and design PID parameters in MATLAB simulation. The second level of control is to apply estimated PID criteria on board and enables feedback control based on motor encoder, pressure sensors and vacuum pressure transducer. The control algorithm of PID tuning is integrated in Arduino micro-controllor board. The design of a close-loop control system for infant suckling simulator achieves frequency matched interactions between vacuum and oral motor functions.

Tongue motor control: The silicone tongue gear is controlled by a micro DC motor with built-in encoder (TT Micro, DFRobot). The transfer function for the open-loop DC motor is presented as:

$$P(s) = \frac{\dot{\theta(s)}}{V(s)} = \frac{K_t}{(Js+b)(Ls+R)+K_e^2} \tag{4.1}$$

where, θ is the degree rotated, V is input voltage, J is the moment of inertia of the rotor, b is the motor viscous friction constant, K_e is electromotive force constant, K_t is the motor torque constant, R is the electric resistance, and L is the electric inductance. Open-loop data reading is used for model identification and parameter estimation (Goppelt et al., 2018). Kalman filter algorithm was utilized to filter the sensor noise. The physical parameters for the tongue gear DC motor are estimated via non-linear least squares algorithm. PID parameters are estimated in MATLAB SIMULINK model using the identified transfer function. Estimated parameters are presented in Table 4.1.

Table 4.1: Transfer function and PID parameters from MATLAB simulation.

<table>
<tr><td rowspan="7">Transfer Function</td><td>parameter</td><td>Tongue motor</td><td>Vacuum Pump</td></tr>
<tr><td>J ($kg \cdot m^2$)</td><td>1.21 $\times 10^{-5}$</td><td>0.50</td></tr>
<tr><td>b ($N \cdot m.s$)</td><td>1.53 $\times 10^{-4}$</td><td>0.84</td></tr>
<tr><td>K_e ($V/rad/sec$)</td><td>0.034</td><td>1</td></tr>
<tr><td>K_t ($N \cdot m/Amp$)</td><td>0.034</td><td>1</td></tr>
<tr><td>R (Ohm)</td><td>1.32</td><td>0.71</td></tr>
<tr><td>L (H)</td><td>0.82</td><td>0.40</td></tr>
<tr><td rowspan="3">PID</td><td>K_p</td><td>0.085</td><td>22.9</td></tr>
<tr><td>K_i</td><td>0.77</td><td>7.5</td></tr>
<tr><td>K_d</td><td>0.005</td><td>1.2</td></tr>
</table>

Vacuum pump feedback control: The vacuum pump generator assembly, as shown in **Figure 4.4**, contains a micro air pump driven by a vacuum DC motor (ROB1038, SparkFun Electronics, USA), a solenoid valve (DN20, DFRobot), and a pressure transducer (PX209, Omega, USA). Vacuum pressure is controlled by the coordination between the DC micro air pump motor and the solenoid pressure valve. The air pump creates vacuum when solenoid valve closes and release air when valve opens. The vacuum transducer captures the pressure generated by the vacuum pump and provides analog signal to Arduino Mega for PID closed-loop feedback control. Parameters of the identified transfer function are listed in Table 4.1. In the closed-loop vacuum pump control, designed PID parameters are embedded into Arduino IDE to generate a control signal with pressure feedback from the sensor and achieve real-time vacuum pressure tracking control under real constraints and disturbances.

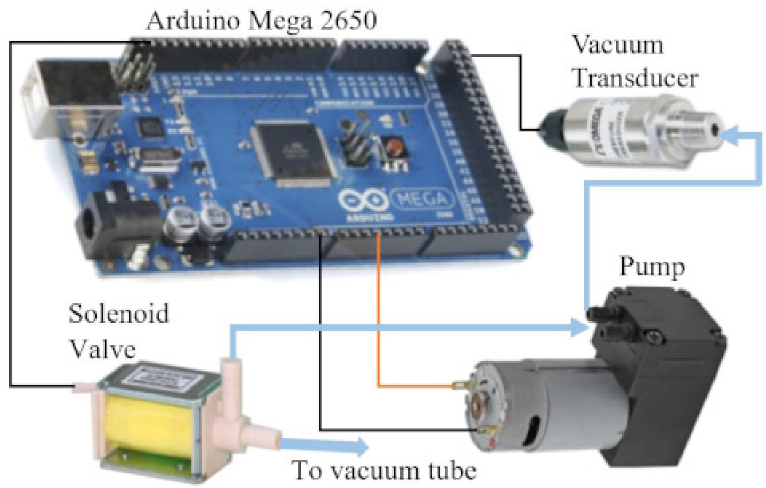

Figure 4.4: Electrical architecture for vacuum motor PID control

4.1.4 Measurement System

Pressure Measurement on the Breast: Pressure variations on the breast, which are performed by the humanoid infant head are measured and recorded with flexible and thin piezoelectric force sensors (FSR^{TM} Interlink 408, Interlink Electronics, Los Angles, USA). The sensor strips are placed on the upper surface and lower surface of the breast with their center-lines coincidence with the mid-sagittal plane of the milk duct following the displacement on (Jiang and Hassanipour, 2020a).

Tongue Motion Image Capture and Processing: The camera module used for capturing the tongue motion and the nipple deformation during suckling is the ArduCAM Mini 2MP. The camera has a resolution of 1600×1200, and an uncertainty of 3×3 pixels. The camera is mounted on a laser cut transparent 3mm thick plastic board, which is inserted in the T-slot of the frame that allows for positioning. **Figure 4.5** provides a sequence of images captured with the camera. The features of the camera measuring system include an OV2640 image sensor, I2C and SPI interfaces support (ArduCAM, 2018). The I2C interface is used for the internal configuration of the sensor and the SPI interface is for the camera configuration and control. Image data is captured and transferred to a PC from Arduino

UNO board via FIFO (First-in-First-out) data class. Sequential images are captured at 15 frames per second. All images are stored on PC through a self-designed Graphical User Interface (GUI). Edge detection of the images are performed using MATLAB programming for tracking the nipple deformation and tongue movement during suckling dynamics.

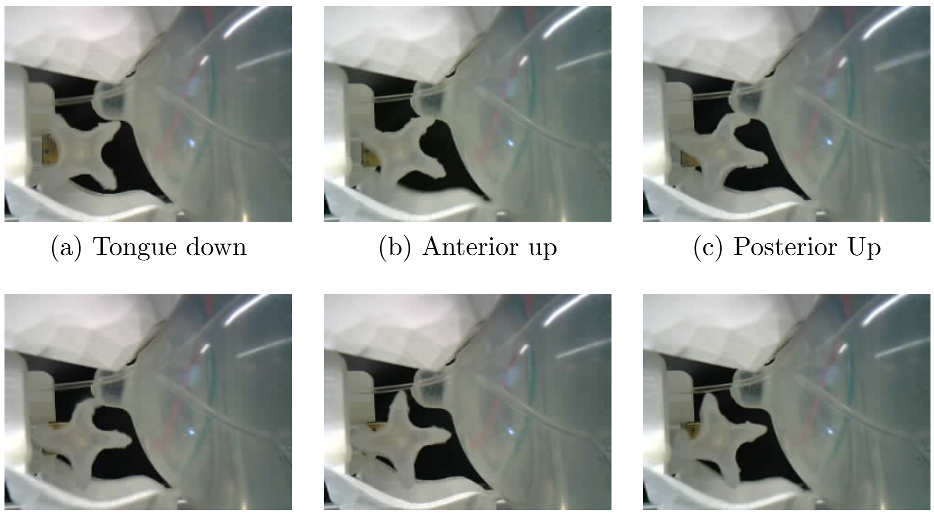

(a) Tongue down (b) Anterior up (c) Posterior Up

(d) Tongue up (e) Posterior down (f) Anterior down

Figure 4.5: Image sequence of tongue motion captured by ArduCAM in the apparatus.

Outlet Flow Measurement: To measure the human milk instantaneous flow rate at the milk duct outlet, two flow measurement systems are utilized synchronously and cross-validated with each other during testing. The mass flow rate is measured with a digital flow meter (Water flow sensor YF-B3, Seeed Technology Co., Ltd) integrated on Arduino Mega 2650 board. Since the flow meter only outputs a digital signal when fluid flows through it, the continuous monitoring of the mass flow rate is depicted using MATLAB data processing after each test. The outlet flow velocity magnitude is measured via time-resolved particle image velocimetry (PIV) flow measurement system (TSI, Inc., MN, USA). The human milk analog fluid for PIV experiments is prepared using the information from the author's previous work (Jiang et al., 2020). Density of the analog fluid is 1.123 g/cm^3. Seeding particles with

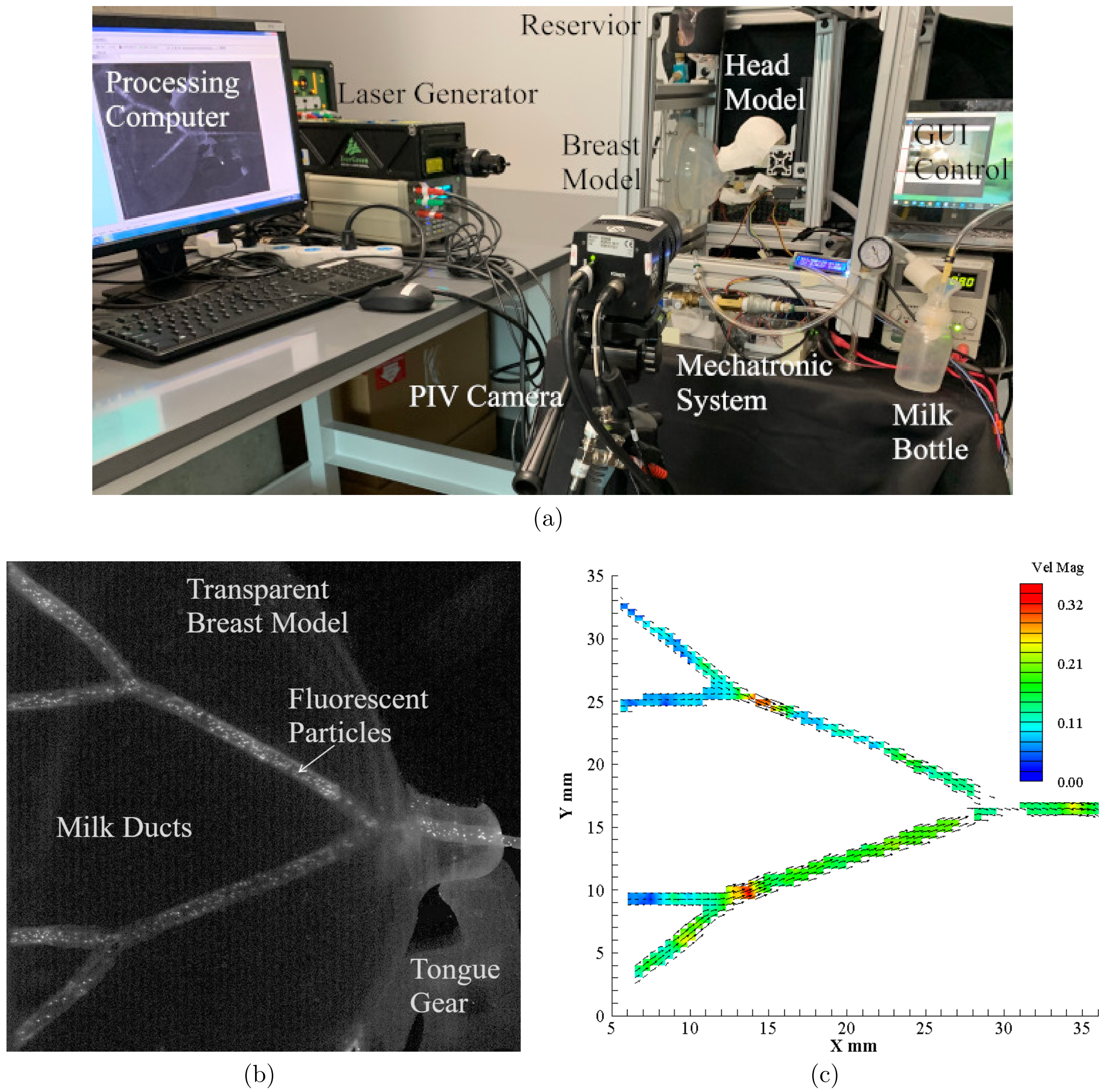

Figure 4.6: (a) BIBS setup with PIV measurement system, (b) Raw PIV image on the breast phantom during experiment, and (c) A sample processed PIV velocity magnitude image during breastfeeding mimicking experiment.

45 μm in diameter (CoSpheric. LLC, Santa Babara, CA, USA) and 1.120 g/cm^3 in density is matched to the analog fluid for PIV visualization.

The PIV measurement system includes a dual pulse Nd-YAG laser, a CCD camera (TSI PowerView 4M Plus), a group of optics, a synchronizer and an image processing software as shown in **Figure 4.6a**. The lasers worked at a frequency of 2 Hz with a wavelength of 532nm and an energy of 100mJ per laser to illuminate a vertical plane parallel to the flow outlet direction. Images on the mid-sagittal plane of the breast phantom were acquired at 2 Hz upon a temporal gate of $500\mu s$. **Figure 4.6b** demonstrates an example of the PIV captured image of the ductal structure during experiment. The thickness of the laser sheet was set as 2 mm to reduce the out-of-plane measuring error (Raffel et al., 2018a). The CCD camera is 2352×1768 pixels resolution with a pixel size of 5.5mm×5.5mm, operates at 16 frames per second and provides a 12-bit or 14-bit output, with a 190ns frame straddle time. Canon adjustable lens are utilized to focus on the area of interest in the experiment. The images pairs are recorded and processed using Insight 4G software. Images of the calibration are captured, processed and calculated based on the known dimensions of the ducts to compute the real particle displacements during each test. A total of 100 images were recorded in each run of the experiment. The instantaneous velocities are processed and analyzed offline using Insight 4G.

4.1.5 Graphical User Interface (GUI) Design

To offer an easy-to-use software interface for users to simulate different oral suckling behavior on this infant suckling simulator, an intuitive GUI is developed using Java-based Processing I^3 IDE under the Windows System. The GUI architecture used for the simulator is illustrated in **Figure 4.7**.

The PC first identifies the number and location of the serial ports that are connected with Arduino controllers. There are two serial port connections: 1) data port is connected to Arduino Mega, and 2) image port is connected to Arduino Mega. After serial ports are identified and classified, it starts to read serial data. The GUI allows the user-define inputs and deliver the data to the corresponding serial port. Arduino IDE reads the inputs and send command signals to the motors in the simulator. GUI then reads the digital and analog data

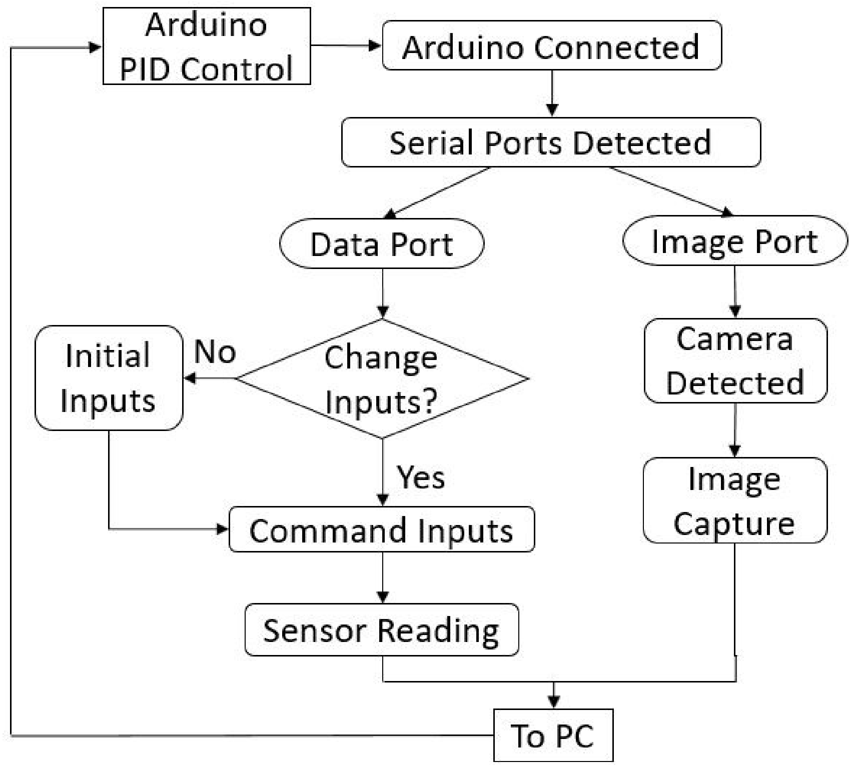

Figure 4.7: GUI Flow Chart for User

from Arduino Mega through the data serial port. Image port transfer data through Arduino UNO independently as the image data is not compatible with the measured pressure and flow rate data. The GUI output contains three parts of information: 1) user-defined inputs; 2) real-time data outputs; 3) motion capture.

User-defined Vacuum and Oral Cavity Dynamics: Frequency match of the tongue, jaw and vacuum pressure is essential to imitate infant oral suckling pattern with high-fidelity. The GUI allows the user to program a vacuum profile using vacuum peak to peak value, frequency, and amplitude shift. Coordinated signals are matched and generated in Arduino IDE.

Real-time Data Outputs: The real-time data readings are presented in the left column of the GUI. Digital readings from digital flow meter are presented in the first row, analog pressure readings from FSR sensors are demonstrated in the second and third rows. Instant data values are presented following the start time of the plot for data monitoring.

Motion Capture: Images are captured at 15 fps by ArduCAM Ov2640. Captured images are saved with frame numbering and time information to the GUI directory folder named "Captures". The image capturing and data outputs operate in a concurrent matter as shown in **Figure 4.8**.

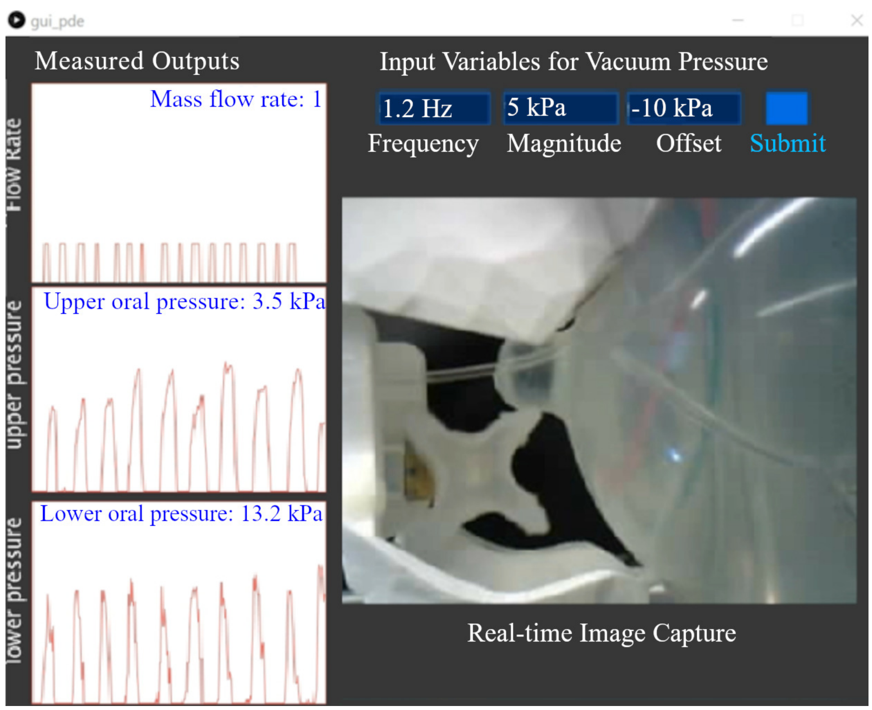

Figure 4.8: GUI results

4.2 Results

To demonstrate the success imitation of the bench-top infant suckling simulator, we have conducted experiments with two user-defined profile.

Case 1: Constant suckling frequency of 1.2 Hz, local minimum vacuum at -15kPa, and local maximum vacuum at -5kPa in the entire duration of 10 seconds (Eq.4.2).

$$P_{vac.}(t) = -5cos(2.4\pi t) - 10, \quad 0 \leq t \leq 10\,s \tag{4.2}$$

Case 2: The vacuum frequency of first 5 seconds is 0.6 Hz, and the frequency for the next 5 seconds is 1.2Hz. Local minimum vacuum and maximum vacuum for the first five seconds is -20 kPa and -8 kPa, whereas the local minimum vacuum and maximum vacuum for the last five seconds is -15 kPa and -5 kPa. (Eq.4.3).

$$P_{vac.} = \begin{cases} -6cos(1.2\pi) - 14 & 0 \leq t \leq 5\,s \\ -5cos(2.4\pi t) - 10 & 5 \leq t \leq 10\,s \end{cases} \tag{4.3}$$

Twenty times of ten-second trials are repeated for each case. Averaged time-resolute results of oral pressures (vacuum, upper palate and jaw) and outlet flow velocity are presented as below, followed by uncertainty analysis for the setup.

4.2.1 Results for User-defined Constant Suckling Frequency (Case-1)

Figure 4.9 shows the dynamics of the vacuum pressure and the positive pressure (compression) on the breast. Vacuum data captured by the related sensors are compared with user-defined inputs. As expected from the MATLAB simulation, the vacuum frequency quickly and closely matched with the given frequency. The tracking error of vacuum pressure decreases to $\pm 1.3\%$ within 5 seconds. Meanwhile, the measured positive pressure on the breast reveals a sinusoidal signal that matches with the vacuum frequency of 1.2 Hz. The jaw motor can stably and dynamically track the above vacuum change with small phase errors. Values of the jaw pressure range from 0 to 15 kPa with an average of 7.8 kPa, which are in good agreement with the in vivo clinical data in (Alatalo et al., 2020). Palate pressure in **Figure 4.9** presents a constant and stable sinusoidal wave range from 2-5 kPa. As the infant's upper head is kept in position during the experiment, the varying pressure is

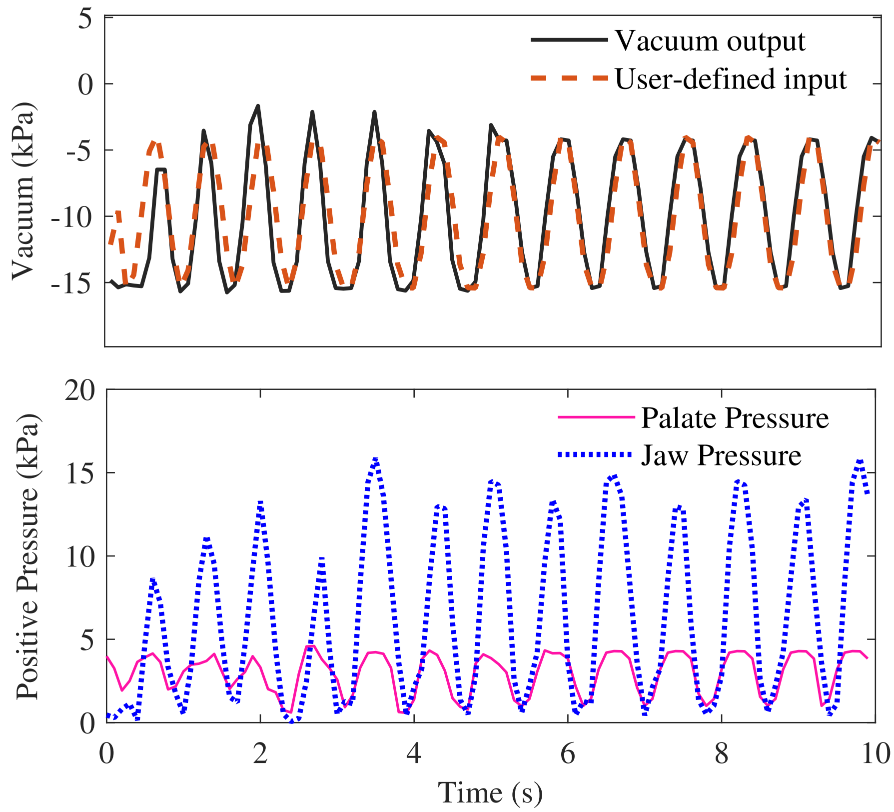

Figure 4.9: Oral pressure results for constant suckling frequency.

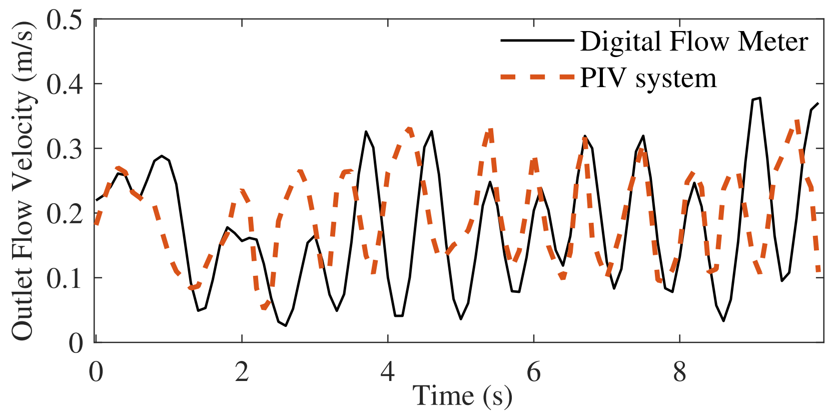

Figure 4.10: Outlet flow velocity for no frequency varying inputs

most likely coming for the breast deformation during active suckling simulations with the apparatus.

Figure 4.10 presents the outlet flow rate under a constant suckling frequency for 10 seconds. As described in section 4.1.4, outlet flow velocity is captured and analyzed using two systems. One is digital flow meter reading via Arduino and GUI interface. The other is the PIV measurement system for validation. Note that the digital meter is connected to the tube extended out from the breast ducts, which cause a phase difference compared to PIV as the it tracks the fluorescent particles in the fluid to measure flow rate at a designated position. Dynamic flow rate measured by both systems demonstrate an arbitrary and nonlinear flow velocity at the outlet of the breast. The mean and standard deviation of the outlet flow velocity is 0.196 ± 0.112 by digital meter and 0.201 ± 0.107 by PIV. Mean value difference between two measurement systems is 4.3%, which indicates the portable digital flow meter measure the flow rate in a good agreement with PIV measurement system and can be used as an alternative portable flow rate measure system for the simulator.

4.2.2 Results for User-defined Variable Suckling Frequency (Case-2)

Figure 4.11 shows measured real-time positive pressures of upper and lower jaw, as well as the tracking performance of the pressures generated by the oral suckling simulator under a varying frequency during the 10 seconds of suction. As can be seen from the output vacuum pressure, frequency matched with the defined inputs in 4 seconds. When frequency changes from 0.6 Hz to 1.2 Hz, the simulator can achieve the desire frequency tracking in one cycle. Tracking error decreases to $\pm 1\%$ at time $= 8s$, 3 seconds after transient variance of vacuum frequency and magnitude. The results show that no significant magnitude change for upper pressure, but frequency matches with the vacuum dynamics. The average palate pressure for lower frequency suckling is $2.31 \pm 0.79kPa$ higher than that for higher frequency suckling. Oral pressure results match with the clinical observation of the infant suckling pattern during breastfeeding (Alatalo et al., 2020).

Figure 4.12 demonstrates the flow rate variation for Case 2. The mean and standard deviation outlet flow rate for lower frequency for the first five seconds is $0.143 \pm 0.122m/s$ by digital meter and $0.157 \pm 0.131m/s$ by PIV. Mean value difference between the digital meter and PIV system for the first five seconds is 9.7%. During 5-10s, when frequency raises from 0.6 Hz to 1.2 Hz, the average flow rate is measured as $0.198 \pm 0.120m/s$ by digital meter and $0.189 \pm 0.133m/s$. Mean value difference between the two systems is 4.54% and in good agreement with those in Case 1.

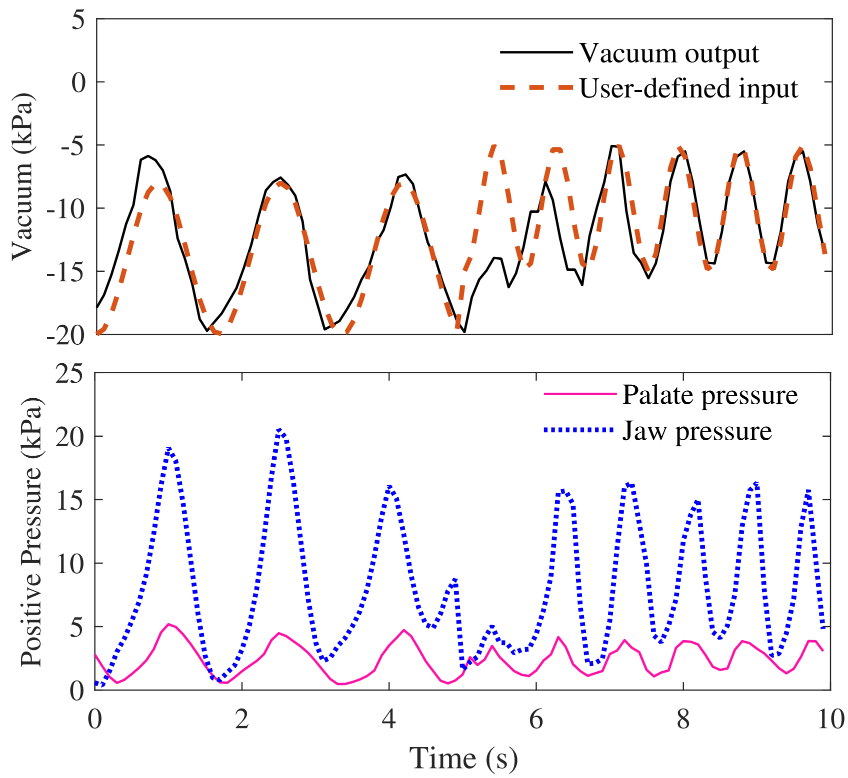

Figure 4.11: Oral pressure results for varying frequency inputs

4.2.3 PIV Flow Rate Analysis on Different Vacuum Pressure and Frequencies

To evaluate the effect of vacuum frequency and strength on flow rate, we conducted a comparison study with various conditions. Mean outlet flow rate and standard deviation of each test repeated twenty times are presented in **Figure 4.13**. Flow rate increases apparently as vacuum pressure becomes stronger, especially for higher frequency. No significant difference

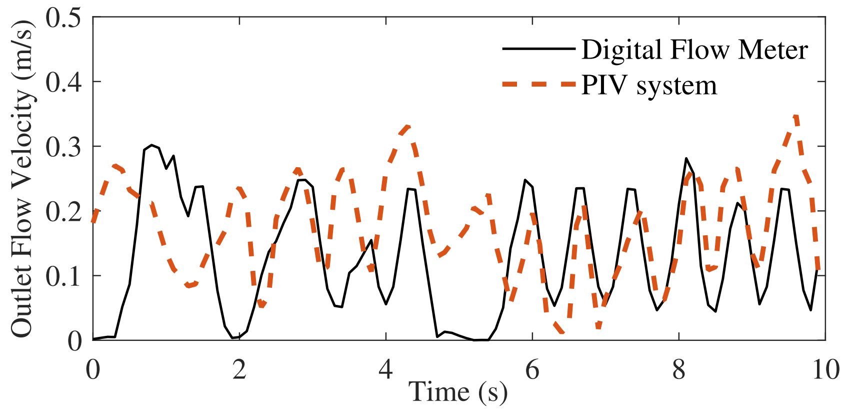

Figure 4.12: Outlet flow velocity for varying frequency inputs

of outlet flow rate is observed between 1.2 Hz and 1.8 Hz groups. The comparison study indicates that vacuum strength plays the most important role for the milk ejection. This finding matches with a previous study of testing the effect on milk ejection of breastfeeding mothers with different pumping pattern using breast pumps (Kent et al., 2003).

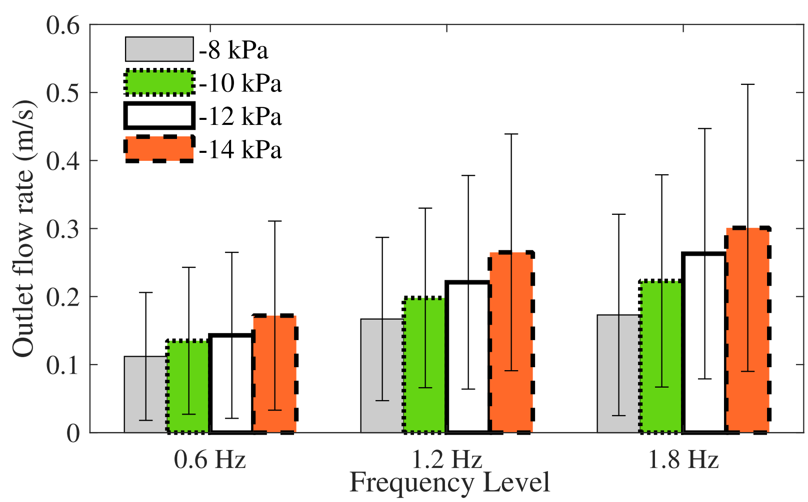

Figure 4.13: Outlet flow rate captured by PIV system of different vacuum frequency and strength.

4.2.4 Uncertainty Analysis

The pressure and flow rate data of the bench-top infant suckling simulator is highly nonlinear and unpredictable due to the complexity of the hardware settings and operation systems.

Maximum absolute error (MAXE) and the root mean square error (RMSE) have been computed from Equation 4.4 and Equation 4.5, respectively. X_i is the actual state during experiments, and X_d is the desired state. N is the number of samples.

$$MAXE = \max_{N} |X_i - X_d| \tag{4.4}$$

$$RMSE = \sqrt{\frac{\sum_{i=1}^{N}(X_i - X_d)^2}{N}} \tag{4.5}$$

The values of MAXE and RMSE are illustrated in Table 4.2 for all tested data sets. The filtered vacuum pressure and motor speed signals are approximately equal to the original signals with the percentage maximum error and the RMSE of 7.67% and 5.65% respectively.

Table 4.2: Error analysis for vacuum pressure and motor rotational speed.

	MAXE	RMSE
Vacuum Pressure (kPa)	1.15 kPa	0.91 kPa
Motor Speed (rpm)	1.13 rpm	0.64 rpm

Sensing error accumulated from sensors are calculated using Kline-McClintock(Kline and McClintock, 1953) analysis in Equation 4.6. Maximum error caused by vacuum motor and tongue motor are also considered.

$$\begin{aligned} U_{pressure} &= \sqrt{U_{FSR_1}^2 + U_{FSR_2}^2 + U_{motor}^2} \\ U_{flowrate} &= \sqrt{U_{vac}^2 + U_{flow}^2 + U_{PIV}^2} \end{aligned} \tag{4.6}$$

U_{FSR}, U_{flow}, and U_{PIV} are calculated based on the sensor uncertainties listed in Table 4.3 from the specific data sheet provided by manufactures.

Table 4.3: Resolution in sensors, camera and image processing

Sensor	Usage	Resolution
Interlink FSR 408 (Lebosse et al., 2011)	Force/Pressure	0.1N/440 Pa
Seeed YF-DN50 (Mulik et al., 2021)	Flow Rate	$< 5\%$
ArduCAM 2MP OV2640 (ArduCAM, 2018)	Images	2×2 pixels
PIV Insight 4G (Raffel et al., 2018b)	Flow rate	<1%

Accumulated percentage uncertainty for pressure sensing and flow rate measuring is 6.79% and 4.21% respectively. All percentage uncertainties less than 10%, which indicates a real-time stability and feedback robustness of the simulator to imitate breastfeeding patterns.

4.3 Discussion

This work presents a bench-top, portable and user-friendly bioinspired breastfeeding simulator (BIBS) integrated with software interface and feedback controllers for the purpose of in vitro monitoring of the infant breastfeeding pattern (Figure4.14). The architecture contains a previous developed bio-inspired breastfeeding simulator (BIBS) (Jiang and Hassanipour, 2020a), linear motor feedback controllers with PID control algorithm, thin and flexible piezoelectric pressure sensors, digital flow meter for outlet flow rate measurement, and particle image velocimetry system for flow rate validation. In particular, a software interface compatible with Arduino has been developed in this work for real-time data monitoring and image capturing and its response has been compared with clinical data presented in (Alatalo et al., 2020). We performed two types of tests in laboratory to test the reliability and robustness of the updated simulator in applying arbitrary user-defined oral pressures and tongue movement. Our results confirmed the better performance with the feedback control loops for vacuum pressure tracking and tongue motor speed control. The updated BIBS mimics infant oral suckling behavior with a better fidelity.

Possible limitations in the use of the integrated simulator may due to the offline PID parameter generation and some of the simplifying assumptions made. The PID control is

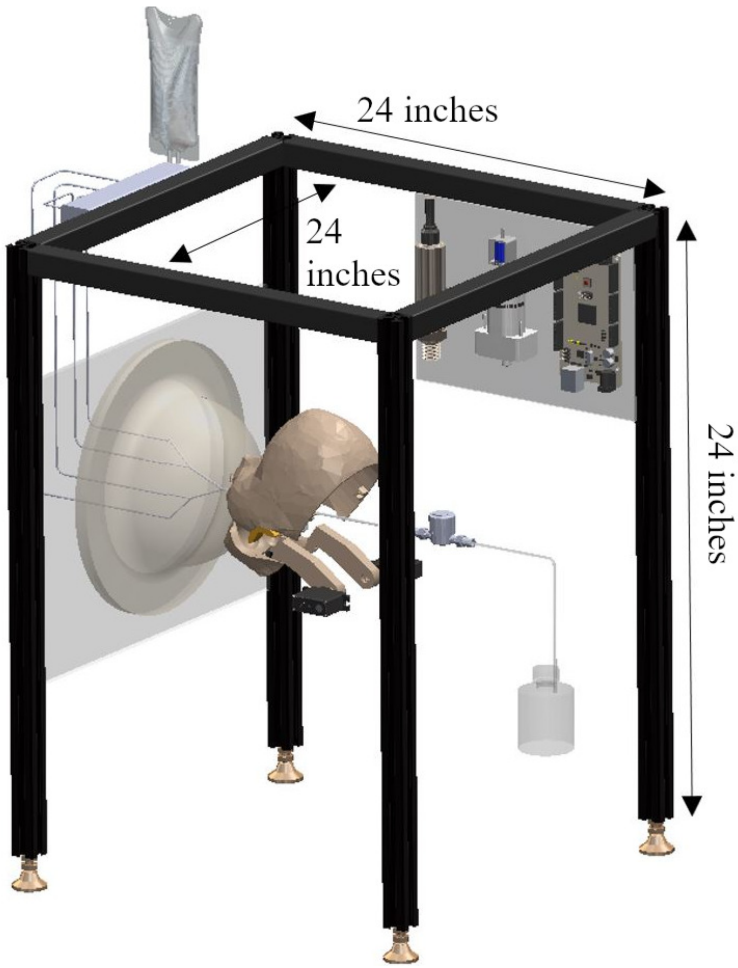

Figure 4.14: A Portable, adjustable and user-friendly BIBS (24x24x24 in^3) integrated with software interface and feedback controllers

based on the transfer function of the motors, which is generated by open-loop testing. Adaptive real-time PID control will be more precise in tracking the vacuum pressure and tongue position, but will also increase the computational cost. The current maximum percentage error in the simulator is $< 10\%$, which is acceptable as a preliminary medical simulator. Additionally, our simulator uses rigid replicas for the infant head and jaw model. The lack of accessory muscle and oral structures limits the deformation caused by infant oral and breast interaction. Future work for this simulator includes adding silicone made infant face, lip, mouth muscle and palate geometry to better represent infant's mouth cavity, and applying advance level of control algorithm to process the data in real-time. This will also help in the study of soft material to semi-soft material interaction. These two material/ structures, the breast and the infant head have different stiffness, deformation behavior and the resulting interaction will be unique.

Despite these challenges, this work provides a much more accessible and robust simulator to evaluate the effect of infant oral suckling on the breast and breast milk extraction. Our new BIBS setup drives oral pressures on the breast with electrical motors and soft tongue gear actuator. Integrated with GUI and PID control unit, the apparatus is the first known fully controllable simulator that replicates the biomechanics of breastfeeding and functions as an educational, training, and research tool. We can tune the jaw and tongue movement based on the varying vacuum frequency and strength to match the physiological mechanics of infant's oral suckling during breastfeeding. Additionally, the simulator evaluates the milk outlet flow rate of various vacuum suckling pattern quantitatively and more sensitive than the existing metrics. Our results show that stronger vacuum yield to a higher milk consumption, which is in accordance with literature findings (Kent et al., 2003). We also process the captured images to compare with ultrasound nipple and breast deformation, which prove the validity of the soft robotic tongue gear to mimic peristaltic like tongue movement during breastfeeding. These results confirm the simulator we developed can be used as a reliable assessment of the suckling behavior for breastfeeding infants at different ages.

4.4 Conclusion

This work implements a software interface and feedback controllers in a bio-inspired breastfeeding simulator (BIBS) to allow real-time data display, user input variables and effective tracking of the command signals. The developed user-friendly and portable apparatus includes multiple sensors to measure and observe the effect of changing oral suckling pattern on milk flow pattern. The acquired data demonstrated the stability of the apparatus to simulate physical movement of infant suckling during breastfeeding, as well as to be used as an educational medical simulator in vitro. This model is an innovative mechatronic system and an effective pedagogical tool for studying the biomechanics of breastfeeding with infant oral mechanism in a user-controlled, interactive manner.

CHAPTER 5

A HUMAN MILK MIMICKING FLUID (HMMF) FOR PARTICLE IMAGE VELOCIMETRY SYSTEMS[1]

5.1 Introduction

Over the past two decades, particle image velocimetry (PIV) systems have been developed extensively for studying bio-fluid transportation (Schröder and Willert, 2008). Optical clearness of the model and particle movement visualization in the fluids are important characteristics and requirements of a successful PIV experiment. However, for some applications, such as vascular models with complex geometry, these requirements cannot be easily satisfied (Yousif et al., 2011).

Refractive index (RI) matching is the key to solve distortion problems and allows more precise PIV measurements with high-speed cameras. Previous models used in PIV experiments on fluid dynamics have been built with transparent materials such as glass, acrylic, and polypropylene. Recently, PDMS/silicone are of particular interest in bio-fluid flow research due to their flexibility, excellent optical clarity, elasticity, and tissue-mimicking abilities. In addition to RI matching fluids with solids in PIV experiments, matching the rheological properties of the non-Newtonian analog fluid in the PIV experiment requires further attention.

Studies in large vessels with shear rates above 500 s^{-1} use solutions of glycerin (Gly) with sodium iodide (NaI) in distilled water (DW) as a Newtonian blood-mimicking fluid (Najjari et al., 2016). When lower shear rates or complex geometries are considered, the addition of xanthan gum (XG) produces a shear-thinning non-Newtonian fluid with viscoelastic properties (Sworn et al., 2011) and is considered the best choice for blood mimicking fluids (Brookshier and Tarbell, 1993). While the viscosity of an experimental fluid is adjusted by varying

[1] © 2020 Reprinted, with permission, from Lin Jiang, Diana L. Alatalo, and Fatemeh Hassanipour. "A human milk-mimicking fluid for PIV experiments." Experiments in Fluids 61.10 (2020): 1-7.

the Gly/DW ratio, the RI increases as the ratio increases (Yousif et al., 2011) and must be adjusted with NaI. The manipulation of these components to develop a RI-matched, optically clear PIV fluid to imitate blood has been reported in multiple studies (Yousif et al., 2011; Brookshier and Tarbell, 1993; Najjari et al., 2016). However, no human milk mimicking fluid with refractive index, density, and the rheological match has been discussed.

Human milk is a complex non-Newtonian bio-fluid with similar rheological behavior as the blood that must flow through a complex system of bifurcating ducts during breastfeeding (Alatalo and Hassanipour, 2020). For *in vitro* flow experiments, a human milk mimicking fluid (HMMF) must exhibit the same non-Newtonian characteristic of human milk while RI matching the phantom materials and maintaining optical clearness.

In this study, a NaI-Gly-XG-DW solution is used to formulate a non-Newtonian HMMF for PIV experiment in a self-designed breast phantom (Jiang and Hassanipour, 2020b). The dynamic viscosity of HMMF is tested under room temperature and compared with human milk at body temperature. The effect of NaI/DW ratio, Gly/DW ratio, and XG/DW ratio on the RI values, density, and viscosity curve is investigated. A formula for HMMF at room temperature with a range of RIs matched to the silicone elastomers in the breast phantom and exhibiting a similar dynamic viscosity of the human milk is derived for use in PIV experiments.

5.2 Methods

5.2.1 Viscosity, Density, & RI Measurements

Frozen human milk was donated by seven moms according to IRB 17-102 approved by The University of Texas at Dallas Internal Review Board. Human milk samples were thawed in warm water tested at $37 \pm 0.2°C$. HMMF samples were tested under room temperature at $22.3 \pm 0.2°C$. Viscosity was tested on a rheometer (Anton Paar MCR 302) using a double-gap concentric cylinder geometry. After a 4 minute pre-shear at 0.001 s^{-1}, a logarithmic shear ramp of 0.01–3000 s^{-1} was applied and data recorded 10 points/decade. A density meter with an accuracy of ± 0.001 g/cm^3 (Anton Paar DMA 501) measured the density of all samples at previously stated temperatures. The RI of PIV materials (solids and fluids) was measured with a refractometer (TORC 5000, Anton Paar), which has an accuracy of ± 0.00002. RI and density of each HMMF sample were repeated five times with mean and standard deviation calculated. Kinematic viscosity curves were derived by dividing dynamic viscosity data by the mean density of each sample for comparison.

5.2.2 Lactating Human Breast Phantom

An optically clear, flexible, and elastic breast phantom was designed to mimic a human breast in the setup as shown in Figure 5.1. The breast phantom contains a breast shell (or skin), transparent filling water-based gel (Zerdine gel, CIRS, Norfolk, VA, USA), and the ductal structure. The phantom was manufactured with idealistic dimensions based on *in vivo* geometric characterization, using injection molding and lost-material casting technique as outlined in (Jiang and Hassanipour, 2020b).

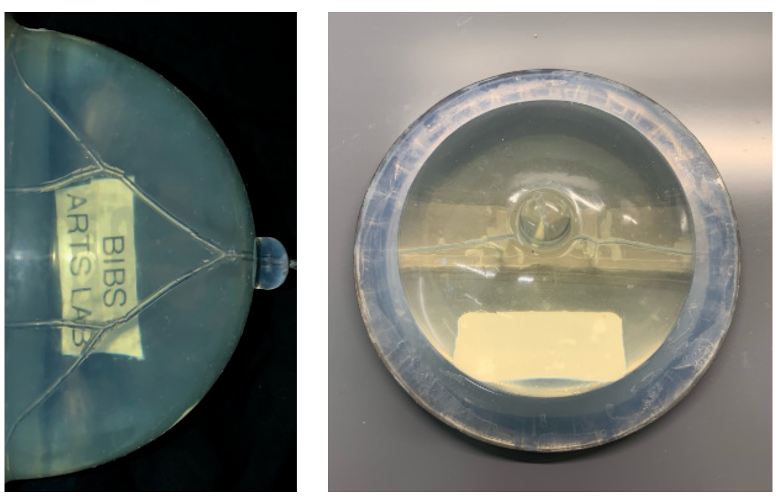

(a) (b)

Figure 5.1: The lactating human breast phantom (a) side view, and (b) top view.

5.2.3 Materials for Development of HMMF

Based on the rheological profile of the raw human milk samples, Gly and DW provided a Newtonian solution to approximate viscosity as shear rate approaches infinity while the addition of XG enabled the HMMF to imitate the non-Newtonian property at relatively low shear rates ($< 10^2 s^{-1}$). NaI enabled matching the target RI of the breast phantom. Materials were weighed by electronic balance with 0.0001 g resolution (Analytical Balances ML204T, Mettler Toledo, Switzerland) and mixed as percentages of weight to total fluid mixture weight (w%w). Each formulation required approximately 30 minutes for the solids to completely dissolve in the Gly before being added to DW.

An initial solution composed of 5% NaI and 10% Gly w%w was prepared toward a RI of 1.357, which was the lower bound of the RI of the breast phantom composite materials. Five fluid samples were prepared for each level of the NaI concentration but increasing ratios of Gly. Four groups of different concentration levels of NaI ranging from 5% to 20% were generated to achieve a range of RI values from 1.357-1.436. The impact of XG on RI was not previously reported. Therefore, two series of solutions were composed, one with just NaI and Gly, the other with NaI, Gly and XG.

5.3 Results and Discussion

The RI of the breast phantom provided the target RI for the HMMF. The RIs for the breast skin and duct are the same, as they are both made of Slygard-184 silicone PDMS material (Dow Corning Corp., Midland, MI, USA). Reported RI for PDMS mixed ratios of the base to the curing agent 10:1 at 532nm wavelength (specific for PIV laser wavelength) is 1.414 ± 0.0008. The measured RI for the Zerdine Gel and the composite breast phantom are 1.363 ± 0.011 and 1.396 ± 0.021, respectively. The target RI matching system for HMMF to optically match with the breast phantom is 1.357-1.417 based on the RI measurements of different materials used in the phantom. RI was found to vary linearly with NaI concentration and Gly concentration as shown in Figure 5.2a. XG failed to significantly impact RI.

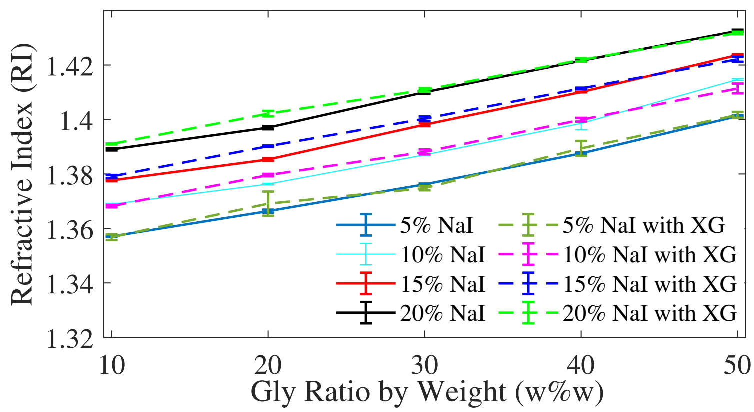

(a)

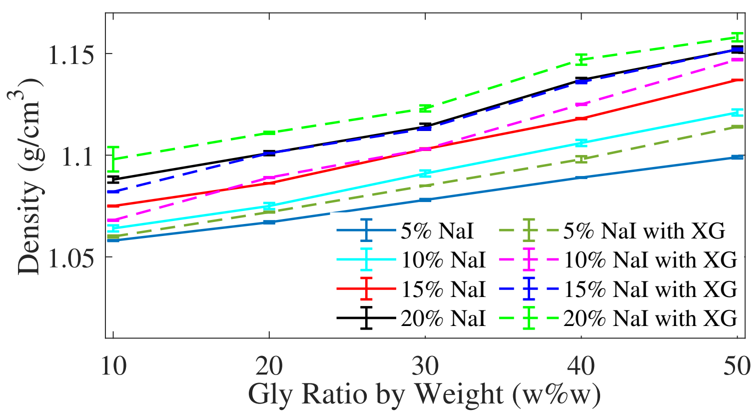

(b)

Figure 5.2: Variations in (a) RI and (b) density for different formulations of HMMF, both with (dashed lines) and without (solid lines) XG.

Table 5.1: Linear empirical expression of RI and Density in terms of NaI and Gly concentrations in weight percentage (w%/w)

Terms	Fitted Equation	R^2	$RMSE$
RI	$n = 1.336 + 2.180 \times 10^{-3} NaI$ $+1.107 \times 10^{-3} Gly + 5.201 \times 10^{-3} XG$	0.9779	0.691×10^{-3}
Density (g/cm^3)	$\rho = 1024 + 2.714 \times 10^{-4} NaI$ $+1.714 \times 10^{-3} Gly + 2.167 \times 10^{-2} XG$	0.9712	5.180×10^{-3}

Similarly, densities of samples were measured to find the appropriate match for HMMF. Figure 5.2b shows the mean density from five times of the measurements of different NaI, Gly, XG, and DW concentrations. Density was also found linearly related to the Gly and NaI concentration for both Newtonian and non-Newtonian fluids. Additionally, adding XG in the NaI-Gly mixture increases the overall density of the fluid by $1.81\% \pm 0.32\%$.

As we observed the linear correlations of both RI and density versus concentration ratio, simple predictions of the RI and density tuning on a multi-component fluid were made using the empirical Arago-Biot (AB) equation (Arago and Biot, 1806), which is based on linear volumetric addition for each component. The AB equation is expressed as $n = \Sigma_i \phi_i n_i$, where n is the RI, ϕ is the volume fraction and i indicate number of components. A linear 2-D regression fit for RI and density in terms of NaI and Gly concentration of the HMMF was described by the equation shown in Table 5.1, where the units for NaI and Gly are weight percentages to total fluid mixture weight ($w\%w$). The accurate fit was achieved in all linear empirical expressions as outlined by R^2 (R-square) and RMSE (Root Mean Square Error) results.

Kinematic viscosity was calculated and reported for both human milk and HMMF samples containing XG in Figures 5.3a and 5.3b, respectively. Non-Newtonian, shear-thinning flow behavior was clearly displayed by milk and imitated in the HMMF samples. A Cross model fit (Cross, 1965) was used to find the nonlinear model for kinematic viscosity (ν) with regards to shear rate ($\dot{\gamma}$). A nonlinear 2-D regression approach was applied to fit the Cross model, which is given by:

$$\nu(\dot{\gamma}) = \nu_\infty + \frac{\nu_0 - \nu_\infty}{1 + K\dot{\gamma}^n} \tag{5.1}$$

where ν_0 and ν_∞ refer to the viscosities as shear rate $\dot{\gamma}$ approaches zero and infinity, respectively. K and n are constants representing the degree and rate of shear thinning. The measured viscosity data for the working fluid and the Cross model fit are shown in Figure 5.4.

An optimized solution for the concentration ratio of NaI, Gly, XG, and DW in HMMF was generated using the genetic algorithm (GA) optimization approach for nonlinear constraints (Homaifar et al., 1994). RI, density, and viscosity curves were input as constraints in the optimization process. The optimized aqueous solution for HMMF is 15.69% NaI, 30.27% Gly, 0.02% XG (w%w) and 54.02% DW. Visual results of the RI matching using the HMMF solution can be seen in Figure 5.5, which fulfilled our PIV experiment requirement to eliminate the effects of tube distortion.

The HMMF is the first transparent liquid that mimics human milk density and the non-Newtonian viscosity properties while matching the RI in the complex silicone breast phantom. The HMMF is inexpensive, non-flammable, and not silicone solvable according to the Material Safety Data Sheet of the PDMS material. The one limitation to be noted is that the HMMF shows a yellowing over time, especially after exposure to air or light for several hours (Narrow et al., 2000). However, this can be resolved by requiring a rinse with DW after use in phantom. Since all the measurements are performed at room temperature, a detailed study of NaI, Gly, and XG-based solutions with regard to temperature fluctuations is required to fully characterize their dependence on temperature and their solubility under heating.

5.4 Conclusion

In this chapter, a sodium iodide (NaI), glycerin (Gly), xanthan gum (XG), and distilled water (DW) solution is used to formulate non-Newtonian human milk mimicking fluid (HMMF) for use in a PIV fluid dynamic experiment with a Y-shaped, bifurcated ductal structure in a silicone lactating breast phantom. Characterization of the RI, density and kinematic viscosity as functions of the NaI concentration and Gly/DW ratio enables the adjustment of the aqueous solution to match the RI of the phantom while maintaining an appropriate density and non-Newtonian viscosity profile of the target biological fluid, human milk.

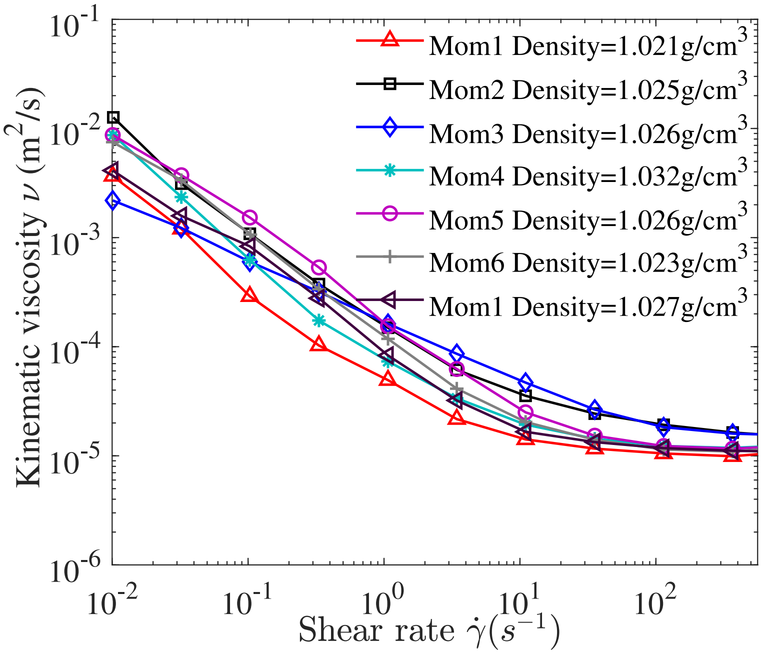

(a)

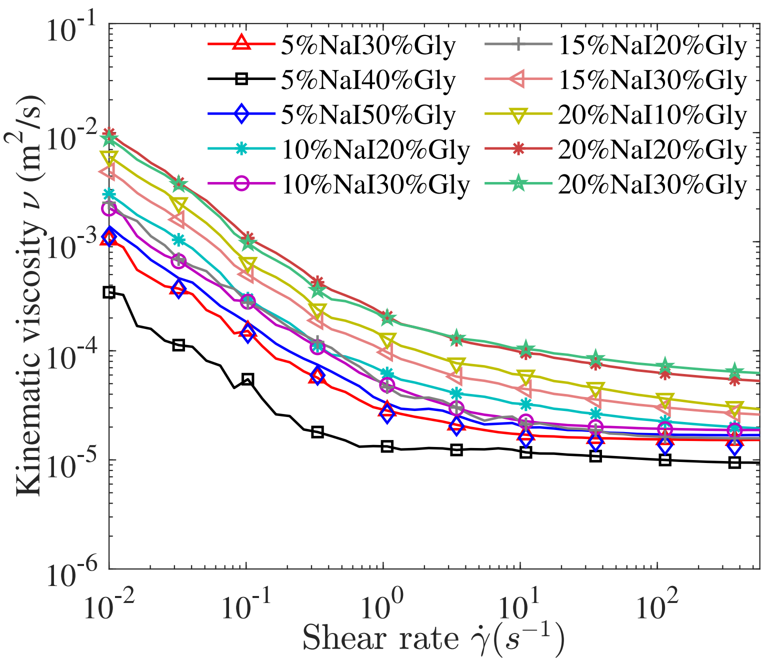

(b)

Figure 5.3: (a) Kinematic viscosity of human milk samples, and (b) Kinematic viscosity of HMMF samples

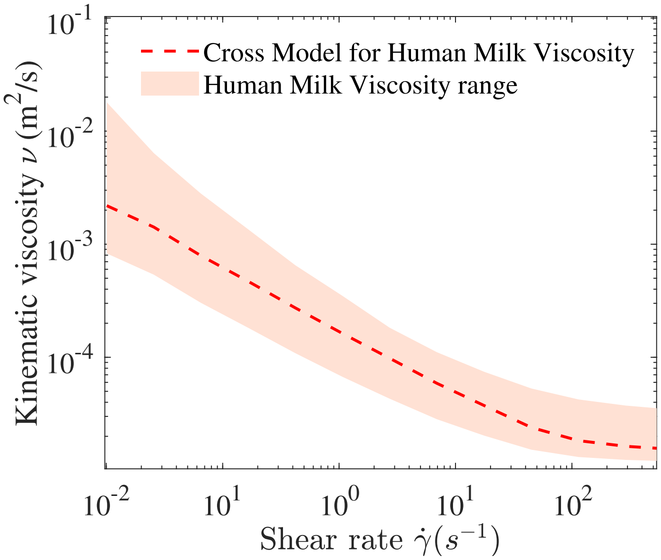

Figure 5.4: Matching the viscosity of human milk.

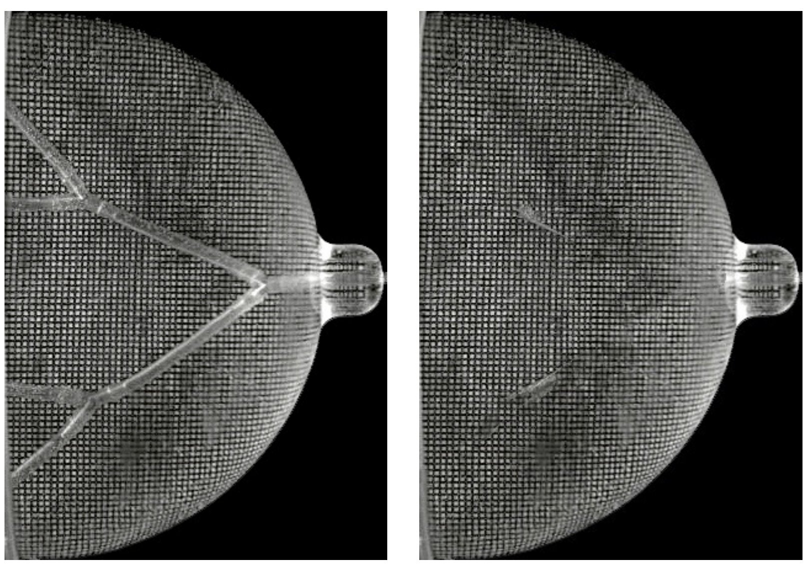

(a) (b)

Figure 5.5: Impact of HMMF in breast phantom. (a) Air in the duct structure illuminates ducts. (b) RI matched HMMF ($n = 1.4012 \pm 0.0007$) in the Y-shaped ducts eliminates visibility of ducts in the breast model

CHAPTER 6

FLOW INVESTIGATION IN MILK DUCTS WITH BIBS

The content of this chapter was adapted from a manuscript to be submitted at the time of writing by the author: Lin Jiang, Fatemeh Hassanipour, "*In Vitro* Flow Visualization in a Bio-inspired Breastfeeding Simulator", *Annuals of Biomedical Engineering*.

6.1 Introduction

The benefit of breastfeeding is well documented. However, only 38% of the infants can receive adequate breast milk during the first month after birth (Schwartz et al., 2002). Decreasing milk supply is largely associated with physical health issues from both mother and child (Odom et al., 2013), such as nipple trauma, nipple infection, breast duct clogging, infant oral malfunctions, and so on. Although mothers work diligently to keep up with the demands of producing milk, they continue to struggle with producing enough volumes of breast milk. Current advice for mothers to increase milk production includes early pumping, hand expression, breast massage, alternative feeding and so on (Becker et al., 2016). However, due to the lack of quantitative measurement of milk velocity and limited access to investigate the instantaneous fluid dynamics in the milk ducts during breastfeeding, the reasons for insufficient milk supply among breastfeeding mothers are unclear. A detailed study is needed in understanding the milk transportation in the breast during breastfeeding.

Efforts to understand the biomechanics of milk flow in the breast have increased in recent years. Some of the well-studied clinical investigations of breastfeeding have explored the oral feeding mechanism (Newton and Newton, 1950), the rhythmic vacuum pressure for milk extraction (Woolridge, 1986), as well as the relationship between the tongue position and the milk ejection (Geddes et al., 2012). While intra-oral pressure can yield adequate volumes of milk for infant consumption, more recent work has demonstrated that mouthing dynamics is also as effective as a vacuum at milk removal (Alekseev and Ilyin, 2016; Alatalo et al., 2020). Besides clinical observations, mathematical modeling (Zoppou et al., 1997; Mortazavi et al., 2015) and computational simulations (Elad et al., 2014; Azarnoosh and Hassanipour, 2020) have studied the milk flow within the breast using the oral applied pressures as boundary conditions. However, clinical studies can only capture flow velocity at the outlet and measure the total milk consumption for the entire feeding period, which contains large randomness and experimental discrepancies. In this study, we aim to use the PIV technique to visualize and measure the flow field in the breast ducts *in vitro* via a bio-inspired breastfeeding simulator (BIBS) (Jiang and Hassanipour, 2020a) created by the authors to mimic infant's suckling mechanism.

This work utilizes a lactating human breast phantom that contains three generations of bifurcated ducts for studying the fluid flow in the breast during lactation. Manipulating of the flow is conducted by a bio-inspired breastfeeding simulator (BIBS) (Jiang and Hassanipour, 2020a). As human milk is a shear-thinning fluid, human milk mimicking liquid that can match the refractive index of the breast phantom is used to provide the similar kinematic viscosity of human milk as discussed in Jiang et al. (Jiang et al., 2020). A non-invasive Particle imaging velocimetry (PIV) experimental system is set to provide a quantitative, instantaneous velocity vector field with good spatial resolution. Temporally resolved velocity measurements are extracted to show the flow field dynamics in the ductal structure in the lactating breast phantom. Wall shear stress of the milk ducts in different generations of the bifurcations is estimated using the method by Charonko et al. (Charonko et al., 2009).

The objective of this study is to investigate the relationship between the oral suckling and milk flow velocity profile in the duct structures *in vitro*. The BIBS setup generates vacuum extraction and oral compression to deform the milk ducts and vary the applied pressure on the breast phantom using real-world infant feeding mechanism conditions. The PIV results show that the oscillatory oral vacuum pressure plays an important role in milk extraction and causes reverse flow in the bifurcated ducts in the artificial lactating human breast. Oral compression and tongue movement affect the geometry in the milk ducts and perform complex fluid dynamics in the duct structure when combined with oral vacuum pressure.

6.2 Methodology

6.2.1 Lactating Breast Model and Infant Applied Pressures

The human breast is a complex organ comprised of bifurcating ducts that evolve during pregnancy and parturition to begin synthesizing and secreting milk. Due to the limitations of reaching the milk ducts from the nipple with catheters *in vivo* beyond the 2nd or 3rd bifurcation (Love and Barsky, 2004b), we design the breast ducts in three generations using the dimensions in Mortazavi et al. (Mortazavi et al., 2015). The synthetic breast model contains bifurcated milk ducts in the breast to mimic the fluid flow path in a lactating breast. This physical model was fabricated and manufactured as outlined in Jiang et al. (Jiang and Hassanipour, 2020a).

To mimic an infant's oral suckling mechanism in vitro, the vacuum pressure, tongue pressure, and jaw pressure are applied by mechanical actuators on the breast phantom to extract milk in the ducts as outlined in (Jiang and Hassanipour, 2020a). Figure 6.1a shows the schematic picture of the position and direction of the applied pressure on the breast model. Figure 6.1b presents the five-second dynamic pattern of the applied pressures. This oral pressure pattern follows the infant's natural suckling. When vacuum peaks, oral compression pressures decrease, whereas when vacuum moves close to atmospheric pressure, oral compression pressure increases. The sinusoidal oral vacuum and the compression pressure values from tongue, jaw, and palate are generated from real-world data from clinical study (Alatalo et al., 2020). Mean and peak values of the input pressures, suckling frequency, and time duration are listed in Table 6.1.

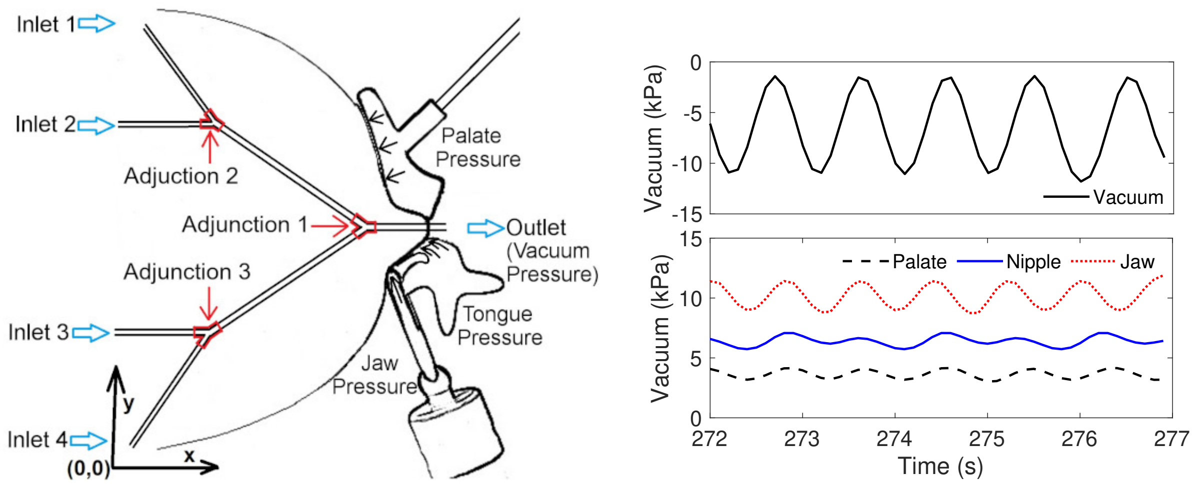

(a) (b)

Figure 6.1: (a) Boundary conditions applied on BIBS, and (b) Averaged pressure data from infants' oral cavity during clinical study (Alatalo et al., 2020)

Table 6.1: Input pressure parameters on BIBS for PIV experiments

	Mean (kPa)	Peak (kPa)	Frequency (Hz)	Time Duration (s)
Vacuum Pressure	-5.35	-11.42	1.19	567.8
Jaw Pressure	9.05	12.36		
Nipple Pressure	5.65	8.04		
Palate Pressure	3.17	4.68		

6.2.2 Working Fluid

Human milk-mimicking Fluid (HMMF), which has been reproduced for use in PIV experiments (Jiang et al., 2020), was utilized in the setup as the working fluid. The non-Newtonian fluid HMMF which also matches the refractive index of the breast phantom at 1.412 is composed of 15.69% NaI, 30.27% Gly, 54.02% water, and 0.02% XG by weight percentage. The clinical data of raw human milk (Alatalo and Hassanipour, 2020) is used to calculate the parameters of the Cross model (Yasuda, 2006), a parametric equation that describes non-Newtonian dynamic viscosity with regards to shear rate. The dynamic viscosity of HMMF used in the PIV experiments is in good agreement with the viscosity of raw human milk.

6.2.3 Experiment Case Configuration

To analyze the fluid dynamics of HMMF in the bifurcated ducts of the breast phantom, comparison experiments that imitate both breast pump suction and natural suckling cases were conducted. Case 1: vacuum only suction, which indicates breast pumps, and Case 2: vacuum plus compression suckling, which mimics infant oral suckling mechanism. The sample input pressure of each component is presented in Table 6.2. Case 1 used arbitrary vacuum pressure only, and Case 2 used the same vacuum profile, but add oral compression pressure from the jaw and tongue. The oral compression pressures have the same vacuum frequency as the vacuum pressure. The correlation between vacuum and oral compression pressure follows the pattern of infant natural suckling during breastfeeding measured by clinical experiments (Alatalo et al., 2020). Each experiment runs last 658.4 seconds and in total 489 sucks. The milk bottle was weighed before and after experiments for liquid weight measurements. Two representative time marks are selected for comparing the velocity magnitude: (1) when the tongue is up, the jaw is up, compression is stronger, and vacuum pressure is weaker; 2) when the tongue is down, the jaw is down, compression is weaker, vacuum pressure is stronger as shown in Table 6.2.

6.2.4 PIV System Setup

Figure 6.2a provides a schematic picture of the PIV experimental setup. Experiments were performed in a transparent, flexible, life-sized lactating breast phantom on a bio-inspired breastfeeding simulator (BIBS) device as outlined in (Jiang and Hassanipour, 2020a). The breast phantom contains three-generation milk ducts that mimic the real-size ducts in the breast. Neutrally buoyant (density designed for HMMF suspension $1.15 g/cc$) fluorescent polyethylene microspheres tracing particles (Cospheric, CA, USA) of a diameter $35 \mu m$ were added to the mixture HMMF for PIV measurements. To perform the experiments, the vacuum pump in the BIBS device draws the HMMF from the IV bags through milk ducts to

Table 6.2: Applied Pressure Condition in PIV Experiment.

Experiment Cases	Input Pressure	Pressure Profile at Nipple
Case 1	Vacuum only	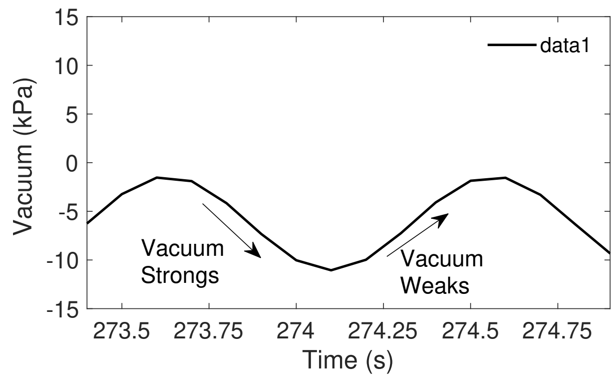
Case 2	Vacuum, tongue&jaw	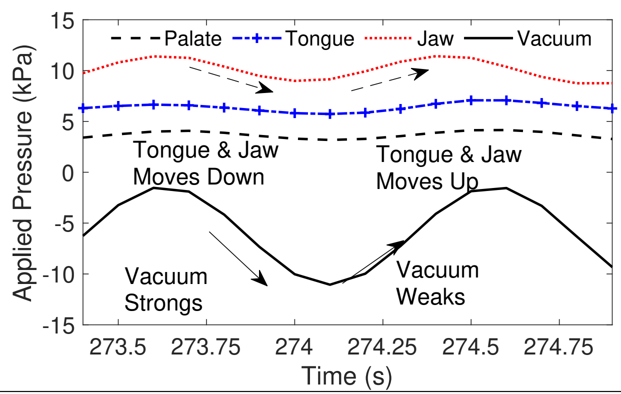

the bottle container by applying an arbitrary suction as outlined in (Jiang and Hassanipour, 2020a). In addition to vacuum, an oral compression pressure from jaw, palate, and tongue movement is applied on the breast phantom to mimic the complete oral feeding mechanism on the breast. Each pressure can be controlled independently. Vacuum Pressure was monitored at the breast phantom outlet tube using an inline pressure transducer (PX209, Omega, USA). Oral compression pressures were measured with piezoelectric force sensors (FSR 408, Interlink Electronics, Los Angles, CA, USA) on the phantom.

A Time-resolved PIV system (TSI, Inc., MN, USA) was utilized to measure the velocity profiles in the mid-sagittal plane of the breast phantom. The PIV measurement system consisted of a dual pulse Nd-YAG laser, a CCD camera (TSI PowerView 4M Plus), a group

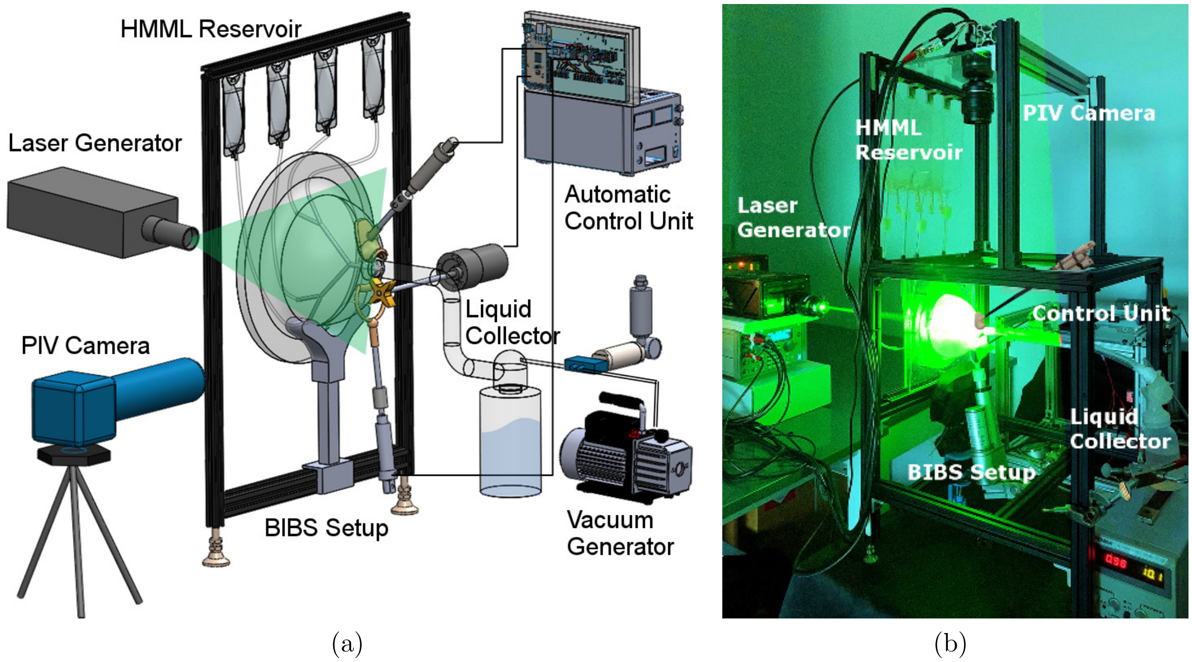

Figure 6.2: (a) Schematic description of the PIV integrated on BIBS setup with laser on mid-sagittal plane of the breast phantom, and (b) Physical PIV setup on BIBS with a top-view camera positions.

of optics, a synchronizer, and an image processing software as shown in Figure 6.2a. The lasers worked at a frequency of 2 Hz with a wavelength of 532nm and energy of 100mJ per laser to illuminate a vertical plane parallel to the flow outlet direction. Images pairs were acquired at 2HZ upon a temporal gate of 500μs for 685s of the total 489 suck cycles. The thickness of the laser sheet was set as 2 mm to reduce the out-of-plane measuring error (Raffel et al., 2018a). The CCD camera is 2352×1768 pixels resolution with a pixel size of 5.5mm$times$5.5mm, operates at 16 frames per second, and provides a 12-bit or 14-bit output, with a 190ns frame straddle time. Canon adjustable lens is utilized to focus on the area of interest in the experiment. In measuring the flow dynamic, both the global view of the milk ducts and its localized adjunction parts were captured separately.

The image pairs were recorded and processed using Insight 4G software. Images of the calibration were captured, processed, and calculated based on the known dimensions of the ducts to compute the real particle displacements during the milk flow test. The interrogation window is 64 pixel×64 pixel with an overlap of 50% to yield the displacement information at the center, borders, and corners of each interrogation region. The second pass used an interrogation area of 32 pixel×32 pixel to enrich the velocity information. The frame frequency is set as 5 Hz, measurement resolution is 142mm×142mm per data point. Cross-correlation between image frames was performed using the fast Fourier transform (FFT) algorithm that reduces interference of noise peaks caused by the random pairings of images of different particles. During the experiment, fifty image pairs were captured each time and then stored in the hard disk. Once this was done, another fifty pairs of the image were captured with the help of the synchronizer. A total of 2000 image pairs of the particles were recorded in each run of the experiment. The mean velocity could be obtained by ensemble averaging the 2000 instantaneous velocities.

6.2.5 Uncertainty Analysis:

The uncertainty for PIV measurements is from several factors depending on the hardware equipment and mathematical analysis. The procedures of PIV measurements include correlating the particle movements (in pixel) and their real displacements (in mm) via calibration, capturing two sequential images of particles, determining the displacement in X, Y direction using cross-correlation algorithm, recording the gate time between the two images, and calculating the velocity using X, Y displacement. Therefore, the uncertainty of measurement is based upon multiple sources of error in PIV image processing, which are calibration error (Uc), pixel displacement (Up), image pre-processing (Upre), and the velocity magnitude (Uv). According to the law of uncertainty propagation, the total uncertainty is calculated as:

$$U_{total} = \sqrt{U_c^2 + U_p^2 + U_{pre}^2 + U_v^2} \tag{6.1}$$

Uc was lower than 0.5% in the experiment using TSI calibration methods. Uncertainty of pixel displacement (Up) is associated with the computational algorithm which transfers the particle images into velocity vectors. Upre generally depends on background subtraction and image enhancement. This kind of uncertainty is generally lower than 2%. The uncertainty magnitude of velocity in PIV image processing can be calculated with equation 6.2 (Raffel et al., 2018b):

$$U_v = |(Mexp(-\frac{1}{2}(\frac{Q-1}{s}^2))^2 + (AQ^B)^2 + C^2| \tag{6.2}$$

where, M, s, A, B, C were coefficients in Insight 4G software. Q is the Primary Peak Ratio (PPR), which is the ratio between primary and secondary correlation peaks and the primary measure of local image quality. Considering the above-listed sources of uncertainty, the total velocity uncertainty was 3.52%.

6.3 Results

6.3.1 PIV Image Capture and Processing

The PIV images were analyzed using INSIGHT 4G (TSI, Inc., MN, USA). All the images were captured with the same gated time during experiments. Images in the x-y plane were acquired throughout the flow field starting from the middle plane of the breast phantom. On each pair of the images selected for cross-correlation treatment, dynamic masking was applied to remove the no-flow area of the image and also define the wall boundaries. The images were pre-processed by background subtraction. A Gaussian-window weighting and a normalized image intensity are applied to identify the tracing particles. Velocity vectors were processed using a fast Fourier-transform (FFT) based cross-correlation algorithm with decrease window size from 64×64 pixels to 32×32. For post-processing, a median filter is used to remove spurious vectors. Figure 6.3 provides sample PIV images for two different measurement window sizes at all locations. The 68mm×52mm window size is for mapping the whole branching of ducts, and the 28mm×21mm window size is for mapping each adjunction. Fluorescent particles are seen in all three generations of bifurcation as shown in Figure 6.3.

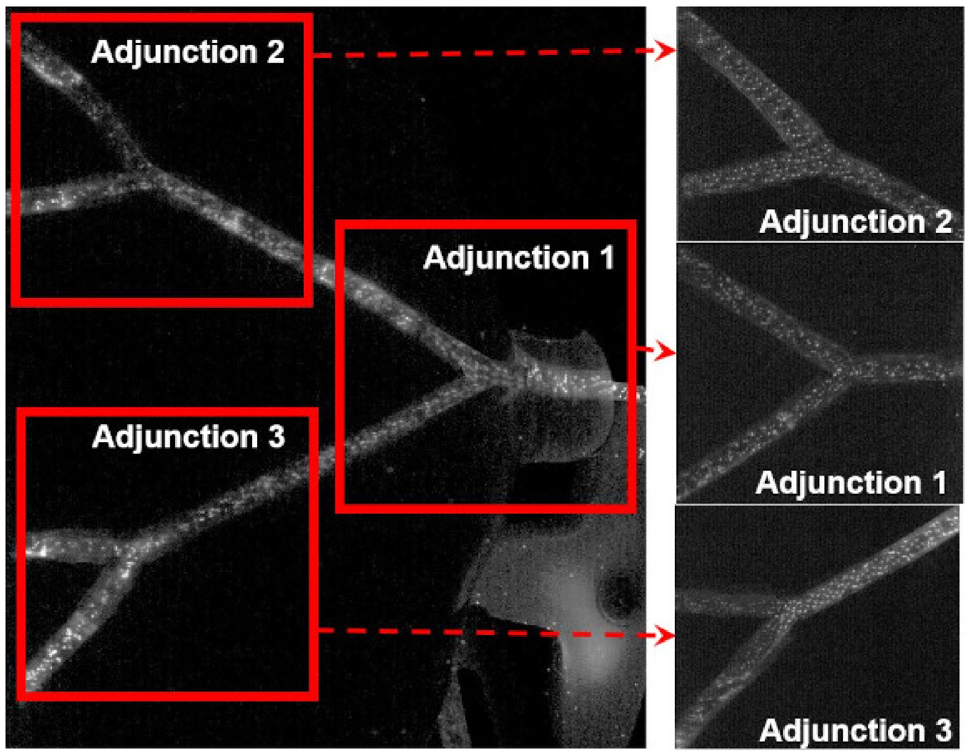

Figure 6.3: Raw PIV images on multi-bifurcation (left), and on each adjunctions (right).

6.3.2 Mean Velocity and Flow rates

Mean & peak inlet velocity, outlet velocity, velocities in adjunctions 1, 2, 3 (in m/s), and total collected milk (in ml) are reported in Table 6.3 for Case 1: vacuum only, and Case 2: vacuum, tongue and jaw pressures. Periodic velocity profiles are seen in both cases. Due to gravity influence, the velocities of inlet 1 and 2 are slightly larger than inlet 3 and 4. Flow velocity in outlet ducts for both cases is higher than the velocity in bifurcation ducts. Averaged maximum jet velocity in the vacuum-only case is 0.9218 m/s, with an increase of 24.1% compares to the averaged maximum jet velocities 0.7789 m/s in vacuum, jaw, and tongue case. The mean outlet velocity of Case 2 when milk is extracted by the coordinated movement of vacuum, jaw, and tongue movement is 0.3766 m/s, 19.25% less than Case 1. The total amount of collected fluid (milk consumption) for vacuum only condition is 105.2 ± 14.5 ml averaging from 50 experiments. The total collected milk liquid for Case 2 is 130.0±26.8, approximately 23.2%±3.7% more than Case 1 under the same suckling frequency and duration time. This phenomenon indicates that natural oral suckling mechanisms collect more milk compare to vacuum only suction under the same vacuum profile.

Mean velocities in three points at three milk duct adjunctions are also compared for two cases. (X,Y) locations of the three points in three adjunctions are (15,20), (15,50), and (42,35) respectively. No significant difference was seen in the velocity of adjunction 1 for Case 1 and Case 2. However, for adjunction 2 and 3, larger velocities were seen in Case 2 (vacuum, tongue, and jaw), which is likely caused by the flow vortices during oscillatory flow and duct deformation causing the oral compression movement from tongue and jaw.

Time-averaged velocity fields for both Case 1 and 2 are presented in Figure 6.4. A jet imposed by vacuum suctions were observed in the outlets for both cases. High velocity was near the outlets for both cases. In vacuum only average velocity field, large velocities were observed in the outlet tube. However, when the tongue and jaw cooperate with vacuum suction, higher velocities and vortices were seen in the adjunctions in the ducts.

6.3.3 Characteristic of Flow Field in Ducts

In-plane velocity fields for the three-generation bifurcation duct structure are investigated for three representative time points in one suckling cycle to understand the oscillatory flow in the ducts during breastfeeding. The contour-plot of velocity mapping and vorticity mapping are shown in Figure 6.5 and Figure 6.6 respectively. The fluid fields are shown for (1) early cycle of -3kPa vacuum; (2) peak cycle of -11kPa vacuum, and (3) late-cycle with vacuum pressure back to -3kPa.

Table 6.3: Inlet and outlet flow rate results of PIV experiments

		Case 1: Vacuum Only		Case 2: Vacuum, tongue&jaw	
		mean	peak	mean	peak
Inlet velocity (m/s)	inlet 1	0.1103	0.1478	0.1286	0.1353
	inlet 2	0.1211	0.1599	0.1361	0.1646
	inlet 3	0.1014	0.1601	0.1243	0.1611
	inlet 4	0.1038	0.1426	0.1121	0.1576
Outlet velocity (m/s)		0.7664	1.0218	0.5727	0.9789
Adjunction 1 (m/s)		0.6097	0.8346	0.6125	0.9715
Adjunction 2 (m/s)		0.4328	0.6115	0.5522	0.7599
Adjunction 3 (m/s)		0.4179	0.5315	0.3248	0.5116
Total collected liquid (ml)		105.2 ± 14.5		130.0 ± 26.8	

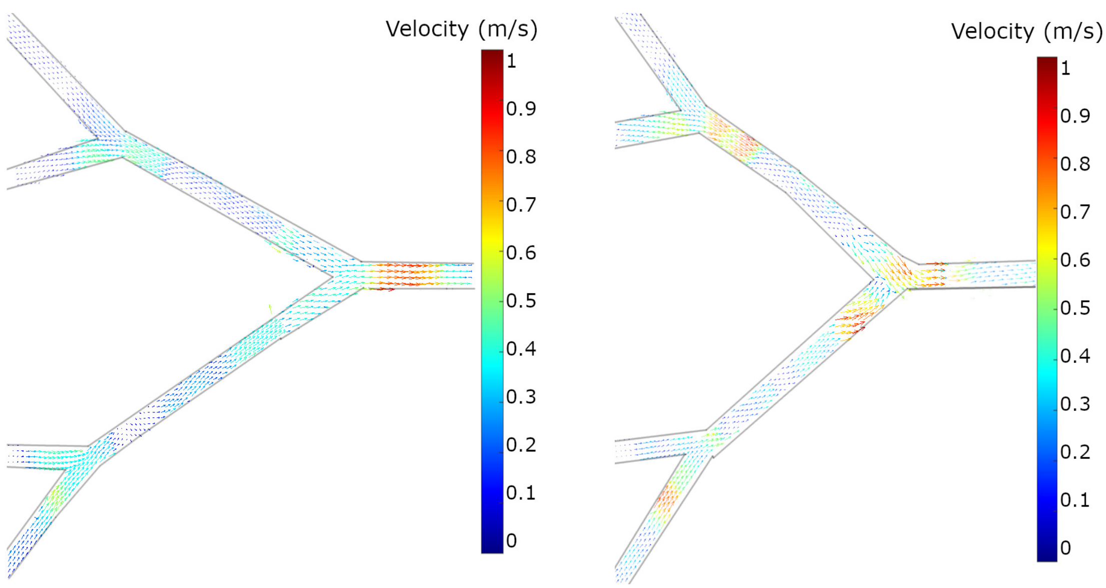

(a) Case 1: Vacuum only

(b) Case 2: Vacuum tongue & jaw

Figure 6.4: Time-averaged velocity maps for Case 1 (a), and Case 2 (b).

In velocity contours, a color bar range from 0-1 m/s is applied on all plots. Local peak velocities are seen in adjunctions and outlet ducts for all times but are rather disordered. In the vorticity distribution contour plots, regions of light yellow indicate clockwise rotation and forward flows, while dark red regions correspond to counter-clockwise rotation and backward flows. Randomized vorticities are observed in the tubes and bifurcations as the tongue and jaw cause the deformation of the outlet duct and suspend the outlet fluid by applying compression pressure on the nipple area.

At the time (1), the suckling pressure is at -3kPa, but the vacuum is descending to getting stronger. Higher velocities are distributed at the outlet in Case 1 but not in Case 2. The outlet duct of Case 2 is compressed at the time (A) and has not been released to the original tube diameter. Therefore, the outlet velocity in Case 2 is lower than that in Case 1. The velocity in adjunction 2 located at the upper left in the plot presents relatively high values compared to other bifurcations. This phenomenon is most like arise from the gravity influence in the flow. In the vorticity plots, both cases present two-direction flows in the ducts. The maximum cross-flow appears at the outlet adjunction of the branching ducts.

At the time (2), when vacuum peaks at maximum strength, velocity fields are generally higher at the outlet position for both cases. However, fluid flow under Case 2 with vacuum tongue & jaw provides higher velocity at the adjunction part for each generation than vacuum only case. Meanwhile, the velocity field in the tubes is slightly different between two cases with Case 1 has a smoother velocity field under the same pressure. The highest magnitudes of vorticities are observed near adjunctions of the outlet tube at the time (2) when a vacuum is at the strongest rate and tongue and jaw detach the nipple. Retract flows are observed in the Y-shape bifurcations in each generation but not as much as time (1) and time (2).

At the time (3) when vacuum returns to -3kPa, retract flows are observed. Overall velocity decreased as vacuum weaks. The higher velocities were seen at the adjunctions in Case 2 but not Case 1. Meanwhile, when a vacuum is at low strength, vorticities are seen in each Y-shaped bifurcation. The number of vortices is decreasing as the bifurcation level increases. Retract flow cause more vortex in the outlet tube and the first generation bifurcation.

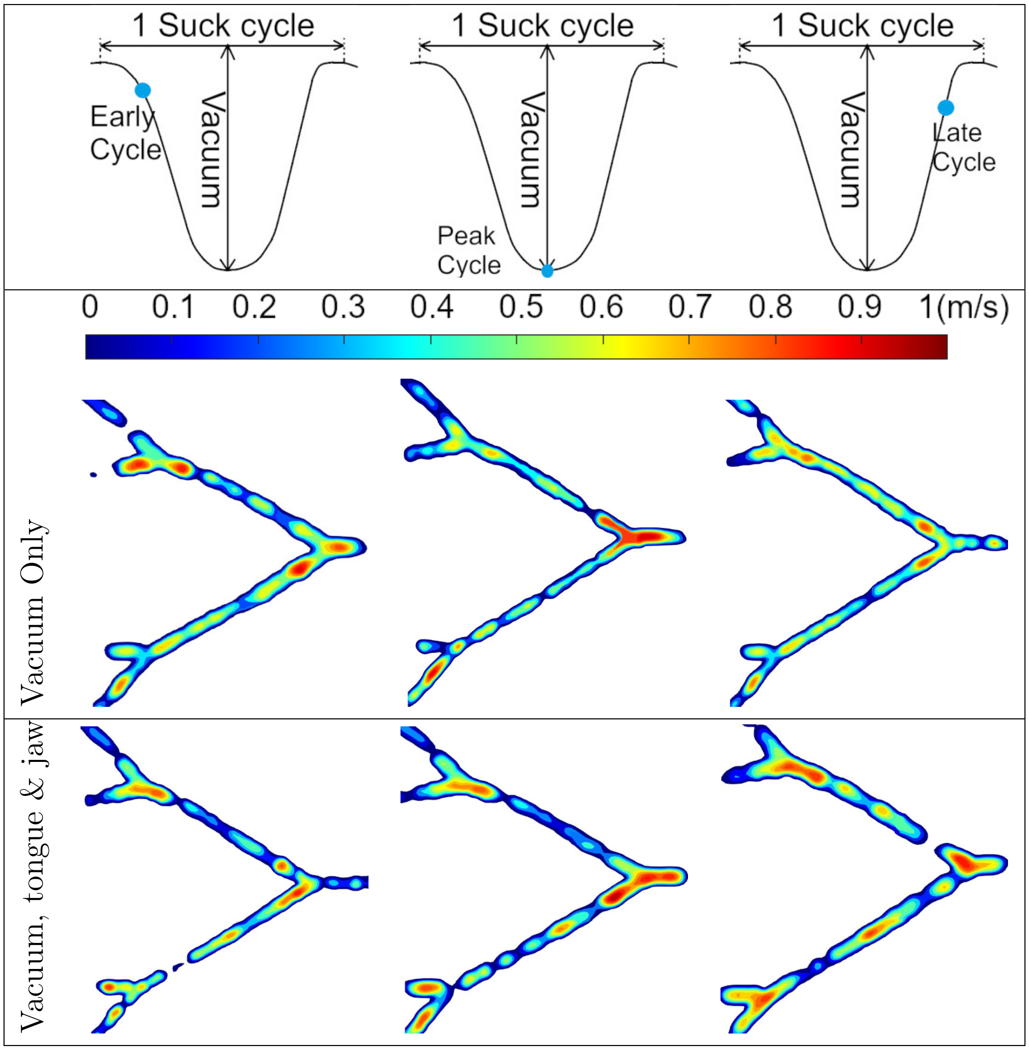

Figure 6.5: Velocity fields acquired from PIV experiments at typical time points in a suck cycle

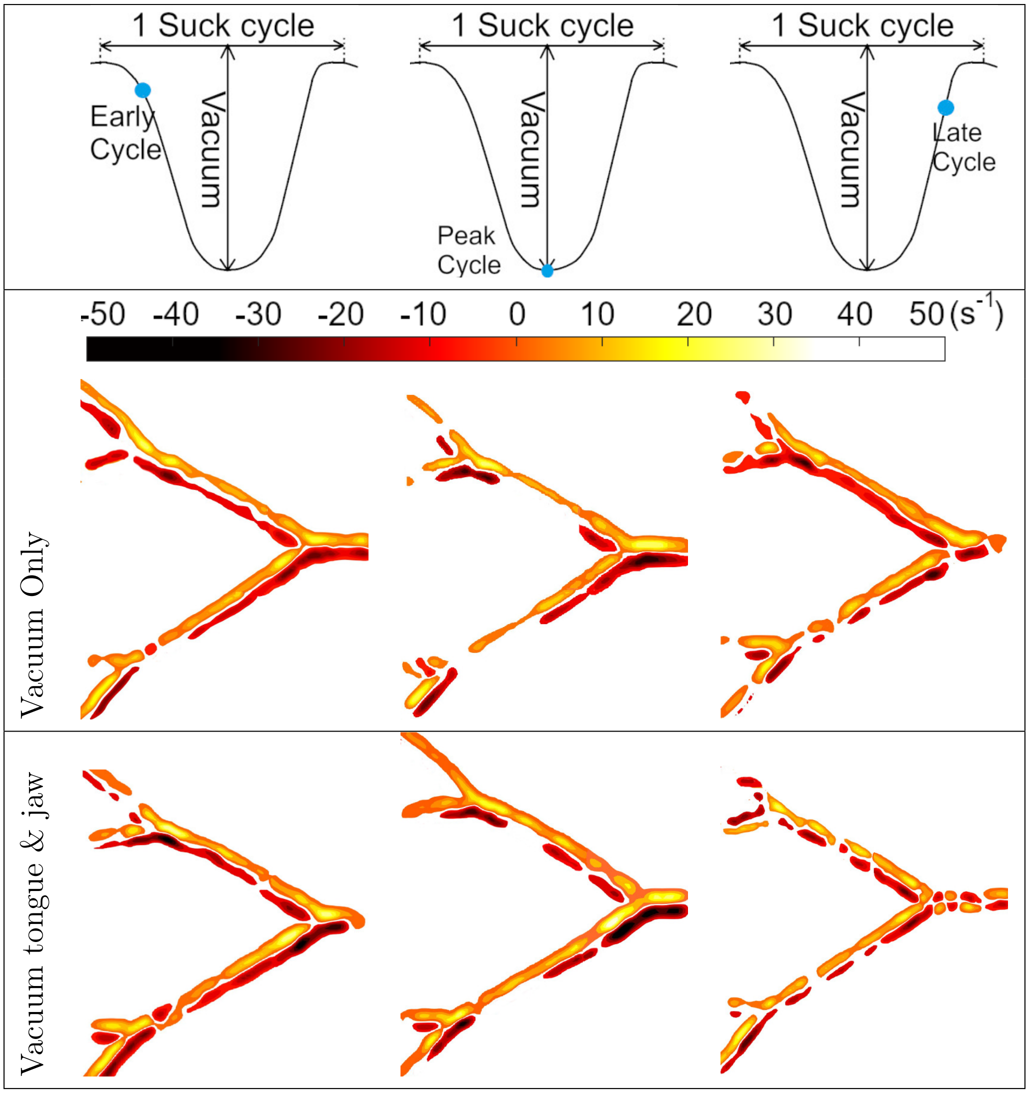

Figure 6.6: Vorticity plots acquired from PIV experiments at typical time points in a suck cycle

6.3.4 Characteristic of Time-resolved Velocity

Time-resolved velocity profiles in the outlet duct and 3 bifurcations at each time step are shown in Figure 6.7 to compare the temporal evolution of the flow field in the ducts. The (X,Y) measurement locations in adjunctions 1,2 and 3 are (42,35), (15,20), and (15,50) respectively as described in Figure 6.3. Time analysis probes are chosen in the middle of the adjunction or tube at x/D = 0.5, where x is the perpendicular distance from the wall to measure point and D is the diameter of the adjunction or tube. The dynamic velocity changes in both case 1 and case 2 are presented for two cycles under the same periodic vacuum suction strength.

Figure 6.7a shows that the peak of velocity profile in the outlet tube appears at approximately the same time phase with the peaks from all three adjunctions for vacuum only case. However, the peak velocity at outlet tubes and adjunctions occurs at different time steps in vacuum, tongue, and jaw movement case. There is about 0.15s time lag between outlet tube and adjunction velocity peak, and 0.1s time lag between the first daughter branch at adjunction 1 and the second daughter branches at adjunction 2 and 3. Meanwhile, the oscillatory velocity amplitude in the ducts is larger in Case 2 compared with Case 1. It is considered that the oscillatory flow at a low frequency can be assumed as quasi-steady flow (Slutsky et al., 1981), but unsteadiness of oscillatory flow appears when the parent duct is compressed and deformed by the soft tongue actuators in BIBS.

6.4 Discussion

This work provides an *in-vitro* fluid dynamic assessment on the velocity and vorticity field in the milk ducts using BIBS setup to understand the bio-fluid transportation under infant suckling mechanism during breastfeeding. Arbitrary flow parameters, such as waveform vacuum pattern, periodic jaw, and rotational tongue motion that cause a structural change

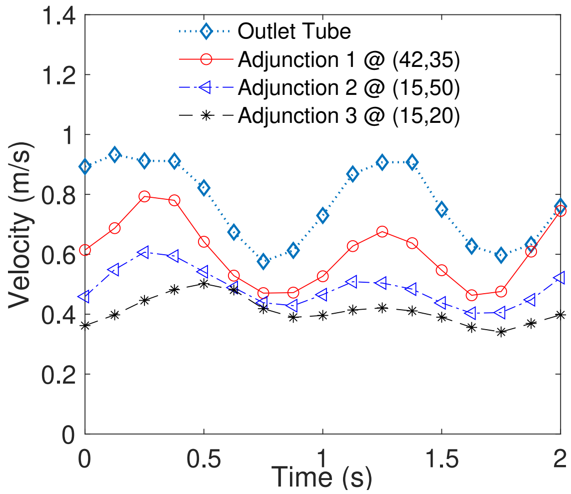

(a) Case 1: Vacuum only

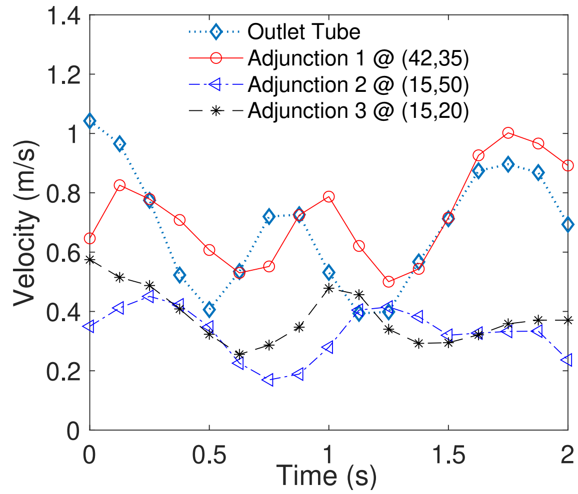

(b) Case 2: Vacuum, tongue & jaw

Figure 6.7: Time-resolved velocity variations at different locations in the milk ducts.

of the breast have been implemented to assess the fluid field in the bifurcated ducts during infant suckling. In order to study the effects of oral movement on the velocimetry variations in the ducts, two suckling cases (Case 1: vacuum only, Case 2: vacuum, tongue & jaw) were implemented. The two cases represent the most common breastfeeding pattern in the real world, that is breast pump and natural breastfeeding through infant suckling. The two cases differ in the oral compression pressure on the breast that causes deformation to the ducts, and we aim to demonstrate how the oral compression from the tongue and jaw can generate a difference in the flow fields.

Clinically observed breastfeeding infants have a wide range of oral suckling vacuum and oral compression pressures (Alatalo et al., 2020). However, previous studies of breast pump vacuum pressures and their effect on extracting milk in nursing efficiency are limited to ultrasound images in the oral cavity of the infant and the amount of intake milk for the entire nursing. No breast model that contains a set of lactating milk ducts is used to investigate the instantaneous milk flow in the bifurcated ducts. Characterization of the flow fields in the ducts yields many interesting insights into the fluid flow environment associated with infant suckling and oral movement during breastfeeding.

In the case of vacuum-only suction, the mean outlet velocity over the entire feeding period is comparably larger than the ejected milk from the natural suckling pattern when there are both oral vacuum and oral compression pressures. However, the total collected milk results indicate that vacuum only suction is less effective in getting milk compare to vacuum, tongue, and jaw oral suckling under the same vacuum pressure profile.

The oscillatory flow on milk extraction along the ductal structure forms the vortex in the experimental area. The randomized vortices in the ducts are observed for both cases but the difference in locations is still seen when compared. The contour plots of the instantaneous velocity and vorticity in the ducts at three representative time points show that the vortices are mostly clustered in the outlet location while the incoming fluid is relatively evenly distributed in the ducts. Further, the strong vortexes can be seen formed in the middle of each tube, whereas the wall has a much weaker vortex. In the case of natural suckling mechanism with vacuum, tongue, and jaw movement, the larger and stronger vortices are generated on the bifurcation of the ducts. This phenomenon indicates that the infant suckling would cause milk duct clogs in the bifurcation adjunctions.

The time-resolved analysis on the flow velocities in the bifurcated milk ducts is essential in locating the peak velocities in the parent and daughter branches. In vacuum only case, the velocities peaks appear in all branches almost simultaneously. However, the velocities in daughter branches are significantly lower than in the parent branch. This phenomenon matches with previous computational simulation results (Mortazavi et al., 2015; Azarnoosh and Hassanipour, 2020) of the velocity distribution on bifurcated ducts. In the case of both vacuum and oral compression from tongue and jaw are applied on the breast, the velocities peaks of outlet and different generations of adjunctions appear at different times. This is likely caused by the peripheral oral mechanism on the soft breast and milk ducts. Deformation in the duct narrows the outlet thus changes the velocity amplitude and brings the unsteadiness of the oscillatory flow. These results indicate that the fluid mechanics in the milk ducts during breastfeeding are very dependent on the nipple-areola deformations that are affected by the infant's oral feeding mechanism.

6.5 Conclusion

In this study, a framework to measure the velocity and map flow field in a phantom model of the lactating breast with branched milk ducts under oscillatory flow conditions is presented using PIV experimental modality. The variations of velocities across the milk ducts under two critical cases (case 1: vacuum only, and case 2: vacuum, tongue, and jaw) are characterized. Increased velocities and flow consumption are observed in vacuum-only cases. Higher mean velocities and larger vorticities appear in vacuum, tongue, and jaw cases. It is also demonstrated that the fluid dynamics in the adjunctions of the milk ducts are strongly dependent on the outlet duct geometry change. Such variations in the flow fields associated with the breast and duct deformation can potentially influence the breastfeeding clinical practice associated with applying positive pressure on the breast.

CHAPTER 7
DISSERTATION SUMMARY

Breastfeeding provides nourishment and other responses in both infants and mothers that promote survival. The biomechanics of breastfeeding have been studied for over half a century, primarily by clinicians. A healthy suckling pattern coordinates oral compressive forces with intra-oral vacuum and swallowing activities to extract milk from the breast. Studying an infant's oral interaction with a mother's breast during breastfeeding both clinically and experimentally helps to understand the biomechanics of breastfeeding.

7.1 Data Processing and Image Analysis on the Physiology of Breastfeeding

To understand the relationship between positive compression and negative vacuum pressures on the geometry of the nipple during suckling with milk expression, the first part of this dissertation processed the clinical data captured from mother-infant dyads. The data set included the positive peripheral oral pressure exerted on the areola (maxilla pressure from upper palate, mandible pressure from lower jaw and tongue movement), intra-oral cavity ultrasound imaging, and vacuum pressures during breastfeeding. A manual designation of the approximate edge on each frame was used to outline the boundaries for the nipple, the infant's hard palate, and tongue, which was validated using an edge detection algorithm. The milk duct deformations and the nipple expansion in both width and length are caused by the infant's oral activities of tongue and jaw movements during breastfeeding. A postprocessing filter-based polynomial denoising algorithm known as BUTTERWORTH was applied for dealing with the overlapped experimental and the noise signals. After data processing, both maxilla and mandible peripheral pressures varied in an oscillatory pattern that corresponded to the oscillatory pattern of the intra-oral vacuum pressure. All infants applied non-negligible peripheral pressures when compared to the mean intra-oral vacuum pressure with occasional spikes of higher pressures noted.

7.2 Experimental Apparatus for Studying the Breastfeeding Mechanism

A bio-inspired breastfeeding simulator (BIBS) that mimics infant oral behavior and milk extraction pattern was then designed and developed to study the breastfeeding mechanism *in vitro*. The construction of the BIBS apparatus followed the clinical study that collects measurements of intra-oral vacuum pressure, the infant's jaw, tongue and upper palate pressure, as well as nipple deformation on the breast areola area. The BIBS consists of a self-programmed vacuum pump assembly that replicates the infant's oral vacuum, two linear actuators mimicking the oral compressive forces, and a motor-driven gear representing the tongue motion. A flexible, transparent, and tissue-like breast phantom with a bifurcated milk duct structure was fabricated to work as the lactating human breast model. Bifurcated ducts were connected with a four-outlet manifold under a reservoir filled with milk-mimicking liquid. Piezoelectric sensors and a CCD (charge-coupled device) camera were used to record and measure the *in vitro* dynamics of the apparatus. All mechanisms were successfully coordinated to mimic the infant's feeding mechanism. Suckling frequency and pressure values on the breast phantom from the experimental apparatus were in good agreement with the clinical data. Also, the change in nipple deformation captured by BIBS matched with those from *in vivo* clinical ultrasound images. The fully-developed breastfeeding simulator provides a powerful tool for understanding the biomechanics of breastfeeding and formulates a foundation for future breastfeeding device development.

Graphical user interface (GUI) and feedback controllers were integrated on the BIBS to demonstrate the feasibility of a bench-top medical simulator to recreate any type of infant-breast interaction during breastfeeding. Adapted from the previous BIBS model, a solid infant head model with upper face, lower jaw, and tongue actuators was developed for a better demonstration of oral cavity movement pattern during breastfeeding simulation. Microcontroller-based proportional–integral–derivative (PID) controllers were designed for vacuum pressure control and motor speed tracking based on the feedback signals. Multiple measurement systems were applied to capture oral pressures, milk flow rate, and instantaneous images, which were displayed instantaneously in GUI. The input panel in the GUI allowed the users to define inputs such as vacuum frequency, strength, and offset, to observe the effect of pattern changing in breastfeeding simulation. The tests with two different types of user-defined profiles confirmed a better fidelity and robustness of the updated BIBS to mimic multi-phase infant oral suckling dynamics *in vitro*. The updated BIBS successfully served as an automatic and physiologically accurate test-bed for studying the biomechanics of breastfeeding.

7.3 PIV Experiment on Understanding the Flow Dynamics in the Breast

The next phase of the dissertation study investigated the flow field in a lactating breast model considering the bifurcated milk ducts and the multi-phase breast-infant interaction. BIBS integrated with GUI and PID feedback controls was utilized to mimic the infant's oral feeding mechanism during breastfeeding with high fidelity. The simulated mechanism extracted a clear human milk-mimicking Fluid (HMMF) from the transparent and elastic lactating breast phantom during experiments. HMMF solution was generated from a multi-constrained empirical optimization. The matched HMMF, suitable for use in the lactating human breast phantom with bifurcated ductal structures, was achieved with the composition of 15.69% NaI, 30.27% Glycerin, 54.02% water, and 0.02% Xanthan Gum by weight percentage resulting in a non-Newtonian viscosity matched with that of human milk.

Using particle image velocimetry (PIV) system, we found that the oscillatory flow under vacuum pressure provides a higher maximum velocity field at the outlet compare to when both vacuum and oral compression pressures were applied. Vacuum-only extraction yielded an increase in flow velocity at the outlet and could be one of the reasons that cause nipple pain, whereas infant's oral activities on the breast generated more vortices in the milk duct adjunctions and might cause milk duct clogs. This phenomenon is rationalized by validating with a previous *in vivo* clinical study (Taffoni et al., 2016) of milk production compare between commercial pumps and infant suckling. Additionally, the milk consumption of vacuum-only extraction was less than that of vacuum plus oral compression, thus further explains the effectiveness of applying natural suckling pattern in human lactation.

7.4 Contributions

A vast number of clinical study has focused on the effectiveness of vacuum pressure exerted by the infants to extract milk from the breast during lactation process. However, the amount of oral compressive forces on the nipple/breast complex was not clear and received limited attention. The present study developed a physical model consists of a soft breast phantom, linear actuators, motors, and soft robots to mimic the infant's oral suckling skills on the breast and allow for the *in vitro* bio-fluid transport in the human breast to study the biomechanics of breastfeeding.

This work first processed the clinical data of oral pressures in both vacuum and compressive pressure, measured the nipple deformation through the ultrasound images on the mid-sagittal plane of an infant's oral cavity, and correlated the relationship of tongue movement with vacuum dynamics (see Chapter 2). Then a bio-inspired breastfeeding simulator was designed and developed to mimic infant oral dynamics of vacuum pressure, compression pressure on the breast (see Chapter 3). The setup was integrated with a graphical user interface and feedback controllers that allowed for the precise control and desired outputs of the vacuum strength and suckling frequency during *in vitro* experiments (see Chapter 4). The last part of this study utilized the particle image velocimetry measurement system on the BIBS as an application of a breastfeeding simulation that can visualize the flow field and quantify the velocity magnitudes in the milk ducts (see Chapter 6).

Compared with the previous tools that have been used for studying the biomechanics of breastfeeding (Ramsay et al., 2005; EGLASH and MALLOY, 2015; Ilyin et al., 2019), the BIBS device developed in this work provides several advantages and benefits, including an optically clear breast phantom with improved flexibility and softness in the breast and milk ducts. With GUI and feedback controllers, the simulator can run simulations under various suckling patterns to find optimal milk consumption. Based on the existing test-bed operations and PIV settings, BIBS can also be used as a potential screening tool for developmental disabilities such as infants' oral abnormalities and mothers' physical lactation problems. BIBS can also be applied towards an educational purpose for understanding the mechanism of breastfeeding. Following the same approach as in the current work, the model can be extended to a better breast pump design by introducing oral compression pressure.

APPENDIX A

BIBS INTERFACE IN LABVIEW

This appendix shows the LabVIEW interface of the BIBS open-loop controlling system as outlined in Chapter 3. The interface includes a front panel and a block diagram in the LabVIEW program. A high-speed programmable coordinator (NI Compact RIO 9074, see Figure A.1) was loaded with a customized arbitrary periodic vacuum pressure profile before initiating the experiment. Using LabVIEW software, the first step was to build a front panel (see Figure A.2a) to include command data and a control diagram. On the NI hardware platform, an analog module (NI 9264) commanded a voltage output and then an analog reading module (NI 9201) monitored feedback signals from the vacuum pressure sensor.

Real-Time First In First Out (RT FIFO) function was chosen to read data from a measured profile and an analog signal was generated with NI 9264 Real-Time module in NI compact RIO platform (see Figure A.2b). The RI FIFO function allows users to access each Input/Output (I/O) device for maximum flexibility and performance in data processing at a consistent rate. Scan mode with a 100ms scanning period per data update was employed in LabVIEW output. Each data was imported into the data buffer and then was exported following the first-in-first-out (FIFO) principle every 100ms(10HZ). Once the program deployed and began running, the front panel was updated with current I/O values plotted on the waveform chart. Figue A.2b presents the control diagram, which includes (a) Initialization (reading and loading data points from the measurement and creating the RT FIFO), (b) Main processing (data preparation, PID control algorithm, and FIFO scanning) and (c) Shut down.

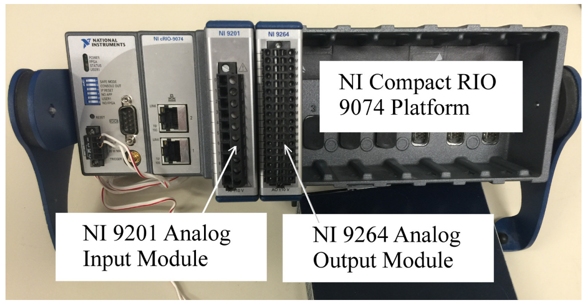

Figure A.1: NI Device, including Compact RIO platform, Analog output and reading modules.

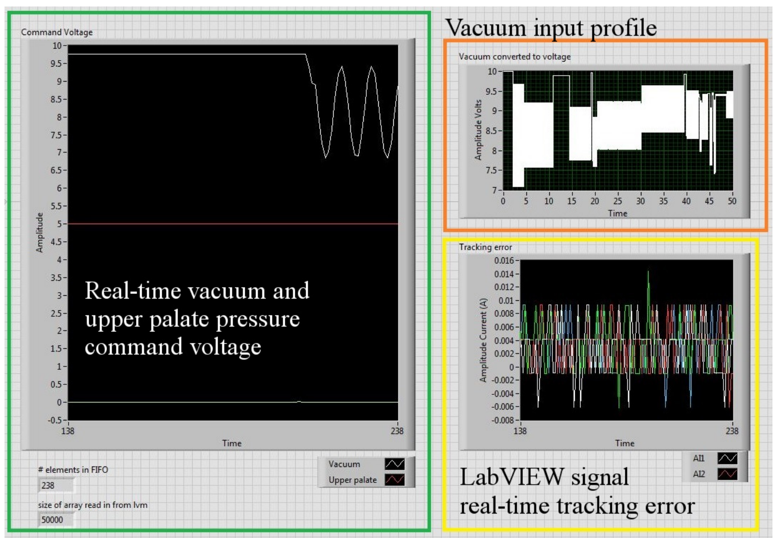

(a)

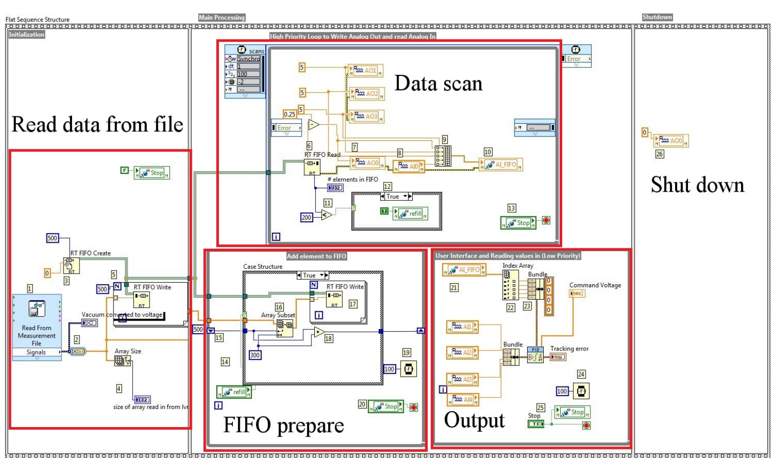

(b)

Figure A.2: LabVIEW Programming: a) Front Panel; b) Scan-Mode Block Diagram.

APPENDIX B

CLINICAL DATA DENOISE AND ULTRASOUND VIDEO PROCESSING ALGORITHMS

A post-processing filter based polynomial denoising algorithm known as BUTTERWORTH with a MATLAB command BUTTER (MATLAB, 2010) was applied for the overlapped experimental and the noise signals. Beginning with the transfer function for an all-pole system of order n, the frequency response of a filter can be modeled as a polynomial of complex variable $s = \sigma + j\omega_c$ (Alarcon et al., 2000). The resulting transfer function appears as:

$$H(s) = \frac{K}{1 + c_1(s/\omega_c) + c_2(s/\omega_c)^2 + ... + c_n(s/\omega_c)^n} = \frac{b_n s^n + b_{n-1}s^{n-1} + ... + b_0}{a_n s^n + a_{n-1}s^{n-1} + ... + a_0}, \qquad \text{(B.1)}$$

where $c_1, c_2, ..., c_n$ are the scalar constants in the denominator of $H(s)$ for the all-pole system, K is the gain of the system, $a_0, a_1, ..., a_n$ are denominator parameters, and $b_0, b_1, ..., b_n$ are numerator parameters. The frequency domain behavior of a BUTTERWORTH filter allows one to attenuate the noise at the unwanted frequency. This method has its advantages in analyzing discontinuities and in keeping the spikes which would reflect some of the oral patterns during breastfeeding. MATLAB achieves the command by [B, A] = butter(N,ω_c,'low'). The first parameter N in this command denotes the order of a digital 'BUTTERWORTH' filter. The order $N = 2$ was chosen because 2nd order is sufficient for typical sensor data. The second parameter ω_c is the normalized cutoff frequency. The cutoff frequency ω_c must be $0.0 < \omega_c < 1.0$, with $\omega_c = 1.0$ corresponding to half of the sample rate. The last string 'low' indicates that the function returns low-pass filter coefficients. The 'BUTTERWORTH' algorithm in MATLAB returned a denominator vector $A = [a_0, a_1, ..., a_n]$ and an numerator vector $B = [b_0, b_1, ..., b_n]$, which were used to construct the filter $H(s)$ to obtain the denoised data.

Ultrasound images were captured as outlined by Geddes et al. (Geddes et al., 2008b). The ultrasound images were used to determine periods of nutritive and non-nutritive suckling by visualization of milk flow. All ultrasound movie analysis were performed using MATLAB for observing the nipple dimension changes inside infants' mouths during breastfeeding.

A self-programmed measurement system was achieved in MATLAB to get average dimensions of the nipple height and length with tongue moving up and tongue moving down. The self-programmed measurement system calibrated the distance indicator with a known dimension in ultrasound images. A manual designation of the approximate edge on each frame was used to outline the boundaries for nipple, hard palate, and tongue. A self-determined baseline or stationary pixel(s) was first fixed for dimension measurements, as shown in Figure 2.3c, to eliminate difficulties in distinguishing the nipple from the areola on ultrasound images. The nipple height and length from the baseline were measured for all infants from ultrasound images for a minimum of ten nutritive suck cycle. All nipple dimension changes measured from ultrasound are given in Table 2.1.

APPENDIX C

MATLAB SIMULATION ON SYSTEM IDENTIFICATION AND PID PARAMETER DESIGN FOR BIBS

This appendix includes MATLAB system identification for a free-body DC motor, SIMULINK simulation to characterize PID controller parameters and the MATLAB simulations results on PID speed control for motors.

• System identification Toolbox in MATLAB, as shown in Figure C.1. General procedures were: 1) input half of the denoised raw data; 2) choose transfer function polynomial based on motor characteristics; 3) identify the motor function; and 4) validate the transfer function model output with the other half set of the data.

• Figure C.2 presents the transfer function and PID controller schematic construction in MATLAB SIMULINK module.

• Figure C.3 presents the simulation results in MATLAB 2020a of a DC motor with PID controller.

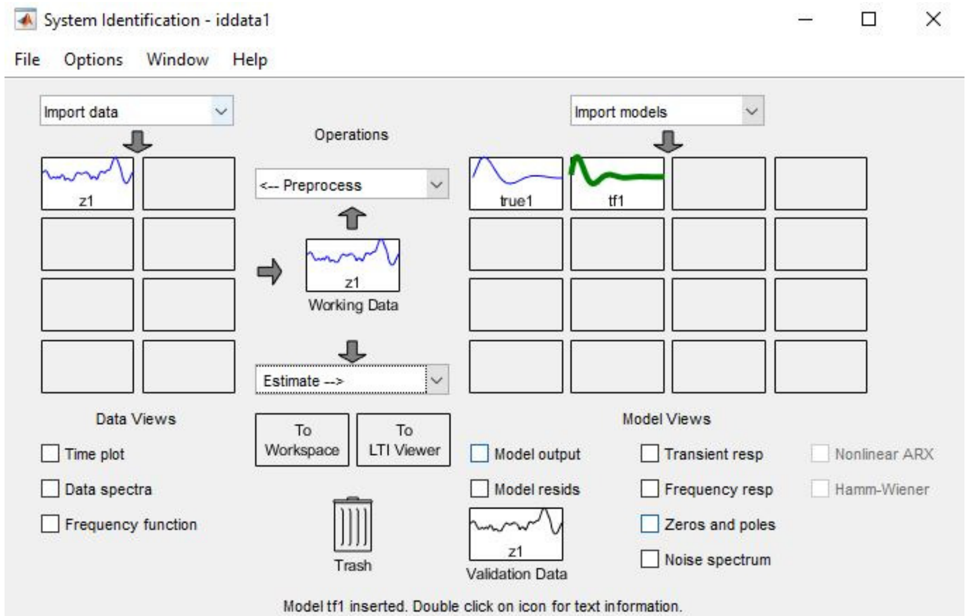

(a)

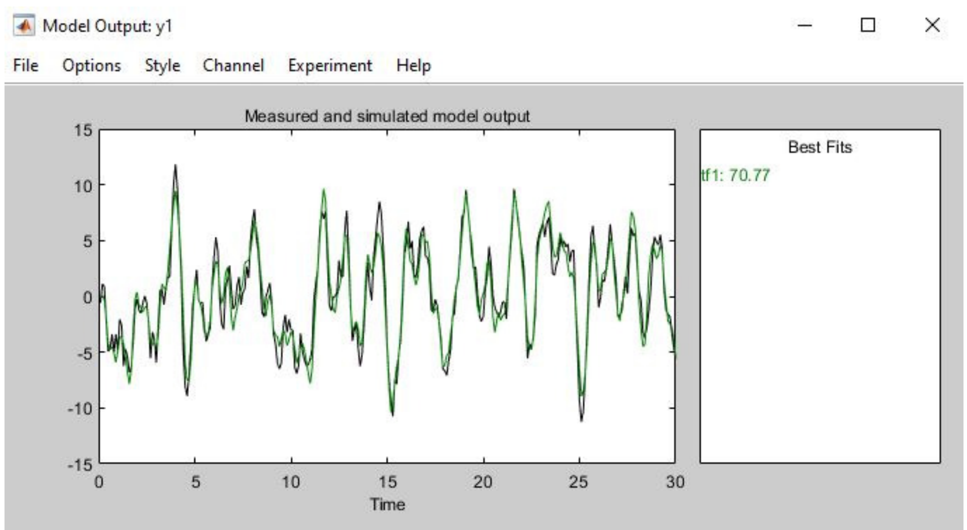

(b)

Figure C.1: (a) System Identification Toolbox in MATLAB for generating a transfer function, and (b) System output validation for the identified transfer function.

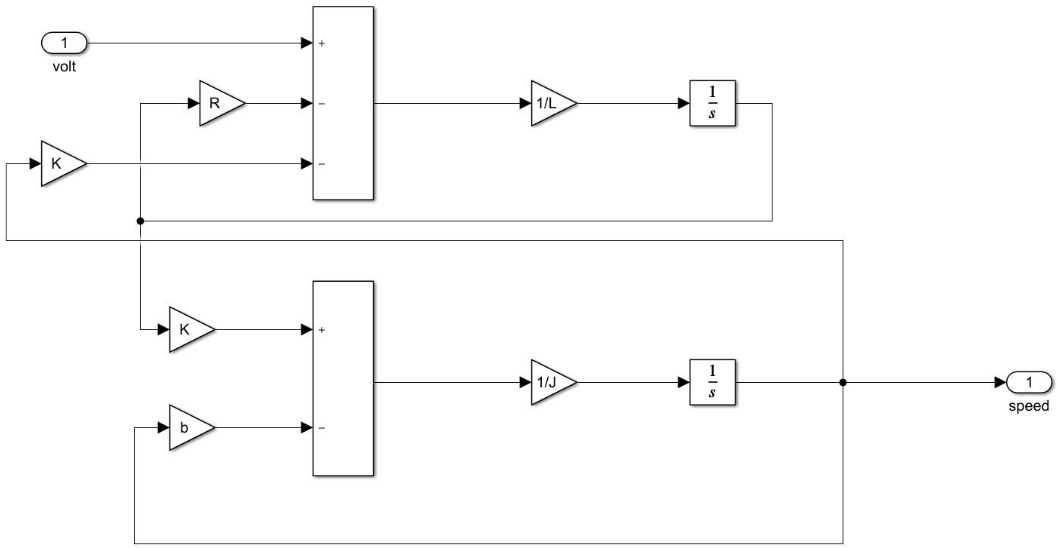

(a)

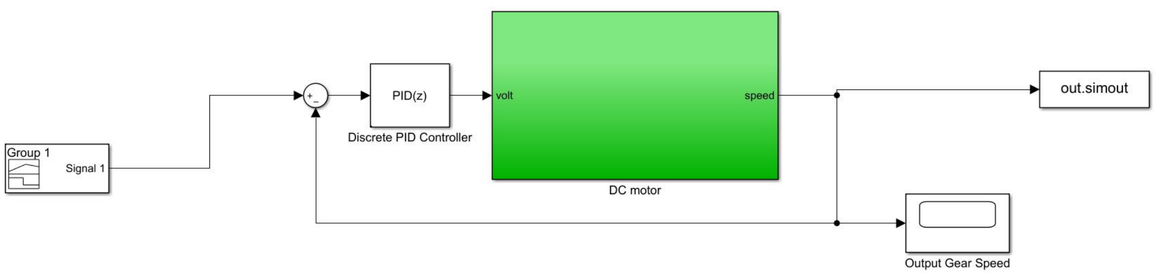

(b)

Figure C.2: (a) Transfer function in SIMULINK, and (b) PID parameter and PID control in a feedback loop.

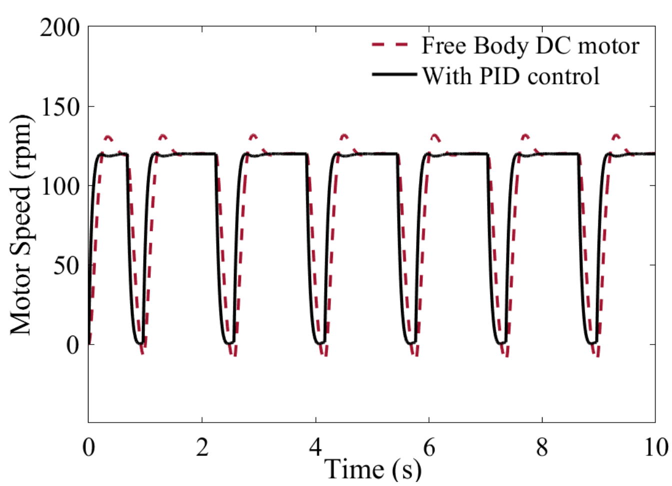

Figure C.3: PID simulation results.

REFERENCES

Alarcon, G., C. Guy, and C. Binnie (2000). A simple algorithm for a digital three-pole butterworth filter of arbitrary cut-off frequency: application to digital electroencephalography. *Journal of Neuroscience Methods 104*(1), 35–44.

Alatalo, D. and F. Hassanipour (2016). An experimental study on human milk viscosity. In *ASME 2016 International Mechanical Engineering Congress and Exposition*, pp. 94–104. American Society of Mechanical Engineers.

Alatalo, D. and F. Hassanipour (2020). An experimental study on human milk rheology: Behavior changes from external factors. *Fluids 5*(2), 42.

Alatalo, D., L. Jiang, D. Geddes, and F. Hassanipour (2020). Nipple deformation and peripheral pressure on the areola during breastfeeding. *Journal of Biomechanical Engineering 142*(1), 1–11.

Alekseev, N., V. Ilyin, V. Yaroslavski, S. Gaidukov, T. Tikhonova, Y. Specivcev, E. Omelyanjuk, and N. Tkachenko (1998). Compression stimuli increase the efficacy of breast pump function. *European Journal of Obstetrics & Gynecology and Reproductive Biology 77*(2), 131–139.

Alekseev, N., E. Omel'ianuk, and N. Talalaeva (2000). [dynamics of milk ejection reflex during continuous rhythmic stimulation of areola-nipple complex of the mammary gland]. *Rossiiskii fiziologicheskii zhurnal imeni IM Sechenova/Rossiiskaia akademiia nauk 86*(6), 711–719.

Alekseev, N. P. and V. I. Ilyin (2016). The mechanics of breast pumping: Compression stimuli increased milk ejection. *Breastfeeding Medicine 11*(7), 370–375.

Arago, D. and J. Biot (1806). Refractive properties of binary mixtures. *Mem Acad Fr 15*, 7–11.

ArduCAM (2018). Arducam mini released.

Azarnoosh, J. and F. Hassanipour (2020). Fluid-structure interaction modeling of lactating breast. *Journal of biomechanics 103*, 109640.

Barlow, S. M. (2009). Central pattern generation involved in oral and respiratory control for feeding in the term infant. *Current opinion in otolaryngology & head and neck surgery 17*(3), 187.

Becker, G. E., H. A. Smith, and F. Cooney (2016). Methods of milk expression for lactating women. *Cochrane Database of Systematic Reviews 1*(9).

Berggren, K., M. Eriksson, P. Hall, M. G. Wallis, and E. Fredenberg (2018). In vivo measurement of the effective atomic number of breast skin using spectral mammography. *Physics in Medicine & Biology 63*(21), 215023.

Brookshier, K. and J. Tarbell (1993). Evaluation of a transparent blood analog fluid: aqueous xanthan gum/glycerin. *Biorheology 30*(2), 107–116, http://doi.org/10.3233/BIR–1993–30202.

Burton, P., J. Deng, D. McDonald, and M. S. Fewtrell (2013). Real-time 3d ultrasound imaging of infant tongue movements during breast-feeding. *Early human development 89*(9), 635–641.

Butterworth, S. (1930). On the theory of filter amplifiers. *Wireless Engineer 7*(6), 536–541.

Cannon, L. M., A. J. Fagan, and J. E. Browne (2011). Novel tissue mimicking materials for high frequency breast ultrasound phantoms. *Ultrasound in medicine & biology 37*(1), 122–135.

Canny, J. (1987). A computational approach to edge detection. In *Readings in computer vision*, pp. 184–203. Elsevier.

Carl Ward, T. and J. Timothy Perry (1981). Dynamic mechanical properties of medical grade silicone elastomer stored in simulated body fluids. *Journal of biomedical materials research 15*(4), 511–525.

Charonko, J., S. Karri, J. Schmieg, S. Prabhu, and P. Vlachos (2009). In vitro, time-resolved piv comparison of the effect of stent design on wall shear stress. *Annals of biomedical engineering 37*(7), 1310–1321.

Cobo, E. (1993). Characteristics of the spontaneous milk ejecting activity occurring during human lactation. *Journal of perinatal medicine 21*(1), 77–85.

Cross, M. M. (1965). Rheology of non-newtonian fluids: a new flow equation for pseudoplastic systems. *J Colloid Science 20*(5), 417–437, https://doi.org/10.1016/0095–8522(65)90022–X.

Dabling, J. G., A. Filatov, and J. W. Wheeler (2012). Static and cyclic performance evaluation of sensors for human interface pressure measurement. In *2012 Annual International Conference of the IEEE Engineering in Medicine and Biology Society*, pp. 162–165. IEEE.

Dahl, L. (2015). *Anatomy and Physiology of Breastfeeding*. Springer.

Dewey, K. G., D. A. Finley, and B. Lönnerdal (1984). Breast milk volume and composition during late lactation (7-20 months). *Journal of pediatric gastroenterology and nutrition 3*(5), 713–720.

EGLASH, A. and M. L. MALLOY (2015). Breastmilk expression and breast pump technology. *Clinical obstetrics and gynecology 58*(4), 855–867.

Eishima, K. (1991). The analysis of sucking behaviour in newborn infants. *Early Human Development 27*(3), 163–173.

Elad, D., P. Kozlovsky, O. Blum, A. F. Laine, M. J. Po, E. Botzer, S. Dollberg, M. Zelicovich, and L. B. Sira (2014). Biomechanics of milk extraction during breast-feeding. *Proceedings of the National Academy of Sciences 111*(14), 5230–5235.

FEŞTILĂ, D., M. Ghergie, A. Muntean, D. Matiz, and A. ŞERBANESCU (2014). Suckling and non-nutritive sucking habit: what should we know? *Clujul Medical 87*(1), 11.

Field, T. M., S. M. Schanberg, F. Scafidi, C. R. Bauer, N. Vega-Lahr, R. Garcia, J. Nystrom, and C. M. Kuhn (1986). Tactile/kinesthetic stimulation effects on preterm neonates. *Pediatrics 77*(5), 654–658.

Fucile, S., E. Gisel, and C. Lau (2002). Oral stimulation accelerates the transition from tube to oral feeding in preterm infants. *The Journal of pediatrics 141*(2), 230–236.

Geddes, D. T. (2007a). The anatomy of the lactating breast: Latest research and clinical implications. *Infant 3*(2), 59–63.

Geddes, D. T. (2007b). Inside the lactating breast: the latest anatomy research. *Journal of Midwifery & Womens Health 52*(6), 556–563.

Geddes, D. T., J. C. Kent, L. R. Mitoulas, and P. E. Hartmann (2008a). Tongue movement and intra-oral vacuum in breastfeeding infants. *Early human development 84*(7), 471–477.

Geddes, D. T., J. C. Kent, L. R. Mitoulas, and P. E. Hartmann (2008b). Tongue movement and intra-oral vacuum in breastfeeding infants. *Early Human Development 84*(7), 471–477.

Geddes, D. T., V. S. Sakalidis, A. R. Hepworth, H. L. McClellan, J. C. Kent, C. T. Lai, and P. E. Hartmann (2012). Tongue movement and intra-oral vacuum of term infants during breastfeeding and feeding from an experimental teat that released milk under vacuum only. *Early human development 88*(6), 443–449.

Goldfield, E. C., C. Buonomo, K. Fletcher, J. Perez, S. Margetts, A. Hansen, V. Smith, S. Ringer, M. J. Richardson, and P. H. Wolff (2010). Premature infant swallowing: patterns of tongue-soft palate coordination based upon videofluoroscopy. *Infant Behavior and Development 33*(2), 209–218.

Goldfield, E. C., M. J. Richardson, K. G. Lee, and S. Margetts (2006). Coordination of sucking, swallowing, and breathing and oxygen saturation during early infant breast-feeding and bottle-feeding. *Pediatric Research 60*(4), 450.

Goppelt, F., T. Hieninger, and R. Schmidt-Vollus (2018). Modeling centrifugal pump systems from a system-theoretical point of view. In *2018 18th International Conference on Mechatronics-Mechatronika (ME)*, pp. 1–8. IEEE.

Hassiotou, F. and D. Geddes (2013). Anatomy of the human mammary gland: Current status of knowledge. *Clinical anatomy 26*(1), 29–48.

Homaifar, A., C. X. Qi, and S. H. Lai (1994). Constrained optimization via genetic algorithms. *Simulation 62*(4), 242–253, https://doi.org/10.1177/003754979406200405.

Ilyin, V. I., N. P. Alekseev, M. M. Troschkin, and V. A. Uleziko (2019). Comparative assessment of excretion of milk from two breast pumps with different vacuum strength and duration. *Breastfeeding Medicine 14*(3), 177–184.

Jiang, L., D. L. Alatalo, and F. Hassanipour (2020). A human milk-mimicking fluid for piv experiments. *Experiments in Fluids 61*(10), 1–7.

Jiang, L. and F. Hassanipour (2020a). Bio-inspired breastfeeding simulator (bibs): A tool for studying the infant feeding mechanism. *IEEE Transactions on Biomedical Engineering 67*(11), 3242–3252.

Jiang, L. and F. Hassanipour (2020b). Bio-inspired breastfeeding simulator (BIBS): A tool for studying the infant feeding mechanism. *IEEE Trans on Biomed Eng 67*(11), 3242–3252.

Jütte, J., A. Hohoff, C. Sauerland, D. Wiechmann, and T. Stamm (2014). In vivo assessment of number of milk duct orifices in lactating women and association with parameters in the mother and the infant. *BMC pregnancy and childbirth 14*(1), 1–8.

Kent, J., M. Cregan, D. Doherty, L. Mitoulas, D. Ramsay, and P. Hartmann (2006). The effect of vacuum on the removal of milk using an electric breastpump. *Breastfeed. Med. 1*(1).

Kent, J. C., L. Mitoulas, D. B. Cox, R. A. Owens, and P. E. Hartmann (1999). Breast volume and milk production during extended lactation in women. *Experimental physiology 84*(2), 435–447.

Kent, J. C., D. T. Ramsay, D. Doherty, M. Larsson, and P. E. Hartmann (2003). Response of breasts to different stimulation patterns of an electric breast pump. *Journal of Human Lactation 19*(2), 179–186.

Kline, S. J. and F. A. McClintock (1953, Jan). Describing uncertainties in single-sample experiments. *Mechanical Engineering 75*, 3–8.

Koyama, S., H.-J. Wu, T. Easwaran, S. Thopady, and J. Foley (2013). The nipple: a simple intersection of mammary gland and integument, but focal point of organ function. *Journal of mammary gland biology and neoplasia 18*(2), 121–131.

Lau, C., S. Fucile, and E. Gisel (2012). Impact of nonnutritive oral motor stimulation and infant massage therapy on oral feeding skills of preterm infants. *Journal of Neonatal-perinatal medicine 5*(4), 311–317.

Lebosse, C., P. Renaud, B. Bayle, and M. de Mathelin (2011). Modeling and evaluation of low-cost force sensors. *IEEE Transactions on Robotics 27*(4), 815–822.

Li, R., S. B. Fein, J. Chen, and L. M. Grummer-Strawn (2008). Why mothers stop breastfeeding: mothers' self-reported reasons for stopping during the first year. *Pediatrics 122*(Supplement 2), S69–S76.

Love, S. M. and S. H. Barsky (2004a). Anatomy of the nipple and breast ducts revisited. *Cancer 101*(9), 1947–1957.

Love, S. M. and S. H. Barsky (2004b). Anatomy of the nipple and breast ducts revisited. *Cancer 101*(9), 1947–1957.

MATLAB (2010). *version 7.10.0 (R2010a)*. Natick, Massachusetts: The MathWorks Inc.

McClellan, H., D. Geddes, J. Kent, C. Garbin, L. Mitoulas, and P. Hartmann (2008). Infants of mothers with persistent nipple pain exert strong sucking vacuums. *Acta Paediatrica 97*(9), 1205–1209.

McNamara, J. D., D. King, and J. E. Browne (2009). 1405: Development of a vessel mimicking material for use in anatomical flow phantoms. *Ultrasound in Medicine and Biology 35*(8), S209.

Moore, A. (2010). The practice of breast ultrasound: Techniques, findings, differential diagnosis. *Ultrasound in Medicine and Biology 36*(2), 358.

Mortazavi, S. N., D. Geddes, and F. Hassanipour (2017). Lactation in the human breast from a fluid dynamics point of view. *Journal of biomechanical engineering 139*(1), 011009.

Mortazavi, S. N., F. Hassiotou, D. Geddes, and F. Hassanipour (2015). Mathematical modeling of mammary ducts in lactating human females. *Journal of biomechanical engineering 137*(7), 071009.

Morton, J., J. Hall, R. Wong, L. Thairu, W. Benitz, and W. Rhine (2009). Combining hand techniques with electric pumping increases milk production in mothers of preterm infants. *Journal of Perinatology 29*(11), 757.

Mulik, S. S., A. D. Patange, R. Jegadeeshwaran, S. S. Pardeshi, and A. Rahegaonkar (2021). Development and experimental assessment of a fluid flow monitoring system using flow sensor and arduino interface. In *Innovative Design, Analysis and Development Practices in Aerospace and Automotive Engineering*, pp. 115–122. Springer.

Najjari, M. R., J. A. Hinke, K. V. Bulusu, and M. W. Plesniak (2016). On the rheology of refractive-index-matched, non-Newtonian blood-analog fluids for PIV experiments. *Exp Fluids 57*(6), 96, http://doi.org/10.1007/s00348–016–2185–x.

Narrow, T., M. Yoda, and S. Abdel-Khalik (2000). A simple model for the refractive index of sodium iodide aqueous solutions. *Exp Fluids 28*(3), 282–283, http://doi.org/10.1007/s003480050389.

Newton, N. R. and M. Newton (1950). Relation of the let-down reflex to the ability to breast feed. *Pediatrics 5*(4), 726–733.

Niikawa, T., C. Hagino, E. Nishi, R. Kawachi, K. Minato, and Y. Takada (2012). Measurement of tongue–artificial nipple contact pressure during infant sucking. *IEEJ transactions on electrical and electronic engineering 7*(2), 190–196.

Nowak, A. J., W. L. Smith, and A. Erenberg (1994). Imaging evaluation of artificial nipples during bottle feeding. *Archives of pediatrics & adolescent medicine 148*(1), 40–42.

Odom, E. C., R. Li, K. S. Scanlon, C. G. Perrine, and L. Grummer-Strawn (2013). Reasons for earlier than desired cessation of breastfeeding. *Pediatrics*, peds–2012.

Perrella, S. L., K. Nancarrow, A. Rea, K. Murray, D. T. Geddes, K. N. Simmer, D. Dowling, and E. Schierholz (2020). Estimates of preterm infants' breastfeeding transfer volumes are not reliably accurate. *Advances in Neonatal Care 20*(5), E93–E99.

Quezada, A. and K. Vafai (2014). Modeling and analysis of transport in the mammary glands. *Physical biology 11*(4), 045004.

Raffel, M., C. E. Willert, F. Scarano, C. J. Kähler, S. T. Wereley, and J. Kompenhans (2018a). *Particle image velocimetry: a practical guide*. Springer.

Raffel, M., C. E. Willert, F. Scarano, C. J. Kähler, S. T. Wereley, and J. Kompenhans (2018b). *PIV uncertainty and measurement accuracy*. Springer.

Ramsay, D., J. Kent, R. Hartmann, and P. Hartmann (2005). Anatomy of the lactating human breast redefined with ultrasound imaging. *Journal of anatomy 206*(6), 525–534.

Ramsay, D. T., L. R. Mitoulas, J. C. Kent, M. Larsson, and P. E. Hartmann (2005). The use of ultrasound to characterize milk ejection in women using an electric breast pump. *Journal of Human Lactation 21*(4), 421–428.

Sandholm, L.-E. (1968). The effect of intravenous and intranasal oxytocin on intramammary pressure during early lactation. *Acta obstetricia et gynecologica Scandinavica 47*(2), 145–154.

Schröder, A. and C. E. Willert (2008). *Particle image velocimetry: new developments and recent applications*, Volume 112. Springer Science & Business Media.

Schwartz, K., H. J. D'arcy, B. Gillespie, J. Bobo, M. Longeway, and B. Foxman (2002). Factors associated with weaning in the first 3 months postpartum. *Journal of Family Practice 51*(5), 439–445.

Scott, J. A., C. W. Binns, W. H. Oddy, and K. I. Graham (2006). Predictors of breastfeeding duration: evidence from a cohort study. *Pediatrics 117*(4), e646–e655.

Siebert, J. (1985). A morphometric study of normal and abnormal fetal to childhood tongue size. *Archives of oral biology 30*(5), 433–440.

Slutsky, A. S., G. G. Berdine, and J. M. Drazen (1981). Oscillatory flow and quasi-steady behavior in a model of human central airways. *Journal of Applied Physiology 50*(6), 1293–1299.

Smith, W., A. Erenberg, A. Nowak, and E. Franken Jr (1985). Physiology of sucking in the normal term infant using real-time us. *Radiology 156*(2), 379–381.

Smith, W. L., A. Erenberg, and A. Nowak (1988). Imaging evaluation of the human nipple during breast-feeding. *American Journal of Diseases of Children 142*(1), 76–78.

Stuebe, A. M., B. J. Horton, E. Chetwynd, S. Watkins, K. Grewen, and S. Meltzer-Brody (2014). Prevalence and risk factors for early, undesired weaning attributed to lactation dysfunction. *Journal of women's health 23*(5), 404–412.

Sworn, G., I. Norton, F. Spyropoulos, and P. Cox (2011). Xanthan gum–functionality and application. *Practical food rheology: An interpretive approach*, 85–112, https://doi.org/10.1002/9781444391060.ch5.

Tadesse, Y., D. Hong, and S. Priya (2011). Twelve degree of freedom baby humanoid head using shape memory alloy actuators. *Journal of Mechanisms and Robotics 3*(1).

Taffoni, F., E. Tamilia, M. Giorgino, G. Morbidoni, A. Rosi, A. Scaini, A. M. Visco, E. Schena, and D. Formica (2016). A novel system to study the coordination of sucking and breathing in newborns during bottle feeding. *IEEE Sensors Journal 16*(23), 8589–8596.

Taki, M., K. Mizuno, M. Murase, Y. Nishida, K. Itabashi, and Y. Mukai (2010). Maturational changes in the feeding behaviour of infants–a comparison between breast-feeding and bottle-feeding. *Acta paediatrica 99*(1), 61–67.

Taneri, F., O. Kurukahvecioglu, N. Akyurek, E. H. Tekin, M. N. İlhan, C. Cifter, S. Bozkurt, A. Dursun, O. Bayram, and E. Onuk (2006). Microanatomy of milk ducts in the nipple. *European surgical research 38*(6), 545–549.

Tekscan^{TM} ((accessed June 15, 2017)). *How does the level of accuracy change as curvature of surfaces increases?* https://www.tekscan.com/support/faqs/how-does-level-accuracy-change-curvature-surfaces-increases.

Vazirinejad, R., S. Darakhshan, A. Esmaeili, and S. Hadadian (2009). The effect of maternal breast variations on neonatal weight gain in the first seven days of life. *International breastfeeding journal 4*(1), 13.

Waller, H. (1936). The force exerted by the baby. *Clinical Studies in lactation*.

Wang, Y.-L., J.-S. Hung, L.-Y. Wang, M.-J. Ko, W. Chou, H.-C. Kuo, and B.-S. Lin (2014). Development of a wireless oral-feeding monitoring system for preterm infants. *IEEE journal of biomedical and health informatics 19*(3), 866–873.

Weber, F., M. Woolridge, and J. Baum (1986). An ultrasonographic study of the organisation of sucking and swallowing by newborn infants. *Developmental Medicine & Child Neurology 28*(1), 19–24.

Wiener, N., N. Wiener, C. Mathematician, N. Wiener, N. Wiener, and C. Mathématicien (1949). *Extrapolation, interpolation, and smoothing of stationary time series: with engineering applications*. Massachusettes Insitute of Technology (MIT) press Cambridge.

Wilson-Clay, B. and K. Hoover (2008). *Breastfeeding atlas*. LactNews Press.

Woolridge, M., J. Baum, and R. Drewett (1980). Effect of a traditional and of a new nipple shield on sucking patterns and milk flow. *Early Human Development 4*(4), 357–364.

Woolridge, M., T. How, R. Drewett, P. Rolfe, and J. D. Baum (1982). The continuous measurement of milk intake at a feed in breast-fed babies. *Early human development 6*(4), 365–373.

Woolridge, M. W. (1986). The 'anatomy' of infant sucking. *Midwifery 2*(4), 164–171.

Woolridge, M. W. and J. D. Baum (1988). The regulation of human milk flow. *Perinatal nutrition* (6), 243.

Yasuda, K. (2006). A multi-mode viscosity model and its applicability to non-newtonian fluids. *Journal of Textile Engineering 52*(4), 171–173.

Yousif, M. Y., D. W. Holdsworth, and T. L. Poepping (2011). A blood-mimicking fluid for particle image velocimetry with silicone vascular models. *Exp Fluids 50*(3), 769–774, http://doi.org/10.1007/s00348–010–0958–1.

Zoppou, C., S. Barry, and G. Mercer (1997). Dynamics of human milk extraction: A comparative study of breast feeding and breast pumping. *Bulletin of mathematical biology 59*(5), 953–973.

BIOGRAPHICAL SKETCH

Lin Jiang received her BS and MS from Nanjing University of Aeronautics and Astronautics in Aerospace Engineering and Control Engineering. She started her PhD in the Spring of 2016 and joined the research group of Dr. Hassanipour in the Advanced Research in Thermo-Fluid Systems (ARTS) Laboratory at UTD. Her research area was in bio-inspired engineering with application to studying the biomechanics of breastfeeding. Her dissertation is in the clinical and experimental study of breastfeeding mechanisms. She has five journal and multiple conference publications. One of her conference papers was among the best paper award finalist (nine total on the list) from the 2018 ASME International Mechanical Engineering Congress and Exposition. She received the Dissertation Research Award in 2020, PhD Small Grants in 2018, and People's Choice of Three Minutes Thesis in 2018 from the Office Graduate Education (OGE). She is also the recipient of the diversity award from the 2019 Summer Biomechanics, bioengineering, and bio-transport Conference. Besides research, she was recognized with an Exemplary Teaching Award in 2019 from Erik Jonsson School of Engineering and Computer Science (ECS) due to her excellence in teaching heat transfer lab in the department of mechanical engineering.

CURRICULUM VITAE

Lin Jiang

March 31, 2021

Contact Information:

Email: lin.jiang@utdallas.edu
Department of Mechanical Engineering
The University of Texas at Dallas
800 W. Campbell Rd.
Richardson, TX 75080-3021, U.S.A.

Education:

PhD, Mechanical Engineering, The University of Texas at Dallas, 2021

MS, Mechanical Engineering, The University of Texas at Dallas, 2020

MS, Control Engineering, Nanjing University of Aeronautics and Astronautics, 2011

BS, Aerospace Engineering, Nanjing University of Aeronautics and Astronautics, 2011

Professional Experience:

Research Assistant, Department of Mechanical Engineering, University of Texas at Dallas, 2016-now

Instructor and Teaching Assistant, Heat transfer Laboratory, Department of Mechanical Engineering, University of Texas at Dallas, 2016-now

Research Assistant, College of Automatic Engineering, Nanjing University of Aeronautics and Astronautics, 2011-2014

Teaching Assistant, Systems and Controls, College of Automatic Engineering, Nanjing University of Aeronautics and Astronautics, 2012-2014

Teaching Assistant, Linear System, College of Automatic Engineering, Nanjing University of Aeronautics and Astronautics, 2011-2012

Software Engineer, Jiangsu Guoxin Union Energy Co., Ltd., Wuxi, China, 2013-2015

Honors and Awards:

Dissertation Research Award, University of Texas at Dallas, 2020

Exemplary Teaching Award, University of Texas at Dallas, 2019

Diversity Travel Award, Summer Biomechanics, Bioengineering and Biotransport (SB3C) Conference, 2019

Phil Ritter Fellowship, University of Texas at Dallas, 2018-2019

Best Paper Award Finalist, ASME IMECE (International Mechanical Engineering Congress & Exposition), 2018

Ph.D. Small Grant ($ 1500), University of Texas at Dallas, 2018-2020

People's Choice, Three Minute Thesis (3MT) competition, Office of Graduate Educations, University of Texas at Dallas, 2018

Jonsson School Graduate Study Scholarships, University of Texas at Dallas, 2016-2017

Graduate Student Fellowship, Nanjing University of Aeronautics and Astronautics, 2011-2014

National Student Fellowship, Nanjing University of Aeronautics and Astronautics, 2007-2011

Journal Publications:

1. **Lin Jiang**, Fatemeh Hassanipour, "Bio-inspired Breastfeeding Simulator (BIBS): A Tool for Studying the Infant Feeding Mechanics", *IEEE Transaction on Biomedical Engineering*, **Featured Article**, vol 67, no. 11, Nov. 2020. link
2. **Lin Jiang**, Diana Alatalo, Fatemeh Hassanipour, "A Human Milk Mimicking Fluid for PIV Experiments", *Experiments in Fluids*, vol 61, no. 224, Oct. 2020. link
3. **Lin Jiang**, Diana Alatalo, Donna Geddes, and Fatemeh Hassanipour, "Nipple Deformation and Peripheral Pressure on the Areola During Breastfeeding", *Journal of Biomechanical Engineering*, vol 142, no.1, Jan. 2020. link
4. Xudong An, **Lin Jiang**, Fatemeh Hassanipour, "Numerical Analysis of Air Vortex Interaction with Porous Screen", Fluids, vol 6, no.70, Feb. 2021.link
5. **Lin Jiang**, and Ruiyun Qi. "Adaptive actuator fault compensation for discrete-time T-S fuzzy systems with multiple input-output delays", *The International Journal of Innovative Computing, Information and Control*, vol.12, no.4, pp.1043-1058, Aug. 2016. link

Conference Publications:

1. **Lin Jiang**, Diana Alatalo,and Fatemeh Hassanipour, " Effects of Nutritive and Non-nutritive Suckling on Human Nipple Deformation during Breastfeeding", in Proceedings of Biomedical Engineering Society Annual Meeting, Philadelphia, PA, October 2019.
2. **Lin Jiang**, Diana Alatalo, Donna Geddes, and Fatemeh Hassanipour, "Lactating Human Breast Response To Infant Oral Movements", in Proceedings of Summer Biomechanics, Bioengineering and Biotransport Conference, Seven Springs, PA, June 2019.
3. **Lin Jiang**, Diana Alatalo, Donna Geddes, and Fatemeh Hassanipour, "A Clinical Experiment on Infant Applied Pressures during Breastfeeding", in Proceedings of ASME 2018 International Mechanical Engineering Congress and Exposition, **Best paper award finalist**, 2018.

4. **Lin Jiang**, Diana Alatalo, Donna Geddes, and Fatemeh Hassanipour, "Preliminary Study on Infant Applied Pressures during Breastfeeding and Poisson Ratio in Lactating Human Nipple", 8th World Congress of Biomechanics, Ireland, June 2018.
5. **Lin Jiang**, Fatemeh Hassanipour, "Infant Oral Cavity Pressure Data Processing", in Proceedings of Summer Biomechanics, Bioengineering and Biotransport Conference, **PhD student Paper Competition finalist**, Tucson, AZ, June 2017.
6. **Lin Jiang**, Ruiyun Qi. "An adaptive actuator failure compensation scheme for discrete-time TS Fuzzy systems." in Proceedings of Chinese Control and Decision Conference (CCDC) pp:4757-4762, IEEE.

Professional Memberships and Services:

- Student Honor Member, IEEE HKN Kappa Kappa Chapter Honor Society. 2019-now
- Student Member, BMES (Biomedical Engineering Society) 2019-now
- Student Member, ASME (American Society of Mechanical Engineers). 2018-now
- Member, ISRHML (International Society for Research in Human Milk & Lactation) 2018-now
- Volunteer, Galerstein Gender Center, The University of Texas at Dallas 2016-2018
- Student Volunteer, Texas Systems Day, The University of Texas at Dallas 2018
- Reviewer, Chinese Control and Decision Conference 2013-2014
- Reviewer, Experimental in Fluids 2019-2020